



Search for non-resonant Higgs boson pair production in the $bb\ell\nu\ell\nu$ final state with the ATLAS detector in pp collisions at $\sqrt{s} = 13$ TeV



The ATLAS Collaboration ^{*}

ARTICLE INFO

Article history:

Received 19 August 2019
 Received in revised form 4 December 2019
 Accepted 5 December 2019
 Available online 13 December 2019
 Editor: M. Doser

ABSTRACT

A search for non-resonant Higgs boson pair production, as predicted by the Standard Model, is presented, where one of the Higgs bosons decays via the $H \rightarrow bb$ channel and the other via one of the $H \rightarrow WW^*/ZZ^*/\tau\tau$ channels. The analysis selection requires events to have at least two b -tagged jets and exactly two leptons (electrons or muons) with opposite electric charge in the final state. Candidate events consistent with Higgs boson pair production are selected using a multi-class neural network discriminant. The analysis uses 139 fb^{-1} of pp collision data recorded at a centre-of-mass energy of 13 TeV by the ATLAS detector at the Large Hadron Collider. An observed (expected) upper limit of $1.2 (0.9^{+0.4}_{-0.3}) \text{ pb}$ is set on the non-resonant Higgs boson pair production cross-section at 95% confidence level, which is equivalent to $40 (29^{+14}_9)$ times the value predicted in the Standard Model.

© 2019 The Author(s). Published by Elsevier B.V. This is an open access article under the CC BY license (<http://creativecommons.org/licenses/by/4.0/>). Funded by SCOAP³.

1. Introduction

In 2012, the ATLAS and CMS Collaborations reported the observation of a new particle in the search for the Standard Model (SM) Higgs boson (H) [1,2]. So far, measurements of the spin and couplings of the new particle are consistent with those predicted by the Brout–Englert–Higgs (BEH) mechanism of the SM [3–12]. The SM predicts non-resonant production of Higgs boson pairs (HH) in proton–proton (pp) collisions, referred to as *non-resonant* HH production, with the dominant production modes at the LHC proceeding via the gluon–gluon fusion (ggF) process. The ggF process has two leading order contributions: the first corresponds to the so-called ‘triangle diagram’, which includes the Higgs boson self-coupling, and the second is the so-called ‘box diagram’, which includes a heavy-quark loop with two fermion–fermion–Higgs (ffH) vertices. These two amplitudes interfere destructively, resulting in a low cross-section of only $31.05 \pm 1.90 \text{ fb}$ for the ggF HH production mode, computed at next-to-next-to-leading order (NNLO) and including finite top-quark mass effects [13–20]. Feynman diagrams illustrating these two contributions are shown in Fig. 1. The measurement of non-resonant HH production at the LHC stands as an important test of the BEH mechanism. In many beyond-the-SM (BSM) theories, HH production can be enhanced by modifying the Higgs boson self-coupling, λ_{HHH} , or the top-quark Yukawa coupling, y_t , and/or by introducing new contact interactions between

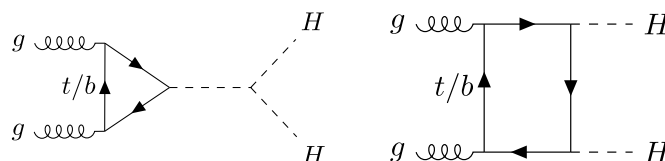


Fig. 1. Feynman diagrams for leading order ggF production of Higgs boson pairs: the ‘triangle diagram’ sensitive to the Higgs boson self-coupling on the left and the ‘box diagram’ on the right.

two top-quarks or gluons and two Higgs bosons or introducing production mechanisms via intermediate BSM particles [21–23].

The ATLAS and CMS Collaborations have performed searches for non-resonant HH production in a variety of final states at 13 TeV [24–33]. No significant excess of events beyond SM expectations is observed in these searches, with the ATLAS and CMS data-analyses setting observed (expected) limits on non-resonant HH production to be no larger than 6.9 (10.0) and 22.2 (12.8) times the predicted rate in the SM, respectively [34,35].

This Letter describes a search for non-resonant HH production in the $bb\ell\nu\ell\nu$ final state, where ℓ refers to a lepton (either an electron or a muon), using 13 TeV pp collision data collected with the ATLAS detector during 2015–2018 and corresponding to a total integrated luminosity of 139 fb^{-1} . The analysis uses machine-learning techniques based on feedforward neural network architectures [36] to construct an event-level classifier trained to distinguish between the HH signal and SM backgrounds. Analyses searching for non-resonant HH production via similar decay channels were performed previously in the single-lepton final state

^{*} E-mail address: atlas.publications@cern.ch.

by ATLAS in searches for $HH \rightarrow bbWW^*$ [28] and in the dilepton channel by CMS in searches for $HH \rightarrow bbWW^*/bbZZ^*$ [31].

2. ATLAS detector

The ATLAS detector [37–39] is a general-purpose particle detector with forward–backward symmetric cylindrical geometry.¹ It includes an inner tracking detector (ID), immersed in an axial magnetic field, which provides precision tracking of charged particles over the range of $|\eta| < 2.5$. Calorimeter systems with either liquid argon or scintillator tiles as the active medium provide energy measurements over the range of $|\eta| < 4.9$. The muon spectrometer (MS) is positioned outside the calorimeters and includes three air-core toroidal magnets. The MS is composed of several types of muon detectors which provide trigger and high-precision tracking capabilities for $|\eta| < 2.4$ and $|\eta| < 2.7$, respectively. A hardware-based trigger followed by a software-based trigger reduce the recorded event rate to an average of 1 kHz [40].

3. Dataset and simulated events

The data used for this search were collected in pp collisions at the LHC with a centre-of-mass energy of 13 TeV. Only those data collected during stable LHC beam conditions and with all ATLAS detector subsystems fully operational are used, and correspond to an integrated luminosity of 139 fb^{-1} . The selection of candidate events with oppositely charged leptons is based on a combination of single-lepton and dilepton triggers.² The use of a given trigger depends on the flavour and the transverse momenta (p_T) of the two (p_T -ordered) leptons in the event, and on the data-taking period. Single-lepton triggers with p_T thresholds between 22 and 28 GeV are given priority over dilepton triggers. The criteria of the dilepton triggers are checked only if no single-lepton trigger criteria are met and have p_T thresholds as low as 19 (10) GeV for the leading (subleading) lepton. At least one reconstructed lepton (or lepton pair) has to match a corresponding trigger object, in which case their offline p_T must be higher than the trigger threshold by at least 2 GeV, in order to be on the efficiency plateau of the corresponding trigger.

Monte Carlo (MC) simulation [41] is used to model the signal processes and in the estimation of SM background processes. A GEANT4 [42] simulation of the ATLAS detector was used for the background processes. The signal MC samples were processed with a fast simulation that relies on a parameterisation of the calorimeter response [41] and on GEANT4 for the tracking detectors. Simulated events are reconstructed using the same algorithms as used for data and include the effects of multiple pp interactions in the same or neighbouring bunch crossings, collectively referred to as pile-up. The simulation of pile-up collisions was performed with PYTHIA 8.186 [43] using the ATLAS A3 set of tuned parameters [44] and the NNPDF2.3LO parton distribution function (PDF) set [45]. Simulated events were reweighted to match the distribution of pile-up interactions in data. The average amount of pile-up in the data collected during 2015–2018 was 33.7.

The signal processes with ggF-initiated non-resonant HH production in the $bb\ell\nu\ell\nu$ final state were generated with an effective

Lagrangian in the infinite top-quark mass approximation. The generated signal events were reweighted with form factors that take into account the finite mass of the top-quark [46,47]. SM background processes were simulated using different MC event generators. The MC matrix element (ME) event generators and PDF sets, the parton showering (PS) and the underlying event (UE) modelling, UE tuned parameters (tune), and the accuracy of the theoretical cross-sections used to normalise the simulated processes are summarised in Table 1. Each SM background process is normalised to the best available respective theoretical cross-section. The mass of the Higgs boson was set to 125 GeV for all signal and background processes. The HH branching fractions (BF) predicted by the SM [13] are used for all Higgs boson decays. MADSPIN [48] was used to model top-quark spin correlations and EVTGEN [49] was used to model properties of b - and c -hadron decays for processes using PYTHIA and for the signal processes.

SM top-quark pair production ($t\bar{t}$) and the production of single top-quarks in association with W bosons (Wt) contribute with significant background contamination in the $bb\ell\nu\ell\nu$ final state. At next-to-leading-order (NLO) accuracy, there exists non-trivial interference between these two processes that may be enhanced in phase-space regions wherein there are high fractions of Wt events [50]. Two schemes are typically used to remove the overlap between these two processes: the so-called diagram removal (DR) and diagram subtraction (DS) schemes [51]; the former is used in the present analysis to remove the overlapping events and the latter is used to evaluate the systematic uncertainty in corresponding background event yields. Because of these effects, the sum of the simulated $t\bar{t}$ and Wt processes is considered as a single background process and referred to as the ‘Top’ process in what follows.

4. Event selection and object definitions

Selected events are required to have at least one pp interaction vertex reconstructed from at least two ID tracks with $p_T > 0.4$ GeV. The primary vertex for each event is defined as the vertex with the highest $\sum (p_T)^2$ of associated ID tracks [102]. Events that contain at least one jet arising from non-collision sources or detector noise are rejected by a set of quality criteria [103].

Loose and signal criteria are defined in order to select reconstructed lepton and jet candidates, where the latter is a subset of the former. Compared to the loose objects, the signal objects are required to satisfy tighter identification or quality criteria that are designed to suppress background contributions. Reconstructed loose (signal) electrons are required to satisfy the ‘Loose’ (‘Tight’) likelihood identification criteria [104]. Loose electrons are required to have $p_T > 10$ GeV and to be within $|\eta| < 2.47$. In addition, signal electrons are required to be outside the range $1.37 < |\eta| < 1.52$, which corresponds to the transition regions between the barrel and endcaps of the electromagnetic calorimeters. In order to reduce background contributions from jets misidentified as electrons, signal electrons are required to be isolated according to the ‘Gradient’ selection criteria [104]. Reconstructed loose and signal muon candidates are required to have $p_T > 10$ GeV, to be within $|\eta| < 2.4$, and to satisfy the ‘Medium’ identification criteria [105]. Additionally, signal muons are required to be isolated according to the ‘FixedCutLoose’ selection criteria [105]. Signal electron (muon) candidates are required to originate from the primary vertex by demanding that the significance of the transverse impact parameter, defined as the absolute value of the track transverse impact parameter, d_0 , measured relative to the primary vertex, divided by its uncertainty, σ_{d_0} , satisfy $|d_0|/\sigma_{d_0} < 5$ (3). The difference Δz_0 between the value of the z coordinate of the point on the track at which d_0 is defined and the longitudinal position of the primary

¹ ATLAS uses a right-handed coordinate system with its origin at the nominal interaction point (IP) in the centre of the detector and the z -axis along the beam pipe. The x -axis points from the IP to the centre of the LHC ring, and the y -axis points upwards. Cylindrical coordinates (r, ϕ) are used in the transverse plane, ϕ being the azimuthal angle around the z -axis. The pseudorapidity is defined in terms of the polar angle θ as $\eta = -\ln \tan(\theta/2)$. The angular distance is measured in units of $\Delta R \equiv \sqrt{(\Delta\eta)^2 + (\Delta\phi)^2}$.

² Distinct sets of single-lepton triggers are used for electrons and muons. Dilepton triggers require either two electrons, two muons, or one electron and one muon.

Table 1

List of the ME generators and PS/UE modelling algorithms used in the simulation. Alternative generators and PS/UE models, used to estimate systematic uncertainties, are shown in parentheses. The PDF sets, tunes, and the perturbative QCD highest-order accuracy (leading-order, LO; next-to-leading-order, NLO; next-to-next-to-leading-order, NNLO; next-to-next-to-leading-logarithm, NNLL) used for the normalisation of the samples are also included. The top-quark mass is set to 172.5 GeV.

| Process | ME generator (alternative) | ME PDF | PS/UE model (alternative) | UE tune | Prediction order for total cross-section |
|--|--|------------------|-------------------------------------|-------------------------|---|
| $t\bar{t}$ [52,53] | POWHEG-BOX v2 [54,55] (MADGRAPH 5_aMC@NLO) | NNPDF3.0NLO [56] | PYTHIA 8.230 [57] (HERWIG 7.0.4) | A14 [58] (H7-MMHT14) | NNLO + NNLL [59–65] |
| Single-top s -channel, Wt [52,66,67] | POWHEG-BOX (MADGRAPH 5_aMC@NLO) | NNPDF3.0NLO | PYTHIA 8.230 (HERWIG 7.0.4) | A14 (H7-MMHT14) | NLO + NNLL [68,69] |
| Single-top t -channel [52,66] | POWHEG-BOX, MADSPIN [48] (MADGRAPH 5_aMC@NLO) | NNPDF3.04fNLO | PYTHIA 8.230 (HERWIG 7.0.4) | A14 (H7-MMHT14) | NLO + NNLL [70] |
| $W, Z/\gamma^* + \text{jets}$ [71] ($Z/\gamma^* + \text{jets}$) | SHERPA 2.2.1 [72,73] (MADGRAPH 5_aMC@NLO) | NNPDF3.0NNLO | SHERPA 2.2.1 (PYTHIA 8.230) | SHERPA default (A14) | NLO(LO) $\leq 2(4)$ partons [74–78] |
| Diboson (WW, WZ, ZZ) [79] | SHERPA 2.2.2 | NNPDF3.0NNLO | SHERPA 2.2.2 | SHERPA default | NLO(LO) $\leq 1(3)$ partons [75–78] |
| $t\bar{t}W, t\bar{t}Z$ [80] | MADGRAPH 5_aMC@NLO [81] | NNPDF3.0NLO | PYTHIA 8.210 | A14 | NLO [82,83] |
| $t\bar{t}H$ [80] | MADGRAPH 5_aMC@NLO | NNPDF3.0NLO | PYTHIA 8.210 | A14 | NLO [84,85] |
| WH, ZH [86] | PYTHIA 8.186 [43] | NNPDF3.0LO [45] | PYTHIA 8.186 | A14 | NNLO QCD + NLO EW [87–93] |
| $ggF H$ [94] | POWHEG-BOX v2 NNLOPS [95] | CT10 [96] | PYTHIA 8.212 | AZNLO [97] | NNLO QCD + NLO EW [98] |
| SM $HH \rightarrow b\bar{b}l\nu\ell\nu$ [99] | MADGRAPH 5_aMC@NLO 2.6.2 | CT10 | HERWIG 7.0.4 [100] | H7-MMHT14 [101] | NNLO [14–20] |

vertex is required to satisfy $|\Delta z_0 \times \sin\theta| < 0.5$ mm, where θ is the polar angle of the track with respect to the z -axis.

Jets are reconstructed from topological clusters of energy deposits in the calorimeters [106] using the anti- k_t algorithm [107, 108] with a radius parameter of $R = 0.4$ and calibrated as described in Ref. [109]. Candidate loose jets are required to have $p_T > 20$ GeV. Signal jets are required to have $|\eta| < 2.8$ and must satisfy pile-up suppression requirements based on the output of a multivariate classifier [110], which identifies jets consistent with a primary vertex in the region $|\eta| < 2.4$ and $p_T < 120$ GeV. The MV2c10 multivariate algorithm [111] is used to identify jets containing b -hadrons (b -tagged jets). An MV2c10 working point with a b -tagging efficiency of 70%, estimated from simulated $t\bar{t}$ events [112], is used. The b -tagged jets must have $p_T > 20$ GeV and $|\eta| < 2.5$. The momentum of b -tagged jets is adjusted using the muon-in-jet correction, as described in Ref. [6], by accounting for momentum losses due to muons originating from in-flight semileptonic b -hadron decays occurring within the b -tagged jet.

The missing transverse momentum $\mathbf{p}_T^{\text{miss}}$, the magnitude of which is denoted by E_T^{miss} , is constructed from the negative vectorial sum of the transverse momenta of calibrated loose objects in the event. An additional term is included to account for the energy of ID tracks that are matched to the primary vertex in the event but not to any of the selected loose objects [113].

To avoid double-counting, loose objects are subject to the overlap removal procedure defined as follows. If a reconstructed electron and muon share a track in the ID, the electron is removed. However, if the muon sharing the track with the electron is calorimeter-tagged,³ then the muon is removed instead of the electron. If a jet and an electron are reconstructed within $\Delta R = 0.2$ of each other, then the jet is removed. If a jet and a muon are within $\Delta R = 0.2$ of each other, and the jet has less than three tracks or carries less than 50% of the muon p_T , then the jet is removed; otherwise, the muon is removed. Electrons or muons separated from the remaining jets by $\Delta R < 0.4$ are removed.

The analysis selects candidate events with exactly two oppositely charged signal leptons, electrons or muons, and at least two signal b -tagged jets. To enhance sensitivity to the signal process

and to maximise rejection of the expected SM backgrounds, the analysis uses a multivariate approach to select signal events.

5. Analysis strategy

The analysis relies on the use of a multivariate discriminant designed to select candidate events consistent with non-resonant HH production. Section 5.1 describes the architecture and the training of the deep neural network (DNN) classifier from which the discriminant is constructed. Section 5.2 describes the signal region selection criteria. Section 5.3 describes the final background estimation procedure.

5.1. Deep learning approach to target HH

The discriminant uses the outputs of a DNN classifier that is built using the KERAS library with TENSORFLOW as a backend [114, 115] and uses the LWTNN library [116] to interface with the analysis software infrastructure of the ATLAS experiment. The sample of events used for training is composed of equal numbers of events from the signal and each of the dominant background processes: Top (as defined in Section 3), $Z/\gamma^* \rightarrow \ell\ell$ (Z - $\ell\ell$), and $Z/\gamma^* \rightarrow \tau\tau$ (Z - $\tau\tau$) production. The signal sample used in the training of the classifier contains only the $HH \rightarrow bbWW^*$ component due to its larger BF relative to the $HH \rightarrow bb\tau\tau$ and $HH \rightarrow bbZZ^*$ components. However, the sum of all three signal components is evaluated as the signal when performing the statistical analysis. Additionally, all processes that make up the training sample ($HH \rightarrow bbWW^*$, Top, Z - $\ell\ell$, and Z - $\tau\tau$) have the same weight during the training of the classifier. The training sample is composed of simulated candidate events with $m_{\ell\ell} > 20$ GeV and having one or more b -tagged jets, where events with exactly one b -tagged jet are included to increase the number of events available for training. For the training events with exactly one b -tagged jet, each observable that requires at least two b -tagged jets is set to its mean value as computed with the full set of training events that contain at least two b -tagged jets. Observables that require two b -tagged jets are defined using the leading two b -tagged jets. The classifier contains two fully connected hidden layers each with 250 nodes. Rectified linear unit (ReLU) activations are used for each layer [117]. In order to improve the robustness of the training and to reduce effects due to overtraining, there is a dropout layer that randomly drops 50% of the nodes between the two fully connected layers during training [118]. The classifier produces four outputs that are passed through a softmax activation, constraining their sum to one [36].

³ A calorimeter-tagged muon has only a reconstructed track in the ID matched to energy deposits in the calorimeter compatible with a minimum ionising particle, but no corresponding track segment in the MS.

Table 2

Description of the variables used as inputs to the DNN classifier.

| | |
|---|--|
| (p_T, η, ϕ) | $p_T, \eta,$ and ϕ of the leptons, leading two jets (not necessarily b -tagged), and leading two b -tagged jets |
| Dilepton flavour | Whether the event is composed of two electrons, two muons, or one of each (encoded as 3 booleans) |
| $\Delta R_{\ell\ell}, \Delta\phi_{\ell\ell} $ | ΔR and magnitude of the $\Delta\phi$ between the two leptons |
| $m_{\ell\ell}, p_T^{\ell\ell}$ | Invariant mass and the transverse momentum of the dilepton system |
| $E_T^{\text{miss}}, E_T^{\text{miss}-\phi}$ | Magnitude of the missing transverse momentum vector and its ϕ component |
| $ \Delta\phi(\mathbf{p}_T^{\text{miss}}, \mathbf{p}_T^{\ell\ell}) $ | Magnitude of the $\Delta\phi$ between the $\mathbf{p}_T^{\text{miss}}$ and the transverse momentum of the dilepton system |
| $ \mathbf{p}_T^{\text{miss}} + \mathbf{p}_T^{\ell\ell} $ | Magnitude of the vector sum of the $\mathbf{p}_T^{\text{miss}}$ and the transverse momentum of the dilepton system |
| Jet multiplicities | Numbers of b -tagged and non- b -tagged jets |
| $ \Delta\phi_{bb} $ | Magnitude of the $\Delta\phi$ between the leading two b -tagged jets |
| m_{T2}^{bb} | m_{T2} [120] using the leading two b -tagged jets as the visible inputs and $\mathbf{p}_T^{\text{miss}}$ as invisible input |
| H_{T2} | Scalar sum of the magnitudes of the momenta of the $H \rightarrow \ell\nu\ell\nu$ and $H \rightarrow bb$ systems, |
| | $H_{T2} = \mathbf{p}_T^{\text{miss}} + \mathbf{p}_T^{\ell,0} + \mathbf{p}_T^{\ell,1} + \mathbf{p}_T^{b,0} + \mathbf{p}_T^{b,1} $ |
| H_{T2}^R | Ratio of H_{T2} and scalar sum of the transverse momenta of the H decay products, |
| | $H_{T2}^R = H_{T2} / (E_T^{\text{miss}} + \mathbf{p}_T^{\ell,0} + \mathbf{p}_T^{\ell,1} + \mathbf{p}_T^{b,0} + \mathbf{p}_T^{b,1}),$ |
| | where $\mathbf{p}_T^{\ell(b),0(1)}$ are the transverse momenta of the leading {subleading} lepton (b -tagged jet) |

The resulting four outputs, each constrained to values between 0 and 1, are referred to as p_i ($i \in \{HH, \text{Top}, Z\text{-}\ell\ell, Z\text{-}\tau\tau\}$). Values of p_i nearer to 1 indicate that the event likely belongs to class i and values nearer to 0 indicate otherwise. The main discriminant in the analysis, d_{HH} , is constructed from the four p_i and is defined as $d_{HH} = \ln[p_{HH} / (p_{\text{Top}} + p_{Z\text{-}\ell\ell} + p_{Z\text{-}\tau\tau})]$.

The $HH \rightarrow bb\ell\nu\ell\nu$ signal events are characterised by two distinct ‘Higgs hemispheres’. One hemisphere contains the two b -tagged jets from the $H \rightarrow bb$ decay and it is typically opposite in the transverse plane to the second hemisphere that contains the two leptons and E_T^{miss} from the $H \rightarrow WW^*/ZZ^*/\tau\tau$ decay. The final-state objects in the SM backgrounds, the Top process in particular, are distributed more uniformly within the event and they typically do not exhibit the same opposite hemispheres topology as the HH signal. These Higgs hemispheres thus provide a topological criterion that distinguishes the signal from the background and motivates the choice of input observables that are provided to the classifier. Thirty-five such variables are provided as inputs to the classifier, ranging from momentum components of the visible final-state objects to observables using event-wide information, and are constructed using only calibrated final state objects that have well-understood uncertainties (Section 6). A complete list is provided in Table 2. The event-wide input observables are sensitive to the presence of Higgs hemispheres in the signal and are largely angular in nature or take advantage of the fact that the final state objects from each of the Higgs bosons in the signal tend to be near to each other. The observables H_{T2}^R and m_{T2}^{bb} are non-standard high-level observables that are not straightforward functions of the momenta of the final-state objects. By construction, H_{T2}^R can take values between zero and one; it peaks near one for signal and is more broadly distributed for background. The m_{T2}^{bb} observable is defined similarly to the M_{T2}^{bb} observable in Ref. [119] but does not include the final-state leptons. As discussed in Ref. [119], for the Top backgrounds m_{T2}^{bb} generally has values below the mass of the top-quark due to kinematic constraints while for the Z/γ^* processes, which have little-to-no E_T^{miss} , m_{T2}^{bb} is typically below 45 GeV. The use of dropout regularisation during the training of the classifier allows it to more effectively use the information contained in the full set of inputs presented in Table 2 by reducing its susceptibility to overtraining effects that may otherwise appear as a result of using such an extended input feature space in the case where no such regularisation is performed. To verify this, the performance of the classifier was checked using an independent sample of events not used in the training of the classifier and was

found to be compatible to its performance when presented with those of the training sample.

5.2. Signal selection criteria

To define signal selection criteria, the analysis relies on the invariant mass of the two leptons, $m_{\ell\ell}$, and the invariant mass of the two leading (p_T -ordered) b -tagged jets, m_{bb} . Due to spin-correlation effects present in the $H \rightarrow WW^* \rightarrow \ell\nu\ell\nu$ decay within the dominant $HH \rightarrow bbWW^*$ signal process, the signal events exhibit values of $m_{\ell\ell}$ that are typically below 60 GeV. By selecting low values of $m_{\ell\ell}$, the signal purity can therefore be enhanced while rejecting a large component of the SM Z boson and Top backgrounds. Additionally, m_{bb} has a peak at the mass of the Higgs boson for the signal process and therefore provides an effective means to define selections in which the HH contribution is enhanced. The signal selection criteria therefore require $m_{\ell\ell} \in (20, 60)$ GeV and $m_{bb} \in (110, 140)$ GeV. The $m_{\ell\ell} > 20$ GeV requirement is enforced in order to remove contamination from low-mass resonances and Z/γ^* processes. The signal selection criteria are further broken down into same-flavour (SF), i.e. ee or $\mu\mu$, or different-flavour (DF), i.e. $e\mu$, regions. Separating by dilepton flavour enhances the separation power between the signal and Z/γ^* background; the former has roughly equal probabilities for the SF and DF final states and the latter leads predominantly to SF final states.

In addition to the $m_{\ell\ell}$ and m_{bb} requirements, the same-flavour and different-flavour signal regions, SR-SF and SR-DF, respectively, are defined by requiring high values of d_{HH} and are presented in Table 3. The chosen threshold values of $d_{HH} > 5.45$ (5.55) for SR-SF (SR-DF) are found to maximise the expected sensitivity to the non-resonant HH process. The predicted $HH \rightarrow bb\ell\nu\ell\nu$ signal yields in SR-SF and SR-DF are shown in Table 3, and are composed of 90% $HH \rightarrow bbWW^*$, 9% $HH \rightarrow bb\tau\tau$, and 1% $HH \rightarrow bbZZ^*$. The predominance of the $HH \rightarrow bbWW^*$ process over the other two is a result of both its larger overall BF and of the classifier having been trained only on this component of the signal.

5.3. Background estimation

As mentioned in Section 5.1, the dominant backgrounds expected to contaminate the signal regions are the Top and Z/γ^* processes, specifically Z/γ^* production in association with jets

Table 3

Analysis region and background estimation summary. Shown are the definitions of the control, validation, and signal regions used in the analysis as well as the predicted and observed event yields in each of these regions. The predicted yields are shown after background-only fits to data in the control regions. The Top and Z/γ^* + HF post-fit normalisation factors, obtained from background-only fits in the corresponding control regions, are shown at the bottom of the table. Also shown is the predicted $HH \rightarrow bb\ell\nu\ell\nu$ signal yield in each of the regions, multiplied by a factor of 20. Of the HH yield in the signal regions, 90% comes from the $HH \rightarrow bbWW^*$ process, 9% from the $HH \rightarrow bb\tau\tau$ process, and 1% from the $HH \rightarrow bbZZ^*$ process. The uncertainties in each yield and in the normalisation correction factors account for the statistical and systematic uncertainties described in Section 6, with those on the normalisation corrections due only to experimental sources.

| Region definitions | | | | | | |
|------------------------------------|---------------------------------------|-----------------|-----------------|------------------------------|----------------|-----------------|
| Observable | CR-Top | VR-1 | CR-Z+HF | VR-2 | SR-SF | SR-DF |
| Dilepton flavour | DF | SF | DF or SF | SF | SF | DF |
| $m_{\ell\ell}$ [GeV] | (20, 60) | (20, 60) | (81.2, 101.2) | (71.2, 81.2) or (101.2, 115) | (20, 60) | (20, 60) |
| m_{bb} [GeV] | \notin (100, 140) | > 140 | (100, 140) | (100, 140) | (110, 140) | (110, 140) |
| d_{HH} | > 4.5 | > 4.5 | > 0 | > 0 | > 5.45 | > 5.55 |
| Event yields | | | | | | |
| Data | 108 | 171 | 852 | 157 | 16 | 9 |
| Total Bkg. | 108 ± 10 | 162 ± 10 | 852 ± 29 | 147 ± 11 | 14.9 ± 2.1 | 4.9 ± 1.2 |
| Top | 92 ± 11 | 77 ± 10 | 55 ± 7 | 71 ± 10 | 4.8 ± 1.4 | 3.8 ± 1.1 |
| Z/γ^* + HF | 3.2 ± 0.5 | 70 ± 4 | 686 ± 33 | 60 ± 4 | 7.8 ± 1.4 | 0.21 ± 0.05 |
| Other | 13.1 ± 3.4 | 14.2 ± 1.9 | 110 ± 13 | 15.8 ± 1.2 | 2.3 ± 0.5 | 0.9 ± 0.4 |
| HH ($\times 20$) | 2.70 ± 0.25 | 1.03 ± 0.22 | 1.97 ± 0.11 | 1.22 ± 0.05 | 5.0 ± 0.6 | 4.8 ± 0.8 |
| Post-fit normalisation | | | | | | |
| $\mu_{\text{Top}} = 0.79 \pm 0.10$ | $\mu_{Z/\gamma^*+HF} = 1.36 \pm 0.07$ | | | | | |

originating from heavy-flavour hadrons (bb , bc , or cc), subsequently referred to as Z/γ^* + HF. Subdominant SM processes contribute via $t\bar{t}$ production in association with an electroweak vector boson, single Higgs boson production (predominantly via the $t\bar{t}H$ mode), Z/γ^* production in association with light-flavour jets, and electroweak diboson processes. There is additionally a minor contribution of background events from non-prompt leptons produced in semileptonic decays of heavy-flavour hadrons and from misidentified electron candidates arising from photon conversions and jets. This background is estimated using events with a same-charge lepton pair, following procedures described in Ref. [121], after subtracting the prompt-lepton contribution. The rest of the SM background processes detailed in Table 1 are estimated primarily using simulation.

Dedicated control regions are defined to derive data-driven normalisation corrections for the dominant background processes: CR-Top for Top and CR-Z+HF for Z/γ^* + HF. These normalisation corrections have a uniform prior and are checked in two validation regions, VR-1 and VR-2, enriched with events from the Top and Z/γ^* + HF processes. The control and validation regions are defined in Table 3 and are kinematically close to the signal regions. CR-Top (CR-Z+HF) and VR-1 (VR-2) are defined by inverting the m_{bb} ($m_{\ell\ell}$) requirements relative to those of the signal regions but retain a selection of the high d_{HH} region similar to the signal regions. The d_{HH} selections were relaxed to increase statistical power, independent checks showed that this did not have a significant impact on the post-fit normalisation corrections in Table 3.

VR-1 keeps only those events with $m_{bb} > 140$ GeV, excluding the region $m_{bb} < 100$ GeV which is included in CR-Top, due to significant contamination of Z/γ^* + HF events. The correlations between the $m_{\ell\ell}$ and m_{bb} observables and d_{HH} after the preselection are observed to be small and do not prevent the use of the former two in the construction of the analysis regions defined in Table 3, as d_{HH} is found to rely mainly on the information provided by the additional input observables listed in Table 2. This absence of strong correlation ensures that the measurements made in the tails of d_{HH} in the control regions can be extrapolated to those in the signal regions.

The Top background in the signal regions is expected to be composed of approximately equal contributions from the $t\bar{t}$ and single-top-quark Wt process and therefore susceptible to the in-

terference effects as described in Section 3. For this reason, CR-Top and the validation regions are defined so that they have predicted $t\bar{t}$ and Wt compositions similar to that of the signal regions. This ensures that the normalisation correction determined in the fit for the Top background results in an accurate estimate of the combined $t\bar{t}$ and Wt process in the signal regions, accounting for potential interference effects present in data but not necessarily modelled in MC simulation. Table 3 compares the observed and predicted event yields, where the background event yields obtained after background-only fits in the corresponding control regions are also shown. The post-fit normalisation correction factors for the Top and Z/γ^* + HF background processes, respectively $\mu_{\text{Top}} = 0.79 \pm 0.10$ and $\mu_{Z/\gamma^*+HF} = 1.36 \pm 0.07$, are also shown in Table 3. The uncertainties in μ_{Top} and μ_{Z/γ^*+HF} take into account the statistical and systematic uncertainties due to the experimental sources, as described in Section 6.

Distributions of d_{HH} in the control regions after performing background-only fits to data in the control regions and applying the Top and Z/γ^* + HF normalisation corrections are shown in Fig. 2. In the control and validation regions, good agreement between the data and SM prediction provided by the post-fit MC simulation is observed for the observables relevant to the analysis.

6. Systematic uncertainties

The analysis evaluates several sources of systematic uncertainty for the signal and background processes, which are classified as either *experimental* (detector or luminosity related) or *theoretical* modelling uncertainties. Statistical uncertainties of the simulated event samples are also taken into account. The main uncertainty components are summarised in Table 4. MC modelling uncertainties in the Top and Z/γ^* + HF background estimates are dominant, followed by statistical and detector uncertainties.

The normalisation corrections of the Top and Z/γ^* + HF background processes are determined primarily by the data events in the control regions when performing the statistical analysis. These corrections take into account the statistical and systematic uncertainties due to the experimental sources, as described later in this section. In addition, the systematic uncertainties in the theoretical modelling of these processes are applied as uncertainties in

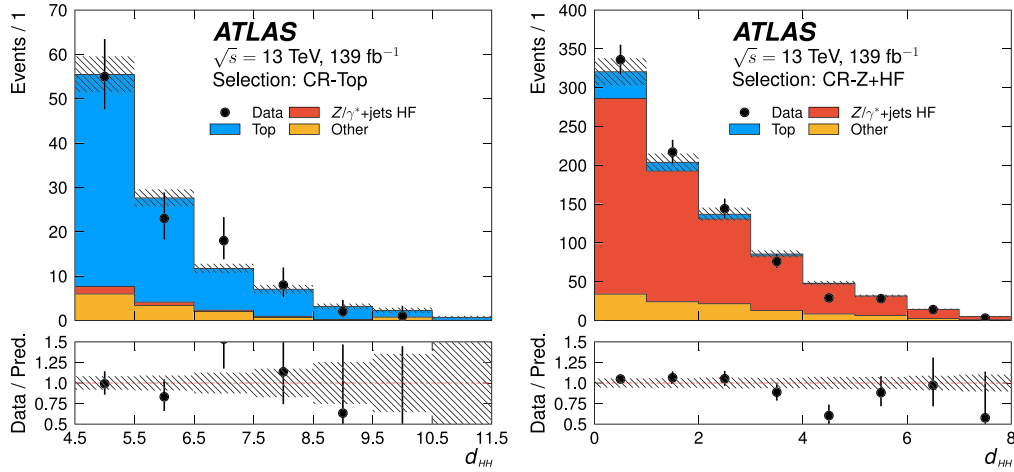


Fig. 2. Distributions of d_{HH} in CR-Top (left) and CR-Z+HF (right). Distributions are shown after the fit to data under the background-only hypothesis in the shown control regions. The ratio of the data to the sum of the backgrounds is shown in the lower panel. The hatched bands indicate the combined statistical and systematic uncertainty.

the corrected predictions in the signal regions using the following procedures. The uncertainties in the estimated Top background event yields due to parton shower modelling are assessed as the difference between the predictions of POWHEG-Box showered with PYTHIA or HERWIG, and those due to the choice of event generator are assessed by comparing the predictions of POWHEG-Box or MADGRAPH 5_aMC@NLO [122], both showered with PYTHIA. The uncertainties due to missing higher-order corrections are estimated by changing the renormalisation and factorisation scales (μ_R and μ_F , respectively) up and down by a factor of two (8-points variation). The uncertainties due to the modelling of initial- and final-state radiation (ISR and FSR, respectively) in the generators used to simulate the Top background processes are evaluated using the method described in Ref. [122]. The Top background composition is varied within the uncertainties in the theoretical predictions for the $t\bar{t}$ and single-top-quark Wt cross-sections [65,68,123]. The uncertainty arising from the interference between the NLO predictions for $t\bar{t}$ and Wt processes is estimated by taking the difference between the predicted Top background yields obtained with the DR and DS schemes used for the NLO Wt calculation [122]. The uncertainties due to PDF variations are computed as the envelope of the central values of the nominal NNPDF3.0 PDF set and the CT14, MMHT14, and PDF4LHC15_30PDF PDF sets [124]. All uncertainties except those in the scale variations, cross-section, and interference are considered as fully correlated between the $t\bar{t}$ and Wt processes. The $Z/\gamma^* + \text{HF}$ modelling uncertainties are estimated using the nominal SHERPA 2.2.1 samples by considering different merging (CKKW-L) [125] and resummation scales. The uncertainties due to PDF variations and changes in μ_R and μ_F are calculated using the same procedures as for the Top backgrounds. An additional uncertainty in the Z/γ^* process is computed by taking the difference between the nominal SHERPA 2.2.1 samples with samples generated using MADGRAPH 5_aMC@NLO+PYTHIA8. The dominant uncertainties in the total background estimates in SR-SF are the $Z/\gamma^* + \text{HF}$ modelling uncertainties (8%), primarily that due to comparison of SHERPA 2.2.1 and MADGRAPH 5_aMC@NLO, and the parton shower uncertainty affecting the Top background process (5%). The uncertainties in the background estimates in SR-DF are dominated by the uncertainty due to the parton shower affecting the Top background process (12%), the uncertainty in the Top normalisation correction μ_{Top} (10%), the uncertainty due to the comparison between the generators used for the Top process (7.5%), and the

uncertainty due to the modelling of ISR and FSR in the Top process (5%).

Systematic uncertainties in the signal acceptance due to varying μ_R and μ_F , as well as PDF-induced uncertainties, are evaluated using the same procedure as for the Top background process. The resulting scale (PDF) uncertainties are $< 3\%$ ($< 1\%$) in both signal regions. The uncertainty due to the parton shower modelling is computed by comparing HERWIG7 with PYTHIA8, and is found to be 8% (9%) in SR-SF (SR-DF). The uncertainty in the HH production cross-section, evaluated to be 5%, is included as an uncertainty in $\sigma^{\text{SM}}(gg \rightarrow HH)$ when computing the upper limits on the cross-section ratio in Table 5. This value is the quadrature sum of the scale, PDF+ α_s , and top mass contributions as reported by the LHCXSWG [20].

The uncertainties due to experimental sources arise primarily from the mismeasurement of reconstructed object momenta and from the mismodelling of reconstruction efficiencies. These uncertainties include uncertainties from the mismodelling of the jet energy scale (JES) [109] and jet energy resolution (JER) [126]. Additional uncertainties for b -tagged jets arise from the mismodelling of the b -tagging efficiency [111] and from the mismodelling of the rates at which charm- and light-flavoured jets are selected as b -tagged jets [127,128]. Lepton-related uncertainties arise from the mismodelling of the electron [104] (muon [105]) reconstructed energy (momentum) measurements, as well as in the mismodelling of their reconstruction and identification efficiencies [104, 105]. The $E_{\text{T}}^{\text{miss}}$ scale and resolution [113] uncertainties, as well as uncertainties from the mismodelling of pile-up, trigger efficiency and luminosity, are also taken into account. The uncertainty in the combined 2015–2018 integrated luminosity is 1.7% [129], obtained using the LUCID-2 detector [130] for the primary luminosity measurements. The combined effect of the experimental sources of systematic uncertainty in the predicted background yields is summarised in Table 4 and is dominated by the JER, with all other contributions found to be negligible.

7. Results

In order to extract information about the $HH \rightarrow b\bar{b}l\nu l\nu$ signal cross-section, a counting experiment is performed with a profile-likelihood fit [131] simultaneously across the CR-Top, CR-Z+HF, SR-SF, and SR-DF regions using the predicted and observed event counts in each region as inputs. The Top and $Z/\gamma^* + \text{HF}$ normal-

Table 4

Breakdown of the main uncertainty components in the background estimates in the two signal regions for the Top, $Z/\gamma^* + \text{HF}$, and all other (“Other”) backgrounds. The uncertainty components associated with the total background estimate in the signal regions (the sum of Top, $Z/\gamma^* + \text{HF}$, and Other) is listed under “Total Bkg.”. As in the upper half of Table 3, all uncertainties are shown “post-fit”. The percentages show the size of the uncertainty relative to the expected background in each column and uncertainties can be correlated, not necessarily adding in quadrature to the total uncertainty in each column or across each row. Uncertainties in the post-fit normalisation factors, μ_{Top} and $\mu_{Z/\gamma^* + \text{HF}}$, are only applicable for the Top and $Z/\gamma^* + \text{HF}$ processes.

| Uncertainty [%] | SR-SF | | | | SR-DF | | | |
|--|-------|--------------------------|-------|------------|-------|--------------------------|-------|------------|
| | Top | $Z/\gamma^* + \text{HF}$ | Other | Total Bkg. | Top | $Z/\gamma^* + \text{HF}$ | Other | Total Bkg. |
| Total uncertainty | 28 | 18 | 20 | 14 | 30 | 26 | 41 | 25 |
| Theoretical | 21 | 15 | 17 | 11 | 20 | 15 | 40 | 17 |
| Experimental | 12 | < 5 | 8 | < 5 | 15 | 17 | 8 | 12 |
| MC statistics | 8 | 8 | 6 | 8 | 13 | 13 | 7 | 11 |
| $\mu_{\text{Top}}, \mu_{Z/\gamma^* + \text{HF}}$ | 13 | 5 | n/a | 5 | 13 | 5 | n/a | 10 |

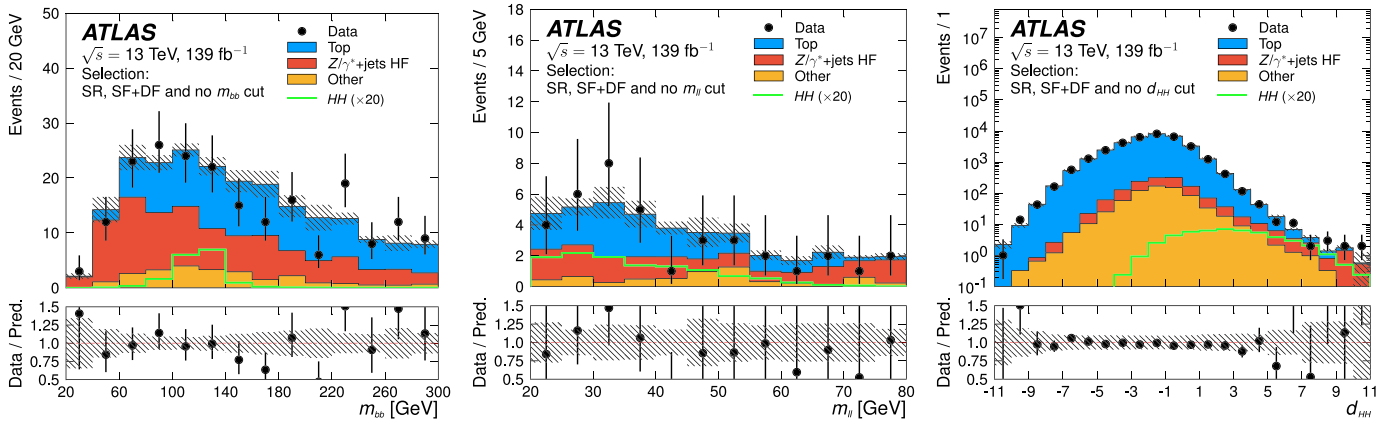


Fig. 3. Distributions of m_{bb} (left), $m_{\ell\ell}$ (middle), and the discriminant d_{HH} (right). The distributions are shown after the fit to data in the control regions under the background-only hypothesis. Each distribution includes both the SF and DF events and imposes signal selection requirements on all quantities except the one being plotted, but the requirement on d_{HH} has been relaxed to $d_{HH} > 5$ for the distributions of m_{bb} and $m_{\ell\ell}$. The $HH \rightarrow b\bar{b}\ell\nu\ell\nu$ signal (“ HH ”) is overlaid and has its cross-section scaled by a factor of 20 relative to the SM prediction for visualisation purposes. The ratio of the data to the sum of the backgrounds is shown in the lower panel of each figure. The hatched bands indicate the combined statistical and systematic uncertainty.

Table 5

Observed and expected upper limits on the ggF-initiated non-resonant HH production cross-section at 95% CL and their ratios to the SM prediction ($\sigma^{\text{SM}}(gg \rightarrow HH) = 31.05 \pm 1.90 \text{ fb}$ [13–20]). The $\pm 1\sigma$ and $\pm 2\sigma$ variations about the expected limit are also shown. Uncertainties in the SM cross-section are taken into account when computing the upper limits on the cross-section ratio.

| | -2σ | -1σ | Expected | $+1\sigma$ | $+2\sigma$ | Observed |
|---|------------|------------|----------|------------|------------|----------|
| $\sigma(gg \rightarrow HH)$ [pb] | 0.5 | 0.6 | 0.9 | 1.3 | 1.9 | 1.2 |
| $\sigma(gg \rightarrow HH) / \sigma^{\text{SM}}(gg \rightarrow HH)$ | 14 | 20 | 29 | 43 | 62 | 40 |

isation corrections are also extracted from this fit and are found to differ negligibly from those presented in Table 3. All sources of systematic and statistical uncertainty in the signal and background models are implemented as deviations from the nominal model, scaled by nuisance parameters that are profiled in the fit. The p -value corresponding to the background-only hypothesis, giving the probability that the data in the signal regions be at least as incompatible with the background-only hypothesis as that observed in SR-SF and SR-DF, is $p_0 = 0.15$ and corresponds to 1.05σ significance. Distributions of m_{bb} , $m_{\ell\ell}$, and d_{HH} after performing background-only fits to data in the control regions and applying the Top and $Z/\gamma^* + \text{HF}$ normalisation corrections are shown in Fig. 3. The signal selection criteria are imposed on all observables shown in Fig. 3 apart from the one being plotted, except that the d_{HH} requirement for the m_{bb} and $m_{\ell\ell}$ distributions is relaxed to $d_{HH} > 5$. No significant excess of events over the expected SM background is observed and upper limits are set on non-resonant Higgs boson pair production at 95% confidence level (CL) using the CL_s method [132]. Table 5 presents these upper limits and comparisons with the SM prediction. The observed (expected) limit at

95% CL is 1.2 (0.9) pb, corresponding to 40 (29) times the SM prediction.

8. Conclusions

A search for non-resonant Higgs boson pair production, as predicted by the SM, is presented in the final state with at least two b -tagged jets and exactly two leptons with opposite electric charge, where one of the Higgs bosons decays to $b\bar{b}$ and the other decays to either WW^* , ZZ^* , or $\tau\tau$. The analysis uses pp collision data recorded at $\sqrt{s} = 13 \text{ TeV}$ by the ATLAS detector at the LHC, corresponding to an integrated luminosity of 139 fb^{-1} . The data are in agreement with the predictions for the SM background processes. An observed (expected) 95% CL upper limit is set on the cross-section for the production of Higgs boson pairs, corresponding to 40 (29) times the SM prediction. These limits are comparable to the previous leading searches for non-resonant Higgs boson pair production performed by the ATLAS and CMS experiments.

Acknowledgements

We thank CERN for the very successful operation of the LHC, as well as the support staff from our institutions without whom ATLAS could not be operated efficiently.

We acknowledge the support of ANPCyT, Argentina; YerPhI, Armenia; ARC, Australia; BMWFW and FWF, Austria; ANAS, Azerbaijan; SSTC, Belarus; CNPq and FAPESP, Brazil; NSERC, NRC and CFI, Canada; CERN; CONICYT, Chile; CAS, MOST and NSFC, China; COLCIENCIAS, Colombia; MSMT CR, MPO CR and VSC CR, Czech Republic; DNRF and DNSRC, Denmark; IN2P3-CNRS, CEA-DRF/IRFU, France; SRNSFG, Georgia; BMBF, HGF, and MPG, Germany; GSRT, Greece; RGC, Hong Kong SAR, China; ISF and Benozio Center, Israel; INFN, Italy; MEXT and JSPS, Japan; CNRS, Morocco; NWO, Netherlands; RCN, Norway; MNiSW and NCN, Poland; FCT, Portugal; MNE/IFA, Romania; MES of Russia and NRC KI, Russian Federation; JINR; MESTD, Serbia; MSSR, Slovakia; ARRS and MIZŠ, Slovenia; DST/NRF, South Africa; MINECO, Spain; SRC and Wallenberg Foundation, Sweden; SERI, SNSF and Cantons of Bern and Geneva, Switzerland; MOST, Taiwan; TAEK, Turkey; STFC, United Kingdom; DOE and NSF, United States of America. In addition, individual groups and members have received support from BCKDF, Canarie, CRC and Compute Canada, Canada; COST, ERC, ERDF, Horizon 2020, and Marie Skłodowska-Curie Actions, European Union; Investissements d'Avenir Labex and Idex, ANR, France; DFG and AvH Foundation, Germany; Herakleitos, Thales and Aristeia programmes co-financed by EU-ESF and the Greek NSRF, Greece; BSF-NSF and GIF, Israel; CERCA Programme Generalitat de Catalunya, Spain; The Royal Society and Leverhulme Trust, United Kingdom.

The crucial computing support from all WLCG partners is acknowledged gratefully, in particular from CERN, the ATLAS Tier-1 facilities at TRIUMF (Canada), NDGF (Denmark, Norway, Sweden), CC-IN2P3 (France), KIT/GridKA (Germany), INFN-CNAF (Italy), NL-T1 (Netherlands), PIC (Spain), ASGC (Taiwan), RAL (UK) and BNL (USA), the Tier-2 facilities worldwide and large non-WLCG resource providers. Major contributors of computing resources are listed in Ref. [133].

References

- [1] ATLAS Collaboration, Observation of a new particle in the search for the Standard Model Higgs boson with the ATLAS detector at the LHC, *Phys. Lett. B* 716 (2012) 1, arXiv:1207.7214 [hep-ex].
- [2] CMS Collaboration, Observation of a new boson at a mass of 125 GeV with the CMS experiment at the LHC, *Phys. Lett. B* 716 (2012) 30, arXiv:1207.7235 [hep-ex].
- [3] ATLAS Collaboration, Study of the spin and parity of the Higgs boson in di-boson decays with the ATLAS detector, *Eur. Phys. J. C* 75 (2015) 476, arXiv:1506.05669 [hep-ex], Erratum: *Eur. Phys. J. C* 76 (2016) 152.
- [4] ATLAS Collaboration, Test of CP invariance in vector-boson fusion production of the Higgs boson using the Optimal Observable method in the ditau decay channel with the ATLAS detector, *Eur. Phys. J. C* 76 (2016) 658, arXiv:1602.04516 [hep-ex].
- [5] ATLAS Collaboration, Observation of Higgs boson production in association with a top quark pair at the LHC with the ATLAS detector, *Phys. Lett. B* 784 (2018) 173, arXiv:1806.00425 [hep-ex].
- [6] ATLAS Collaboration, Observation of $H \rightarrow b\bar{b}$ decays and VH production with the ATLAS detector, *Phys. Lett. B* 786 (2018) 59, arXiv:1808.08238 [hep-ex].
- [7] ATLAS, CMS Collaborations, Measurements of the Higgs boson production and decay rates and constraints on its couplings from a combined ATLAS and CMS analysis of the LHC pp collision data at $\sqrt{s} = 7$ and 8 TeV, *J. High Energy Phys.* 08 (2016) 045, arXiv:1606.02266 [hep-ex].
- [8] CMS Collaboration, Observation of $t\bar{t}H$ production, *Phys. Rev. Lett.* 120 (2018) 231801, arXiv:1804.02610 [hep-ex].
- [9] CMS Collaboration, Observation of Higgs boson decay to bottom quarks, *Phys. Rev. Lett.* 121 (2018) 121801, arXiv:1808.08242 [hep-ex].
- [10] CMS Collaboration, Measurements of the Higgs boson width and anomalous HVV couplings from on-shell and off-shell production in the four-lepton final state, *Phys. Rev. D* 99 (2019) 112003, arXiv:1901.00174 [hep-ex].
- [11] CMS Collaboration, Constraints on anomalous HVV couplings from the production of Higgs bosons decaying to τ lepton pairs, arXiv:1903.06973 [hep-ex], 2019.
- [12] CMS Collaboration, Combined measurements of Higgs boson couplings in proton–proton collisions at $\sqrt{s} = 13$ TeV, *Eur. J. Phys. C* 79 (5) (2018) 421, arXiv:1809.10733 [hep-ex].
- [13] D. de Florian, et al., Handbook of LHC Higgs cross sections: 4. Deciphering the nature of the Higgs sector, arXiv:1610.07922 [hep-ph], 2016.
- [14] S. Dawson, S. Dittmaier, M. Spira, Neutral Higgs-boson pair production at hadron colliders: QCD corrections, *Phys. Rev. D* 58 (1998) 115012, arXiv:hep-ph/9805244 [hep-ph].
- [15] S. Borowka, et al., Higgs boson pair production in gluon fusion at next-to-leading order with full top-quark mass dependence, *Phys. Rev. Lett.* 117 (1) (2016) 012001, arXiv:1604.06447 [hep-ph].
- [16] J. Baglio, et al., Gluon fusion into Higgs pairs at NLO QCD and the top mass scheme, *Eur. Phys. J. C* 79 (2019) 459, arXiv:1811.05692 [hep-ph].
- [17] D. de Florian, J. Mazzitelli, Higgs boson pair production at next-to-next-to-leading order in QCD, *Phys. Rev. Lett.* 111 (2013) 201801, arXiv:1309.6594 [hep-ph].
- [18] D.Y. Shao, C.S. Li, H.T. Li, J. Wang, Threshold resummation effects in Higgs boson pair production at the LHC, *J. High Energy Phys.* 07 (2013) 169, arXiv:1301.1245 [hep-ph].
- [19] D. de Florian, J. Mazzitelli, Higgs pair production at next-to-next-to-leading logarithmic accuracy at the LHC, *J. High Energy Phys.* 09 (2015) 053, arXiv:1505.07122 [hep-ph].
- [20] M. Grazzini, et al., Higgs boson pair production at NNLO with top quark mass effects, *J. High Energy Phys.* 05 (2018) 059, arXiv:1803.02463 [hep-ph].
- [21] G.C. Branco, et al., Theory and phenomenology of two-Higgs-doublet models, *Phys. Rep.* 516 (2012) 1, arXiv:1106.0034 [hep-ph].
- [22] A. Azatov, R. Contino, G. Panico, M. Son, Effective field theory analysis of double Higgs boson production via gluon fusion, *Phys. Rev. D* 92 (2015) 035001, arXiv:1502.00539 [hep-ph].
- [23] P. Huang, A. Joglekar, M. Li, C.E.M. Wagner, Corrections to di-Higgs boson production with light stops and modified Higgs couplings, *Phys. Rev. D* 97 (2018) 075001, arXiv:1711.05743 [hep-ph].
- [24] ATLAS Collaboration, Search for Higgs boson pair production in the $\gamma\gamma b\bar{b}$ final state with 13 TeV pp collision data collected by the ATLAS experiment, *J. High Energy Phys.* 11 (2018) 040, arXiv:1807.04873 [hep-ex].
- [25] ATLAS Collaboration, Search for resonant and nonresonant Higgs boson pair production in the $b\bar{b}\tau^+\tau^-$ decay channel in pp collisions at $\sqrt{s} = 13$ TeV with the ATLAS detector, *Phys. Rev. Lett.* 121 (2018) 191801, arXiv:1808.00336 [hep-ex], Erratum: *Phys. Rev. Lett.* 122 (8) (2019) 089901.
- [26] ATLAS Collaboration, Search for Higgs boson pair production in the $\gamma\gamma WW^*$ channel using pp collision data recorded at $\sqrt{s} = 13$ TeV with the ATLAS detector, *Eur. Phys. J. C* 78 (2018) 1007, arXiv:1807.08567 [hep-ex].
- [27] ATLAS Collaboration, Search for Higgs boson pair production in the $WW^{(*)}WW^{(*)}$ decay channel using ATLAS data recorded at $\sqrt{s} = 13$ TeV, *J. High Energy Phys.* 05 (2019) 124, arXiv:1811.11028 [hep-ex].
- [28] ATLAS Collaboration, Search for Higgs boson pair production in the $b\bar{b}WW^*$ decay mode at $\sqrt{s} = 13$ TeV with the ATLAS detector, *J. High Energy Phys.* 04 (2019) 092, arXiv:1811.04671 [hep-ex].
- [29] ATLAS Collaboration, Search for pair production of Higgs bosons in the $b\bar{b}b\bar{b}$ final state using proton–proton collisions at $\sqrt{s} = 13$ TeV with the ATLAS detector, *J. High Energy Phys.* 01 (2019) 030, arXiv:1804.06174 [hep-ex].
- [30] CMS Collaboration, Search for Higgs boson pair production in events with two bottom quarks and two tau leptons in proton–proton collisions at $\sqrt{s} = 13$ TeV, *Phys. Lett. B* 778 (2018) 101, arXiv:1707.02909 [hep-ex].
- [31] CMS Collaboration, Search for resonant and nonresonant Higgs boson pair production in the $b\bar{b}\ell\nu\ell\nu$ final state in proton–proton collisions at $\sqrt{s} = 13$ TeV, *J. High Energy Phys.* 01 (2018) 054, arXiv:1708.04188 [hep-ex].
- [32] CMS Collaboration, Search for Higgs boson pair production in the $\gamma\gamma b\bar{b}$ final state in pp collisions at $\sqrt{s} = 13$ TeV, *Phys. Lett. B* 788 (2019) 7, arXiv:1806.00408 [hep-ex].
- [33] CMS Collaboration, Search for nonresonant Higgs boson pair production in the $b\bar{b}b\bar{b}$ final state at $\sqrt{s} = 13$ TeV, *J. High Energy Phys.* 04 (2019) 112, arXiv:1810.11854 [hep-ex].
- [34] ATLAS Collaboration, Combination of searches for Higgs boson pairs in pp collisions at $\sqrt{s} = 13$ TeV with the ATLAS detector, arXiv:1906.02025 [hep-ex], 2019.
- [35] CMS Collaboration, Combination of searches for Higgs boson pair production in proton–proton collisions at $\sqrt{s} = 13$ TeV, *Phys. Rev. Lett.* 122 (2019) 121803, arXiv:1811.09689 [hep-ex].
- [36] I. Goodfellow, Y. Bengio, A. Courville, Deep Learning, MIT Press, 2016, <http://www.deeplearningbook.org>.
- [37] ATLAS Collaboration, The ATLAS experiment at the CERN Large Hadron Collider, *J. Instrum.* 3 (2008) S08003.
- [38] ATLAS Collaboration, ATLAS Insertable B-Layer Technical Design Report, ATLAS-TDR-19, URL: <https://cds.cern.ch/record/1291633>, 2010, Addendum: ATLAS-TDR-19-ADD-1, URL: <https://cds.cern.ch/record/1451888>, 2012.

- [39] B. Abbott, et al., Production and integration of the ATLAS insertable B-layer, *J. Instrum.* **13** (2018) T05008, arXiv:1803.00844 [physics.ins-det].
- [40] ATLAS Collaboration, Performance of the ATLAS trigger system in 2015, *Eur. Phys. J. C* **77** (2017) 317, arXiv:1611.09661 [hep-ex].
- [41] ATLAS Collaboration, The ATLAS simulation infrastructure, *Eur. Phys. J. C* **70** (2010) 823, arXiv:1005.4568 [physics.ins-det].
- [42] S. Agostinelli, et al., GEANT4 - a simulation toolkit, *Nucl. Instrum. Methods A* **506** (2003) 250.
- [43] T. Sjöstrand, S. Mrenna, P.Z. Skands, A brief introduction to PYTHIA 8.1, *Comput. Phys. Commun.* **178** (2008) 852, arXiv:0710.3820 [hep-ph].
- [44] ATLAS Collaboration, The Pythia 8 A3 tune description of ATLAS minimum bias and inelastic measurements incorporating the Donnachie-Landshoff diffractive model, ATL-PHYS-PUB-2016-017, URL: <https://cds.cern.ch/record/2206965>, 2016.
- [45] R.D. Ball, et al., Parton distributions with LHC data, *Nucl. Phys. B* **867** (2013) 244, arXiv:1207.1303 [hep-ph].
- [46] R. Frederix, et al., Higgs pair production at the LHC with NLO and parton-shower effects, *Phys. Lett. B* **732** (2014) 142, arXiv:1401.7340 [hep-ph].
- [47] G. Degrandi, P.P. Giardino, R. Gröber, On the two-loop virtual QCD corrections to Higgs boson pair production in the Standard Model, *Eur. Phys. J. C* **76** (2016) 411, arXiv:1603.00385 [hep-ph].
- [48] P. Artoisenet, R. Frederix, O. Mattelaer, R. Rietkerk, Automatic spin-entangled decays of heavy resonances in Monte Carlo simulations, *J. High Energy Phys.* **03** (2013) 015, arXiv:1212.3460 [hep-ph].
- [49] D.J. Lange, The EvtGen particle decay simulation package, *Nucl. Instrum. Methods A* **462** (2001) 152.
- [50] ATLAS Collaboration, Probing the quantum interference between singly and doubly resonant top-quark production in pp collisions at $\sqrt{s} = 13$ TeV with the ATLAS detector, *Phys. Rev. Lett.* **121** (2018) 152002, arXiv:1806.04667 [hep-ex].
- [51] S. Frixione, E. Laenen, P. Motylinski, B.R. Webber, C.D. White, Single-top hadroproduction in association with a W boson, *J. High Energy Phys.* **07** (2008) 029, arXiv:0805.3067 [hep-ph].
- [52] ATLAS Collaboration, Improvements in $t\bar{t}$ modelling using NLO+PS Monte Carlo generators for Run 2, ATL-PHYS-PUB-2018-009, URL: <https://cds.cern.ch/record/2630327>, 2018.
- [53] J.M. Campbell, R.K. Ellis, P. Nason, E. Re, Top-pair production and decay at NLO matched with parton showers, *J. High Energy Phys.* **04** (2015) 114, arXiv:1412.1828 [hep-ph].
- [54] S. Alioli, P. Nason, C. Oleari, E. Re, A general framework for implementing NLO calculations in shower Monte Carlo programs: the POWHEG BOX, *J. High Energy Phys.* **06** (2010) 043, arXiv:1002.2581 [hep-ph].
- [55] S. Frixione, P. Nason, C. Oleari, Matching NLO QCD computations with parton shower simulations: the POWHEG method, *J. High Energy Phys.* **11** (2007) 070, arXiv:0709.2092 [hep-ph].
- [56] R.D. Ball, et al., Parton distributions for the LHC Run II, *J. High Energy Phys.* **04** (2015) 040, arXiv:1410.8849 [hep-ph].
- [57] T. Sjöstrand, et al., An introduction to PYTHIA 8.2, *Comput. Phys. Commun.* **191** (2015) 159, arXiv:1410.3012 [hep-ph].
- [58] ATLAS Collaboration, ATLAS Pythia 8 tunes to 7 TeV data, ATL-PHYS-PUB-2014-021, URL: <https://cds.cern.ch/record/1966419>, 2014.
- [59] M. Beneke, P. Falgari, S. Klein, C. Schwinn, Hadronic top-quark pair production with NNLL threshold resummation, *Nucl. Phys. B* **855** (2012) 695, arXiv:1109.1536 [hep-ph].
- [60] M. Cacciari, M. Czakon, M. Mangano, A. Mitov, P. Nason, Top-pair production at hadron colliders with next-to-next-to-leading logarithmic soft-gluon resummation, *Phys. Lett. B* **710** (2012) 612, arXiv:1111.5869 [hep-ph].
- [61] P. Bärnreuther, M. Czakon, A. Mitov, Percent level precision physics at the Tevatron: first genuine NNLO QCD corrections to $q\bar{q} \rightarrow t\bar{t} + X$, *Phys. Rev. Lett.* **109** (2012) 132001, arXiv:1204.5201 [hep-ph].
- [62] M. Czakon, A. Mitov, NNLO corrections to top-pair production at hadron colliders: the all-fermionic scattering channels, *J. High Energy Phys.* **12** (2012) 054, arXiv:1207.0236 [hep-ph].
- [63] M. Czakon, A. Mitov, NNLO corrections to top pair production at hadron colliders: the quark-gluon reaction, *J. High Energy Phys.* **01** (2013) 080, arXiv:1210.6832 [hep-ph].
- [64] M. Czakon, A. Mitov, Top++: a program for the calculation of the top-pair cross-section at hadron colliders, *Comput. Phys. Commun.* **185** (2014) 2930, arXiv:1112.5675 [hep-ph].
- [65] M. Czakon, P. Fiedler, A. Mitov, Total top-quark pair-production cross section at hadron colliders through $O(\alpha_s^3)$, *Phys. Rev. Lett.* **110** (2013) 252004, arXiv:1303.6254 [hep-ph].
- [66] S. Alioli, P. Nason, C. Oleari, E. Re, NLO single-top production matched with shower in POWHEG: s- and t-channel contributions, *J. High Energy Phys.* **2009** (2009) 111, arXiv:0907.4076 [hep-ph], Erratum: *J. High Energy Phys.* (2010) 11.
- [67] E. Re, Single-top Wt -channel production matched with parton showers using the POWHEG method, *Eur. Phys. J. C* **71** (2011) 1547, arXiv:1009.2450 [hep-ph].
- [68] N. Kidonakis, Two-loop soft anomalous dimensions for single top quark associated production with a W^- or H^- , *Phys. Rev. D* **82** (2010) 054018, arXiv:1005.4451 [hep-ph].
- [69] N. Kidonakis, Next-to-next-to-leading logarithm resummation for s-channel single top quark production, *Phys. Rev. D* **81** (2010) 054028, arXiv:1001.5034 [hep-ph].
- [70] N. Kidonakis, Next-to-next-to-leading-order collinear and soft gluon corrections for t-channel single top quark production, *Phys. Rev. D* **83** (2011) 091503, arXiv:1103.2792 [hep-ph].
- [71] ATLAS Collaboration, ATLAS simulation of boson plus jets processes in Run 2, ATL-PHYS-PUB-2017-006, URL: <https://cds.cern.ch/record/2261937>, 2017.
- [72] T. Gleisberg, et al., Event generation with SHERPA 1.1, *J. High Energy Phys.* **02** (2009) 007, arXiv:0811.4622 [hep-ph].
- [73] E. Bothmann, et al., Event generation with Sherpa 2.2, arXiv:1905.09127 [hep-ph], 2019.
- [74] S. Catani, L. Cieri, G. Ferrera, D. de Florian, M. Grazzini, Vector boson production at Hadron colliders: a fully exclusive QCD calculation at next-to-next-to-leading order, *Phys. Rev. Lett.* **103** (2009) 082001, arXiv:0903.2120 [hep-ph].
- [75] T. Gleisberg, S. Höche, Comix, a new matrix element generator, *J. High Energy Phys.* **12** (2008) 039, arXiv:0808.3674 [hep-ph].
- [76] F. Cascioli, P. Maierhöfer, S. Pozzorini, Scattering amplitudes with open loops, *Phys. Rev. Lett.* **108** (2012) 111601, arXiv:1111.5206 [hep-ph].
- [77] S. Schumann, F. Krauss, A Parton shower algorithm based on Catani-Seymour dipole factorisation, *J. High Energy Phys.* **03** (2008) 038, arXiv:0709.1027 [hep-ph].
- [78] S. Höche, F. Krauss, M. Schönherr, F. Siegert, QCD matrix elements + parton showers: the NLO case, *J. High Energy Phys.* **04** (2013) 027, arXiv:1207.5030 [hep-ph].
- [79] ATLAS Collaboration, Multi-boson simulation for 13 TeV ATLAS analyses, ATL-PHYS-PUB-2017-005, URL: <https://cds.cern.ch/record/2261933>, 2017.
- [80] ATLAS Collaboration, Modelling of the $t\bar{t}H$ and $t\bar{t}V$ ($V = W, Z$) processes for $\sqrt{s} = 13$ TeV ATLAS analyses, ATL-PHYS-PUB-2016-005, URL: <https://cds.cern.ch/record/2120826>, 2016.
- [81] J. Alwall, et al., The automated computation of tree-level and next-to-leading order differential cross sections, and their matching to parton shower simulations, *J. High Energy Phys.* **07** (2014) 079, arXiv:1405.0301 [hep-ph].
- [82] J.M. Campbell, R.K. Ellis, $t\bar{t}W^\pm$ production and decay at NLO, *J. High Energy Phys.* **07** (2012) 052, arXiv:1204.5678 [hep-ph].
- [83] M.V. Garzelli, A. Kardos, C.G. Papadopoulos, Z. Trocsanyi, $t\bar{t}W^\pm$ and $t\bar{t}Z$ hadroproduction at NLO accuracy in QCD with parton shower and hadronization effects, *J. High Energy Phys.* **11** (2012) 056, arXiv:1208.2665 [hep-ph].
- [84] S. Frixione, V. Hirschi, D. Pagani, H.-S. Shao, M. Zaro, Weak corrections to Higgs hadroproduction in association with a top-quark pair, *J. High Energy Phys.* **09** (2014) 065, arXiv:1407.0823 [hep-ph].
- [85] S. Frixione, V. Hirschi, D. Pagani, H.-S. Shao, M. Zaro, Electroweak and QCD corrections to top-pair hadroproduction in association with heavy bosons, *J. High Energy Phys.* **06** (2015) 184, arXiv:1504.03446 [hep-ph].
- [86] ATLAS Collaboration, Evaluation of theoretical uncertainties for simplified template cross section measurements of V-associated production of the Higgs boson, ATL-PHYS-PUB-2018-035, URL: <http://cds.cern.ch/record/2649241>, 2018.
- [87] M.L. Ciccolini, S. Dittmaier, M. Krämer, Electroweak radiative corrections to associated WH and ZH production at hadron colliders, *Phys. Rev. D* **68** (2003) 073003, arXiv:hep-ph/0306234 [hep-ph].
- [88] O. Brein, A. Djouadi, R. Harlander, NNLO QCD corrections to the Higgs-strahlung processes at hadron colliders, *Phys. Lett. B* **579** (2004) 149, arXiv:hep-ph/0307206 [hep-ph].
- [89] G. Ferrera, M. Grazzini, F. Tramontano, Associated Higgs-W-boson production at hadron colliders: a fully exclusive QCD calculation at NNLO, *Phys. Rev. Lett.* **107** (2011) 152003, arXiv:1107.1164 [hep-ph].
- [90] O. Brein, R. Harlander, M. Wiesemann, T. Zirke, Top-quark mediated effects in hadronic Higgs-Strahlung, *Eur. Phys. J. C* **72** (2012) 1868, arXiv:1111.0761 [hep-ph].
- [91] G. Ferrera, M. Grazzini, F. Tramontano, Higher-order QCD effects for associated WH production and decay at the LHC, *J. High Energy Phys.* **04** (2014) 039, arXiv:1312.1669 [hep-ph].
- [92] G. Ferrera, M. Grazzini, F. Tramontano, Associated ZH production at hadron colliders: the fully differential NNLO QCD calculation, *Phys. Lett. B* **740** (2015) 51, arXiv:1407.4747 [hep-ph].
- [93] J.M. Campbell, R.K. Ellis, C. Williams, Associated production of a Higgs boson at NNLO, *J. High Energy Phys.* **06** (2016) 179, arXiv:1601.00658 [hep-ph].
- [94] ATLAS Collaboration, Study of higher-order QCD corrections in the $gg \rightarrow H \rightarrow VV$ process, ATL-PHYS-PUB-2016-006, URL: <https://cds.cern.ch/record/2127515>, 2016.
- [95] K. Hamilton, P. Nason, E. Re, G. Zanderighi, NNLOPS simulation of Higgs boson production, *J. High Energy Phys.* **10** (2013) 222, arXiv:1309.0017 [hep-ph].
- [96] H.-L. Lai, et al., New parton distributions for collider physics, *Phys. Rev. D* **82** (7) (2010) 074024, arXiv:1007.2241 [hep-ph].

- [97] ATLAS Collaboration, Measurement of the Z/γ^* boson transverse momentum distribution in pp collisions at $\sqrt{s} = 7$ TeV with the ATLAS detector, *J. High Energy Phys.* 09 (2014) 145, arXiv:1406.3660 [hep-ex].
- [98] C. Anastasiou, et al., High precision determination of the gluon fusion Higgs boson cross-section at the LHC, *J. High Energy Phys.* 05 (2016) 058, arXiv:1602.00695 [hep-ph].
- [99] ATLAS Collaboration, Validation of signal Monte Carlo event generation in searches for Higgs boson pairs with the ATLAS, detector, ATL-PHYS-PUB-2019-007, URL: <https://cds.cern.ch/record/2665057>, 2019.
- [100] J. Bellm, et al., Herwig 7.0/Herwig++ 3.0 release note, *Eur. Phys. J. C* 76 (2016) 196, arXiv:1512.01178 [hep-ph].
- [101] L.A. Harland-Lang, A.D. Martin, P. Motylinski, R.S. Thorne, Parton distributions in the LHC era: MMHT 2014 PDFs, *Eur. Phys. J. C* 75 (2015) 204, arXiv:1412.3989 [hep-ph].
- [102] ATLAS Collaboration, Vertex reconstruction performance of the ATLAS detector at $\sqrt{s} = 13$ TeV, ATL-PHYS-PUB-2015-026, URL: <https://cds.cern.ch/record/2037717>, 2015.
- [103] ATLAS Collaboration, Selection of jets produced in 13 TeV proton–proton collisions with the ATLAS detector, ATLAS-CONF-2015-029, URL: <https://cds.cern.ch/record/2037702>, 2015.
- [104] ATLAS Collaboration, Electron and photon performance measurements with the ATLAS detector using the 2015–2017 LHC proton–proton collision data, arXiv:1908.00005 [hep-ex], 2019.
- [105] ATLAS Collaboration, Muon reconstruction performance of the ATLAS detector in proton–proton collision data at $\sqrt{s} = 13$ TeV, *Eur. Phys. J. C* 76 (2016) 292, arXiv:1603.05598 [hep-ex].
- [106] ATLAS Collaboration, Topological cell clustering in the ATLAS calorimeters and its performance in LHC Run 1, *Eur. Phys. J. C* 77 (2017) 490, arXiv:1603.02934 [hep-ex].
- [107] M. Cacciari, G.P. Salam, G. Soyez, The anti- k_r jet clustering algorithm, *J. High Energy Phys.* 04 (2008) 063, arXiv:0802.1189 [hep-ph].
- [108] M. Cacciari, G.P. Salam, G. Soyez, Fastjet user manual, *Eur. Phys. J. C* 72 (2012) 1896, arXiv:1111.6097 [hep-ph].
- [109] ATLAS Collaboration, Jet energy scale measurements and their systematic uncertainties in proton–proton collisions at $\sqrt{s} = 13$ TeV with the ATLAS detector, *Phys. Rev. D* 96 (2017) 072002, arXiv:1703.09665 [hep-ex].
- [110] ATLAS Collaboration, Performance of pile-up mitigation techniques for jets in pp collisions at $\sqrt{s} = 8$ TeV using the ATLAS detector, *Eur. Phys. J. C* 76 (2016) 581, arXiv:1510.03823 [hep-ex].
- [111] ATLAS Collaboration, ATLAS b -jet identification performance and efficiency measurement with $t\bar{t}$ events in pp collisions at $\sqrt{s} = 13$ TeV, arXiv:1907.05120 [hep-ex], 2019.
- [112] ATLAS Collaboration, Measurements of b -jet tagging efficiency with the ATLAS detector using $t\bar{t}$ events at $\sqrt{s} = 13$ TeV, *J. High Energy Phys.* 08 (2018) 089, arXiv:1805.01845 [hep-ex].
- [113] ATLAS Collaboration, Performance of missing transverse momentum reconstruction with the ATLAS detector using proton–proton collisions at $\sqrt{s} = 13$ TeV, *Eur. Phys. J. C* 78 (2018) 903, arXiv:1802.08168 [hep-ex].
- [114] F. Chollet, et al., Keras, <https://keras.io>, 2015.
- [115] M. Abadi, et al., TensorFlow: large-scale machine learning on heterogeneous systems, Software available from tensorflow.org, URL: <http://tensorflow.org/>, 2015.
- [116] D.H. Guest, et al., *lwtmn/lwtmn*: version 2.8.1, URL: <https://doi.org/10.5281/zenodo.2583131>, 2019.
- [117] V. Nair, G.E. Hinton, Rectified linear units improve restricted Boltzmann machines, in: Proceedings of the 27th International Conference on International Conference on Machine Learning, ICML'10, Omnipress, ISBN 978-1-60558-907-7, 2010, p. 807, URL: <http://dl.acm.org/citation.cfm?id=3104322.3104425>.
- [118] N. Srivastava, G. Hinton, A. Krizhevsky, I. Sutskever, R. Salakhutdinov, Dropout: a simple way to prevent neural networks from overfitting, *J. Mach. Learn. Res.* 15 (2014) 1929, URL: <http://jmlr.org/papers/v15/srivastava14a.html>.
- [119] CMS Collaboration, Measurement of the top quark mass in the dileptonic $t\bar{t}$ decay channel using the mass observables $M_{b\ell}$, M_{T2} , and $M_{b\ell\nu}$ in pp collisions at $\sqrt{s} = 8$ TeV, *Phys. Rev. D* 96 (2017) 032002, arXiv:1704.06142 [hep-ex].
- [120] A. Barr, C. Lester, P. Stephens, A variable for measuring masses at hadron colliders when missing energy is expected; $m(T2)$: the truth behind the glamour, *J. Phys. G* 29 (2003) 2343, arXiv:hep-ph/0304226 [hep-ph].
- [121] ATLAS Collaboration, Measurement of the $t\bar{t}$ production cross-section using $e\mu$ events with b -tagged jets in pp collisions at $\sqrt{s} = 13$ TeV with the ATLAS detector, *Phys. Lett. B* 761 (2016) 136, arXiv:1606.02699 [hep-ex].
- [122] ATLAS Collaboration, Simulation of top-quark production for the ATLAS experiment at $\sqrt{s} = 13$ TeV, ATL-PHYS-PUB-2016-004, URL: <https://cds.cern.ch/record/2120417>, 2016.
- [123] ATLAS, CMS Collaborations, Combination of ATLAS and CMS results on the mass of the top-quark using up to 4.9 fb^{-1} of $\sqrt{s} = 7$ TeV LHC data, ATLAS-CONF-2013-102, URL: <https://cds.cern.ch/record/1601811>, 2013.
- [124] J. Butterworth, et al., PDF4LHC recommendations for LHC Run II, *J. Phys. G* 43 (2016) 023001, arXiv:1510.03865 [hep-ph].
- [125] L. Lönnblad, S. Prestel, Merging multi-leg NLO matrix elements with parton showers, *J. High Energy Phys.* 03 (2013) 166, arXiv:1211.7278 [hep-ph].
- [126] ATLAS Collaboration, Jet calibration and systematic uncertainties for jets reconstructed in the ATLAS detector at $\sqrt{s} = 13$ TeV, ATL-PHYS-PUB-2015-015, URL: <https://cds.cern.ch/record/2037613>, 2015.
- [127] ATLAS Collaboration, Measurement of b -tagging efficiency of c -jets in $t\bar{t}$ events using a likelihood approach with the ATLAS detector, ATLAS-CONF-2018-001, URL: <https://cds.cern.ch/record/2306649>, 2018.
- [128] ATLAS Collaboration, Calibration of light-flavour b -jet mistagging rates using ATLAS proton–proton collision data at $\sqrt{s} = 13$ TeV, ATLAS-CONF-2018-006, URL: <https://cds.cern.ch/record/2314418>, 2018.
- [129] ATLAS Collaboration, Luminosity determination in pp collisions at $\sqrt{s} = 13$ TeV using the ATLAS detector at the LHC, ATLAS-CONF-2019-021, URL: <https://cds.cern.ch/record/2677054>, 2019.
- [130] G. Avoni, et al., The new LUCID-2 detector for luminosity measurement and monitoring in ATLAS, *J. Instrum.* 13 (2018) P07017.
- [131] G. Cowan, K. Cranmer, E. Gross, O. Vitells, Asymptotic formulae for likelihood-based tests of new physics, *Eur. Phys. J. C* 71 (2011) 1554, arXiv:1007.1727 [physics.data-an], Erratum: *Eur. Phys. J. C* 73 (2013) 2501.
- [132] A.L. Read, Presentation of search results: the CL_s technique, *J. Phys. G* 28 (2002) 2693.
- [133] ATLAS Collaboration, ATLAS computing acknowledgements, ATL-GEN-PUB-2016-002, URL: <https://cds.cern.ch/record/2202407>.

The ATLAS Collaboration

G. Aad¹⁰¹, B. Abbott¹²⁸, D.C. Abbott¹⁰², A. Abed Abud^{70a,70b}, K. Abeling⁵³, D.K. Abhayasinghe⁹³, S.H. Abidi¹⁶⁷, O.S. AbouZeid⁴⁰, N.L. Abraham¹⁵⁶, H. Abramowicz¹⁶¹, H. Abreu¹⁶⁰, Y. Abulaiti⁶, B.S. Acharya^{66a,66b,o}, B. Achkar⁵³, S. Adachi¹⁶³, L. Adam⁹⁹, C. Adam Bourdarios⁵, L. Adamczyk^{83a}, L. Adamek¹⁶⁷, J. Adelman¹²⁰, M. Adersberger¹¹³, A. Adiguzel^{12c}, S. Adorni⁵⁴, T. Adye¹⁴⁴, A.A. Affolder¹⁴⁶, Y. Afik¹⁶⁰, C. Agapopoulou¹³², M.N. Agaras³⁸, A. Aggarwal¹¹⁸, C. Agheorghiesei^{27c}, J.A. Aguilar-Saavedra^{140f,140a,ai}, F. Ahmadov⁷⁹, W.S. Ahmed¹⁰³, X. Ai¹⁸, G. Aielli^{73a,73b}, S. Akatsuka⁸⁵, T.P.A. Åkesson⁹⁶, E. Akilli⁵⁴, A.V. Akimov¹¹⁰, K. Al Khoury¹³², G.L. Alberghi^{23b,23a}, J. Albert¹⁷⁶, M.J. Alconada Verzini¹⁶¹, S. Alderweireldt³⁶, M. Aleksa³⁶, I.N. Aleksandrov⁷⁹, C. Alexa^{27b}, D. Alexandre¹⁹, T. Alexopoulos¹⁰, A. Alfonsi¹¹⁹, F. Alfonsi^{23b,23a}, M. Alhroob¹²⁸, B. Ali¹⁴², G. Alimonti^{68a}, J. Alison³⁷, S.P. Alkire¹⁴⁸, C. Allaire¹³², B.M.M. Allbrooke¹⁵⁶, B.W. Allen¹³¹, P.P. Allport²¹, A. Aloisio^{69a,69b}, A. Alonso⁴⁰, F. Alonso⁸⁸, C. Alpigiani¹⁴⁸, A.A. Alshehri⁵⁷, M. Alvarez Estevez⁹⁸, D. Álvarez Piqueras¹⁷⁴, M.G. Alvigi^{69a,69b}, Y. Amaral Coutinho^{80b}, A. Ambler¹⁰³, L. Ambroz¹³⁵, C. Amelung²⁶, D. Amidei¹⁰⁵, S.P. Amor Dos Santos^{140a}, S. Amoroso⁴⁶, C.S. Amrouche⁵⁴, F. An⁷⁸, C. Anastopoulos¹⁴⁹, N. Andari¹⁴⁵, T. Andeen¹¹, C.F. Anders^{61b}, J.K. Anders²⁰, A. Andreazza^{68a,68b}, V. Andrei^{61a}, C.R. Anelli¹⁷⁶, S. Angelidakis³⁸, A. Angerami³⁹, A.V. Anisenkov^{121b,121a}, A. Annovi^{71a}, C. Antel^{61a}, M.T. Anthony¹⁴⁹, M. Antonelli⁵¹, D.J.A. Antrim¹⁷¹,

F. Anulli ^{72a}, M. Aoki ⁸¹, J.A. Aparisi Pozo ¹⁷⁴, L. Aperio Bella ^{15a}, G. Arabidze ¹⁰⁶, J.P. Araque ^{140a}, V. Araujo Ferraz ^{80b}, R. Araujo Pereira ^{80b}, C. Arcangeletti ⁵¹, A.T.H. Arce ⁴⁹, F.A. Arduh ⁸⁸, J-F. Arguin ¹⁰⁹, S. Argyropoulos ⁷⁷, J.-H. Arling ⁴⁶, A.J. Armbruster ³⁶, A. Armstrong ¹⁷¹, O. Arnaez ¹⁶⁷, H. Arnold ¹¹⁹, Z.P. Arrubarrena Tame ¹¹³, A. Artamonov ^{123,*}, G. Artoni ¹³⁵, S. Artz ⁹⁹, S. Asai ¹⁶³, N. Asbah ⁵⁹, E.M. Asimakopoulou ¹⁷², L. Asquith ¹⁵⁶, J. Assahsah ^{35d}, K. Assamagan ²⁹, R. Astalos ^{28a}, R.J. Atkin ^{33a}, M. Atkinson ¹⁷³, N.B. Atlay ¹⁹, H. Atmani ¹³², K. Augsten ¹⁴², G. Avolio ³⁶, R. Avramidou ^{60a}, M.K. Ayoub ^{15a}, A.M. Azoulay ^{168b}, G. Azuelos ^{109,ax}, H. Bachacou ¹⁴⁵, K. Bachas ^{67a,67b}, M. Backes ¹³⁵, F. Backman ^{45a,45b}, P. Bagnaia ^{72a,72b}, M. Bahmani ⁸⁴, H. Bahrasemani ¹⁵², A.J. Bailey ¹⁷⁴, V.R. Bailey ¹⁷³, J.T. Baines ¹⁴⁴, M. Bajic ⁴⁰, C. Bakalis ¹⁰, O.K. Baker ¹⁸³, P.J. Bakker ¹¹⁹, D. Bakshi Gupta ⁸, S. Balaji ¹⁵⁷, E.M. Baldin ^{121b,121a}, P. Balek ¹⁸⁰, F. Balli ¹⁴⁵, W.K. Balunas ¹³⁵, J. Balz ⁹⁹, E. Banas ⁸⁴, A. Bandyopadhyay ²⁴, Sw. Banerjee ^{181,j}, A.A.E. Bannoura ¹⁸², L. Barak ¹⁶¹, W.M. Barbe ³⁸, E.L. Barberio ¹⁰⁴, D. Barberis ^{55b,55a}, M. Barbero ¹⁰¹, G. Barbour ⁹⁴, T. Barillari ¹¹⁴, M.-S. Barisits ³⁶, J. Barkeloo ¹³¹, T. Barklow ¹⁵³, R. Barnea ¹⁶⁰, S.L. Barnes ^{60c}, B.M. Barnett ¹⁴⁴, R.M. Barnett ¹⁸, Z. Barnovska-Blenessy ^{60a}, A. Baroncelli ^{60a}, G. Barone ²⁹, A.J. Barr ¹³⁵, L. Barranco Navarro ^{45a,45b}, F. Barreiro ⁹⁸, J. Barreiro Guimarães da Costa ^{15a}, S. Barsov ¹³⁸, R. Bartoldus ¹⁵³, G. Bartolini ¹⁰¹, A.E. Barton ⁸⁹, P. Bartos ^{28a}, A. Basalaeu ⁴⁶, A. Bassalat ^{132,aq}, M.J. Basso ¹⁶⁷, R.L. Bates ⁵⁷, S. Batlamous ^{35e}, J.R. Batley ³², B. Batool ¹⁵¹, M. Battaglia ¹⁴⁶, M. Baue ^{72a,72b}, F. Bauer ¹⁴⁵, K.T. Bauer ¹⁷¹, H.S. Bawa ^{31,m}, J.B. Beacham ⁴⁹, T. Beau ¹³⁶, P.H. Beauchemin ¹⁷⁰, F. Becherer ⁵², P. Bechtel ²⁴, H.C. Beck ⁵³, H.P. Beck ^{20,s}, K. Becker ⁵², M. Becker ⁹⁹, C. Becot ⁴⁶, A. Beddall ^{12d}, A.J. Beddall ^{12a}, V.A. Bednyakov ⁷⁹, M. Bedognetti ¹¹⁹, C.P. Bee ¹⁵⁵, T.A. Beermann ⁷⁶, M. Begalli ^{80b}, M. Begel ²⁹, A. Behera ¹⁵⁵, J.K. Behr ⁴⁶, F. Beisiegel ²⁴, A.S. Bell ⁹⁴, G. Bella ¹⁶¹, L. Bellagamba ^{23b}, A. Bellerive ³⁴, P. Bellos ⁹, K. Beloborodov ^{121b,121a}, K. Belotskiy ¹¹¹, N.L. Belyaev ¹¹¹, D. Benckroun ^{35a}, N. Benekos ¹⁰, Y. Benhammou ¹⁶¹, D.P. Benjamin ⁶, M. Benoit ⁵⁴, J.R. Bensinger ²⁶, S. Bentvelsen ¹¹⁹, L. Beresford ¹³⁵, M. Beretta ⁵¹, D. Berge ⁴⁶, E. Bergeaas Kuutmann ¹⁷², N. Berger ⁵, B. Bergmann ¹⁴², L.J. Bergsten ²⁶, J. Beringer ¹⁸, S. Berlendis ⁷, N.R. Bernard ¹⁰², G. Bernardi ¹³⁶, C. Bernius ¹⁵³, F.U. Bernlochner ²⁴, T. Berry ⁹³, P. Berta ⁹⁹, C. Bertella ^{15a}, I.A. Bertram ⁸⁹, O. Bessidskaia Bylund ¹⁸², N. Besson ¹⁴⁵, A. Bethani ¹⁰⁰, S. Bethke ¹¹⁴, A. Betti ²⁴, A.J. Bevan ⁹², J. Beyer ¹¹⁴, D.S. Bhattacharya ¹⁷⁷, P. Bhattarai ²⁶, R. Bi ¹³⁹, R.M. Bianchi ¹³⁹, O. Biebel ¹¹³, D. Biedermann ¹⁹, R. Bielski ³⁶, K. Bierwagen ⁹⁹, N.V. Biesuz ^{71a,71b}, M. Biglietti ^{74a}, T.R.V. Billoud ¹⁰⁹, M. Bindi ⁵³, A. Bingul ^{12d}, C. Bini ^{72a,72b}, S. Biondi ^{23b,23a}, M. Birman ¹⁸⁰, T. Bisanz ⁵³, J.P. Biswal ¹⁶¹, D. Biswas ^{181,j}, A. Bitadze ¹⁰⁰, C. Bittrich ⁴⁸, K. Bjørke ¹³⁴, K.M. Black ²⁵, T. Blazek ^{28a}, I. Bloch ⁴⁶, C. Blocker ²⁶, A. Blue ⁵⁷, U. Blumenschein ⁹², G.J. Bobbink ¹¹⁹, V.S. Bobrovnikov ^{121b,121a}, S.S. Bocchetta ⁹⁶, A. Bocci ⁴⁹, D. Boerner ⁴⁶, D. Bogavac ¹⁴, A.G. Bogdanchikov ^{121b,121a}, C. Boehm ^{45a}, V. Boisvert ⁹³, P. Bokač ^{53,172}, T. Bold ^{83a}, A.S. Boldyrev ¹¹², A.E. Bolz ^{61b}, M. Bomben ¹³⁶, M. Bona ⁹², J.S. Bonilla ¹³¹, M. Boonekamp ¹⁴⁵, C.D. Booth ⁹³, H.M. Borecka-Bielska ⁹⁰, A. Borisov ¹²², G. Borissov ⁸⁹, J. Bortfeldt ³⁶, D. Bortoletto ¹³⁵, D. Boscherini ^{23b}, M. Bosman ¹⁴, J.D. Bossio Sola ¹⁰³, K. Bouaouda ^{35a}, J. Boudreau ¹³⁹, E.V. Bouhova-Thacker ⁸⁹, D. Boumediene ³⁸, S.K. Boutle ⁵⁷, A. Boveia ¹²⁶, J. Boyd ³⁶, D. Boye ^{33b,ar}, I.R. Boyko ⁷⁹, A.J. Bozson ⁹³, J. Bracinik ²¹, N. Brahim ¹⁰¹, G. Brandt ¹⁸², O. Brandt ³², F. Braren ⁴⁶, B. Brau ¹⁰², J.E. Brau ¹³¹, W.D. Breaden Madden ⁵⁷, K. Brendlinger ⁴⁶, L. Brenner ⁴⁶, R. Brenner ¹⁷², S. Bressler ¹⁸⁰, B. Brickwedde ⁹⁹, D.L. Briglin ²¹, D. Britton ⁵⁷, D. Britzger ¹¹⁴, I. Brock ²⁴, R. Brock ¹⁰⁶, G. Brooijmans ³⁹, W.K. Brooks ^{147c}, E. Brost ¹²⁰, J.H. Broughton ²¹, P.A. Bruckman de Renstrom ⁸⁴, D. Bruncko ^{28b}, A. Bruni ^{23b}, G. Bruni ^{23b}, L.S. Bruni ¹¹⁹, S. Bruno ^{73a,73b}, B.H. Brunt ³², M. Bruschi ^{23b}, N. Bruscinò ¹³⁹, P. Bryant ³⁷, L. Bryngemark ⁹⁶, T. Buanes ¹⁷, Q. Buat ³⁶, P. Buchholz ¹⁵¹, A.G. Buckley ⁵⁷, I.A. Budagov ⁷⁹, M.K. Bugge ¹³⁴, F. Bühner ⁵², O. Bulekov ¹¹¹, T.J. Burch ¹²⁰, S. Burdin ⁹⁰, C.D. Burgard ¹¹⁹, A.M. Burger ¹²⁹, B. Burghgrave ⁸, J.T.P. Burr ⁴⁶, C.D. Burton ¹¹, J.C. Burzynski ¹⁰², V. Büscher ⁹⁹, E. Buschmann ⁵³, P.J. Bussey ⁵⁷, J.M. Butler ²⁵, C.M. Buttar ⁵⁷, J.M. Butterworth ⁹⁴, P. Butti ³⁶, W. Buttinger ³⁶, C.J. Buxo Vazquez ¹⁰⁶, A. Buzatu ¹⁵⁸, A.R. Buzykaev ^{121b,121a}, G. Cabras ^{23b,23a}, S. Cabrera Urbán ¹⁷⁴, D. Caforio ⁵⁶, H. Cai ¹⁷³, V.M.M. Cairo ¹⁵³, O. Cakir ^{4a}, N. Calace ³⁶, P. Calafiura ¹⁸, A. Calandri ¹⁰¹, G. Calderini ¹³⁶, P. Calfayan ⁶⁵, G. Callea ⁵⁷, L.P. Caloba ^{80b}, S. Calvente Lopez ⁹⁸, D. Calvet ³⁸, S. Calvet ³⁸, T.P. Calvet ¹⁵⁵, M. Calvetti ^{71a,71b}, R. Camacho Toro ¹³⁶, S. Camarda ³⁶, D. Camarero Muñoz ⁹⁸, P. Camarri ^{73a,73b}, D. Cameron ¹³⁴, R. Caminal Armadans ¹⁰², C. Camincher ³⁶, S. Campana ³⁶, M. Campanelli ⁹⁴, A. Camplani ⁴⁰, A. Campoverde ¹⁵¹, V. Canale ^{69a,69b}, A. Canesse ¹⁰³, M. Cano Bret ^{60c}, J. Cantero ¹²⁹, T. Cao ¹⁶¹, Y. Cao ¹⁷³, M.D.M. Capeans Garrido ³⁶, M. Capua ^{41b,41a}, R. Cardarelli ^{73a}, F. Cardillo ¹⁴⁹, G. Carducci ^{41b,41a},

I. Carli ¹⁴³, T. Carli ³⁶, G. Carlino ^{69a}, B.T. Carlson ¹³⁹, L. Carminati ^{68a,68b}, R.M.D. Carney ^{45a,45b}, S. Caron ¹¹⁸, E. Carquin ^{147c}, S. Carrá ⁴⁶, J.W.S. Carter ¹⁶⁷, M.P. Casado ^{14,e}, A.F. Casha ¹⁶⁷, D.W. Casper ¹⁷¹, R. Castelijin ¹¹⁹, F.L. Castillo ¹⁷⁴, V. Castillo Gimenez ¹⁷⁴, N.F. Castro ^{140a,140e}, A. Catinaccio ³⁶, J.R. Catmore ¹³⁴, A. Cattai ³⁶, J. Caudron ²⁴, V. Cavaliere ²⁹, E. Cavallaro ¹⁴, M. Cavalli-Sforza ¹⁴, V. Cavasinni ^{71a,71b}, E. Celebi ^{12b}, F. Ceradini ^{74a,74b}, L. Cerda Alberich ¹⁷⁴, K. Cerny ¹³⁰, A.S. Cerqueira ^{80a}, A. Cerri ¹⁵⁶, L. Cerrito ^{73a,73b}, F. Cerutti ¹⁸, A. Cervelli ^{23b,23a}, S.A. Cetin ^{12b}, Z. Chadi ^{35a}, D. Chakraborty ¹²⁰, S.K. Chan ⁵⁹, W.S. Chan ¹¹⁹, W.Y. Chan ⁹⁰, J.D. Chapman ³², B. Chargeishvili ^{159b}, D.G. Charlton ²¹, T.P. Charman ⁹², C.C. Chau ³⁴, S. Che ¹²⁶, S. Chekanov ⁶, S.V. Chekulaev ^{168a}, G.A. Chelkov ^{79,aw}, M.A. Chelstowska ³⁶, B. Chen ⁷⁸, C. Chen ^{60a}, C.H. Chen ⁷⁸, H. Chen ²⁹, J. Chen ^{60a}, J. Chen ³⁹, S. Chen ¹³⁷, S.J. Chen ^{15c}, X. Chen ^{15b,av}, Y. Chen ⁸², Y-H. Chen ⁴⁶, H.C. Cheng ^{63a}, H.J. Cheng ^{15a,15d}, A. Cheplakov ⁷⁹, E. Cheremushkina ¹²², R. Cherkaoui El Moursli ^{35e}, E. Cheu ⁷, K. Cheung ⁶⁴, T.J.A. Chevalérias ¹⁴⁵, L. Chevalier ¹⁴⁵, V. Chiarella ⁵¹, G. Chiarelli ^{71a}, G. Chiodini ^{67a}, A.S. Chisholm ²¹, A. Chitan ^{27b}, I. Chiu ¹⁶³, Y.H. Chiu ¹⁷⁶, M.V. Chizhov ⁷⁹, K. Choi ⁶⁵, A.R. Chomont ^{72a,72b}, S. Chouridou ¹⁶², Y.S. Chow ¹¹⁹, M.C. Chu ^{63a}, X. Chu ^{15a}, J. Chudoba ¹⁴¹, A.J. Chuinard ¹⁰³, J.J. Chwastowski ⁸⁴, L. Chytka ¹³⁰, D. Cieri ¹¹⁴, K.M. Ciesla ⁸⁴, D. Cinca ⁴⁷, V. Cindro ⁹¹, I.A. Cioară ^{27b}, A. Ciocio ¹⁸, F. Ciotto ^{69a,69b}, Z.H. Citron ^{180,k}, M. Citterio ^{68a}, D.A. Ciubotaru ^{27b}, B.M. Ciungu ¹⁶⁷, A. Clark ⁵⁴, M.R. Clark ³⁹, P.J. Clark ⁵⁰, C. Clement ^{45a,45b}, Y. Coadou ¹⁰¹, M. Cobal ^{66a,66c}, A. Coccaro ^{55b}, J. Cochran ⁷⁸, H. Cohen ¹⁶¹, A.E.C. Coimbra ³⁶, L. Colasurdo ¹¹⁸, B. Cole ³⁹, A.P. Colijn ¹¹⁹, J. Collot ⁵⁸, P. Conde Muiño ^{140a,f}, E. Coniavitis ⁵², S.H. Connell ^{33b}, I.A. Connelly ⁵⁷, S. Constantinescu ^{27b}, F. Conventi ^{69a,ay}, A.M. Cooper-Sarkar ¹³⁵, F. Cormier ¹⁷⁵, K.J.R. Cormier ¹⁶⁷, L.D. Corpe ⁹⁴, M. Corradi ^{72a,72b}, E.E. Corrigan ⁹⁶, F. Corriveau ^{103,ae}, A. Cortes-Gonzalez ³⁶, M.J. Costa ¹⁷⁴, F. Costanza ⁵, D. Costanzo ¹⁴⁹, G. Cowan ⁹³, J.W. Cowley ³², J. Crane ¹⁰⁰, K. Cranmer ¹²⁴, S.J. Crawley ⁵⁷, R.A. Creager ¹³⁷, S. Crépe-Renaudin ⁵⁸, F. Crescioli ¹³⁶, M. Cristinziani ²⁴, V. Croft ¹¹⁹, G. Crosetti ^{41b,41a}, A. Cueto ⁵, T. Cuhadar Donszelmann ¹⁴⁹, A.R. Cukierman ¹⁵³, W.R. Cunningham ⁵⁷, S. Czekierda ⁸⁴, P. Czodrowski ³⁶, M.J. Da Cunha Sargedas De Sousa ^{60b}, J.V. Da Fonseca Pinto ^{80b}, C. Da Via ¹⁰⁰, W. Dabrowski ^{83a}, T. Dado ^{28a}, S. Dahbi ^{35e}, T. Dai ¹⁰⁵, C. Dallapiccola ¹⁰², M. Dam ⁴⁰, G. D'amen ²⁹, V. D'Amico ^{74a,74b}, J. Damp ⁹⁹, J.R. Dandoy ¹³⁷, M.F. Daneri ³⁰, N.P. Dang ^{181,j}, N.S. Dann ¹⁰⁰, M. Danninger ¹⁷⁵, V. Dao ³⁶, G. Darbo ^{55b}, O. Dartsis ⁵, A. Dattagupta ¹³¹, T. Daubney ⁴⁶, S. D'Auria ^{68a,68b}, W. Davey ²⁴, C. David ⁴⁶, T. Davidek ¹⁴³, D.R. Davis ⁴⁹, I. Dawson ¹⁴⁹, K. De ⁸, R. De Asmundis ^{69a}, M. De Beurs ¹¹⁹, S. De Castro ^{23b,23a}, S. De Cecco ^{72a,72b}, N. De Groot ¹¹⁸, P. de Jong ¹¹⁹, H. De la Torre ¹⁰⁶, A. De Maria ^{15c}, D. De Pedis ^{72a}, A. De Salvo ^{72a}, U. De Sanctis ^{73a,73b}, M. De Santis ^{73a,73b}, A. De Santo ¹⁵⁶, K. De Vasconcelos Corga ¹⁰¹, J.B. De Vivie De Regie ¹³², C. Debenedetti ¹⁴⁶, D.V. Dedovich ⁷⁹, A.M. Deiana ⁴², M. Del Gaudio ^{41b,41a}, J. Del Peso ⁹⁸, Y. Delabat Diaz ⁴⁶, D. Delgove ¹³², F. Deliot ^{145,r}, C.M. Delitzsch ⁷, M. Della Pietra ^{69a,69b}, D. Della Volpe ⁵⁴, A. Dell'Acqua ³⁶, L. Dell'Asta ^{73a,73b}, M. Delmastro ⁵, C. Delporte ¹³², P.A. Delsart ⁵⁸, D.A. DeMarco ¹⁶⁷, S. Demers ¹⁸³, M. Demichev ⁷⁹, G. Demontigny ¹⁰⁹, S.P. Denisov ¹²², D. Denysiuk ¹¹⁹, L. D'Eramo ¹³⁶, D. Derendarz ⁸⁴, J.E. Derkaoui ^{35d}, F. Derue ¹³⁶, P. Dervan ⁹⁰, K. Desch ²⁴, C. Deterre ⁴⁶, K. Dette ¹⁶⁷, C. Deutsch ²⁴, M.R. Devesa ³⁰, P.O. Deviveiros ³⁶, A. Dewhurst ¹⁴⁴, F.A. Di Bello ⁵⁴, A. Di Ciaccio ^{73a,73b}, L. Di Ciaccio ⁵, W.K. Di Clemente ¹³⁷, C. Di Donato ^{69a,69b}, A. Di Girolamo ³⁶, G. Di Gregorio ^{71a,71b}, B. Di Micco ^{74a,74b}, R. Di Nardo ¹⁰², K.F. Di Petrillo ⁵⁹, R. Di Sipio ¹⁶⁷, D. Di Valentino ³⁴, C. Diaconu ¹⁰¹, F.A. Dias ⁴⁰, T. Dias Do Vale ^{140a}, M.A. Diaz ^{147a}, J. Dickinson ¹⁸, E.B. Diehl ¹⁰⁵, J. Dietrich ¹⁹, S. Díez Cornell ⁴⁶, A. Dimitrievska ¹⁸, W. Ding ^{15b}, J. Dingfelder ²⁴, F. Dittus ³⁶, F. Djama ¹⁰¹, T. Djobava ^{159b}, J.I. Djuvsland ¹⁷, M.A.B. Do Vale ^{80c}, M. Dobre ^{27b}, D. Dodsworth ²⁶, C. Doglioni ⁹⁶, J. Dolejsi ¹⁴³, Z. Dolezal ¹⁴³, M. Donadelli ^{80d}, B. Dong ^{60c}, J. Donini ³⁸, A. D'onofrio ⁹², M. D'Onofrio ⁹⁰, J. Dopke ¹⁴⁴, A. Doria ^{69a}, M.T. Dova ⁸⁸, A.T. Doyle ⁵⁷, E. Drechsler ¹⁵², E. Dreyer ¹⁵², T. Dreyer ⁵³, A.S. Drobac ¹⁷⁰, D. Du ^{60b}, Y. Duan ^{60b}, F. Dubinin ¹¹⁰, M. Dubovsky ^{28a}, A. Dubreuil ⁵⁴, E. Duchovni ¹⁸⁰, G. Duckeck ¹¹³, A. Ducourthial ¹³⁶, O.A. Ducu ¹⁰⁹, D. Duda ¹¹⁴, A. Dudarev ³⁶, A.C. Dudder ⁹⁹, E.M. Duffield ¹⁸, L. Duflost ¹³², M. Dührssen ³⁶, C. Dülsen ¹⁸², M. Dumancic ¹⁸⁰, A.E. Dumitriu ^{27b}, A.K. Duncan ⁵⁷, M. Dunford ^{61a}, A. Duperrin ¹⁰¹, H. Duran Yildiz ^{4a}, M. Düren ⁵⁶, A. Durglishvili ^{159b}, D. Duschinger ⁴⁸, B. Dutta ⁴⁶, D. Duvnjak ¹, G.I. Dyckes ¹³⁷, M. Dyndal ³⁶, S. Dysch ¹⁰⁰, B.S. Dziedzic ⁸⁴, K.M. Ecker ¹¹⁴, R.C. Edgar ¹⁰⁵, M.G. Eggleston ⁴⁹, T. Eifert ³⁶, G. Eigen ¹⁷, K. Einsweiler ¹⁸, T. Ekelof ¹⁷², H. El Jarrari ^{35e}, M. El Kacimi ^{35c}, R. El Kosseifi ¹⁰¹, V. Ellajosyula ¹⁷², M. Ellert ¹⁷², F. Ellinghaus ¹⁸², A.A. Elliot ⁹², N. Ellis ³⁶,

J. Elmsheuser²⁹, M. Elsing³⁶, D. Emeliyanov¹⁴⁴, A. Emerman³⁹, Y. Enari¹⁶³, M.B. Epland⁴⁹, J. Erdmann⁴⁷, A. Ereditato²⁰, M. Errenst³⁶, M. Escalier¹³², C. Escobar¹⁷⁴, O. Estrada Pastor¹⁷⁴, E. Etzion¹⁶¹, H. Evans⁶⁵, A. Ezhilov¹³⁸, F. Fabbri⁵⁷, L. Fabbri^{23b,23a}, V. Fabiani¹¹⁸, G. Facini⁹⁴, R.M. Faisca Rodrigues Pereira^{140a}, R.M. Fakhruddinov¹²², S. Falciano^{72a}, P.J. Falke⁵, S. Falke⁵, J. Faltova¹⁴³, Y. Fang^{15a}, Y. Fang^{15a}, G. Fanourakis⁴⁴, M. Fanti^{68a,68b}, M. Faraj^{66a,66c,u}, A. Farbin⁸, A. Farilla^{74a}, E.M. Farina^{70a,70b}, T. Farooque¹⁰⁶, S. Farrell¹⁸, S.M. Farrington⁵⁰, P. Farthouat³⁶, F. Fassi^{35e}, P. Fassnacht³⁶, D. Fassouliotis⁹, M. Fauci Giannelli⁵⁰, W.J. Fawcett³², L. Fayard¹³², O.L. Fedin^{138,p}, W. Fedorko¹⁷⁵, M. Feickert⁴², L. Feligioni¹⁰¹, A. Fell¹⁴⁹, C. Feng^{60b}, E.J. Feng³⁶, M. Feng⁴⁹, M.J. Fenton⁵⁷, A.B. Fenyuk¹²², J. Ferrando⁴⁶, A. Ferrante¹⁷³, A. Ferrari¹⁷², P. Ferrari¹¹⁹, R. Ferrari^{70a}, D.E. Ferreira de Lima^{61b}, A. Ferrer¹⁷⁴, D. Ferrere⁵⁴, C. Ferretti¹⁰⁵, F. Fiedler⁹⁹, A. Filipčič⁹¹, F. Filthaut¹¹⁸, K.D. Finelli²⁵, M.C.N. Fiolhais^{140a,140c,a}, L. Fiorini¹⁷⁴, F. Fischer¹¹³, W.C. Fisher¹⁰⁶, I. Fleck¹⁵¹, P. Fleischmann¹⁰⁵, R.R.M. Fletcher¹³⁷, T. Flick¹⁸², B.M. Flierl¹¹³, L. Flores¹³⁷, L.R. Flores Castillo^{63a}, F.M. Follega^{75a,75b}, N. Fomin¹⁷, J.H. Foo¹⁶⁷, G.T. Forcolin^{75a,75b}, A. Formica¹⁴⁵, F.A. Förster¹⁴, A.C. Forti¹⁰⁰, A.G. Foster²¹, M.G. Foti¹³⁵, D. Fournier¹³², H. Fox⁸⁹, P. Francavilla^{71a,71b}, S. Francescato^{72a,72b}, M. Franchini^{23b,23a}, S. Franchino^{61a}, D. Francis³⁶, L. Franconi²⁰, M. Franklin⁵⁹, A.N. Fray⁹², P.M. Freeman²¹, B. Freund¹⁰⁹, W.S. Freund^{80b}, E.M. Freundlich⁴⁷, D.C. Frizzell¹²⁸, D. Froidevaux³⁶, J.A. Frost¹³⁵, C. Fukunaga¹⁶⁴, E. Fullana Torregrosa¹⁷⁴, E. Fumagalli^{55b,55a}, T. Fusayasu¹¹⁵, J. Fuster¹⁷⁴, A. Gabrielli^{23b,23a}, A. Gabrielli¹⁸, G.P. Gach^{83a}, S. Gadatsch⁵⁴, P. Gadow¹¹⁴, G. Gagliardi^{55b,55a}, L.G. Gagnon¹⁰⁹, C. Galea^{27b}, B. Galhardo^{140a}, G.E. Gallardo¹³⁵, E.J. Gallas¹³⁵, B.J. Gallop¹⁴⁴, G. Galster⁴⁰, R. Gamboa Goni⁹², K.K. Gan¹²⁶, S. Ganguly¹⁸⁰, J. Gao^{60a}, Y. Gao⁵⁰, Y.S. Gao^{31,m}, C. García¹⁷⁴, J.E. García Navarro¹⁷⁴, J.A. García Pascual^{15a}, C. Garcia-Argos⁵², M. Garcia-Sciveres¹⁸, R.W. Gardner³⁷, N. Garelli¹⁵³, S. Gargiulo⁵², V. Garonne¹³⁴, A. Gaudiello^{55b,55a}, G. Gaudio^{70a}, I.L. Gavrilenko¹¹⁰, A. Gavrilyuk¹²³, C. Gay¹⁷⁵, G. Gaycken⁴⁶, E.N. Gazis¹⁰, A.A. Geanta^{27b}, C.M. Gee¹⁴⁶, C.N.P. Gee¹⁴⁴, J. Geisen⁵³, M. Geisen⁹⁹, M.P. Geisler^{61a}, C. Gemme^{55b}, M.H. Genest⁵⁸, C. Geng¹⁰⁵, S. Gentile^{72a,72b}, S. George⁹³, T. Gerialis⁴⁴, L.O. Gerlach⁵³, P. Gessinger-Befurt⁹⁹, G. Gessner⁴⁷, S. Ghasemi¹⁵¹, M. Ghasemi Bostanabad¹⁷⁶, A. Ghosh¹³², A. Ghosh⁷⁷, B. Giacobbe^{23b}, S. Giagu^{72a,72b}, N. Giangiacomi^{23b,23a}, P. Giannetti^{71a}, A. Giannini^{69a,69b}, G. Giannini¹⁴, S.M. Gibson⁹³, M. Gignac¹⁴⁶, D. Gillberg³⁴, G. Gilles¹⁸², D.M. Gingrich^{3,ax}, M.P. Giordani^{66a,66c}, F.M. Giorgi^{23b}, P.F. Giraud¹⁴⁵, G. Giugliarelli^{66a,66c}, D. Giugni^{68a}, F. Giuli^{73a,73b}, S. Gkaitatzis¹⁶², I. Gkialas^{9,h}, E.L. Gkougkousis¹⁴, P. Gkoutoumis¹⁰, L.K. Gladilin¹¹², C. Glasman⁹⁸, J. Glatzer¹⁴, P.C.F. Glaysher⁴⁶, A. Glazov⁴⁶, G.R. Gledhill¹³¹, M. Goblirsch-Kolb²⁶, D. Godin¹⁰⁹, S. Goldfarb¹⁰⁴, T. Golling⁵⁴, D. Golubkov¹²², A. Gomes^{140a,140b}, R. Goncalves Gama⁵³, R. Gonçalves^{140a,140b}, G. Gonella⁵², L. Gonella²¹, A. Gongadze⁷⁹, F. Gonnella²¹, J.L. Gonski⁵⁹, S. González de la Hoz¹⁷⁴, S. Gonzalez-Sevilla⁵⁴, G.R. Gonzalvo Rodriguez¹⁷⁴, L. Goossens³⁶, P.A. Gorbounov¹²³, H.A. Gordon²⁹, B. Gorini³⁶, E. Gorini^{67a,67b}, A. Gorišek⁹¹, A.T. Goshaw⁴⁹, M.I. Gostkin⁷⁹, C.A. Gottardo¹¹⁸, M. Gouighri^{35b}, D. Goujdami^{35c}, A.G. Goussiou¹⁴⁸, N. Govender^{33b}, C. Goy⁵, E. Gozani¹⁶⁰, I. Grabowska-Bold^{83a}, E.C. Graham⁹⁰, J. Gramling¹⁷¹, E. Gramstad¹³⁴, S. Grancagnolo¹⁹, M. Grandi¹⁵⁶, V. Gratchev¹³⁸, P.M. Gravila^{27f}, F.G. Gravili^{67a,67b}, C. Gray⁵⁷, H.M. Gray¹⁸, C. Grefe²⁴, K. Gregersen⁹⁶, I.M. Gregor⁴⁶, P. Grenier¹⁵³, K. Grevtsov⁴⁶, C. Grieco¹⁴, N.A. Grieser¹²⁸, J. Griffiths⁸, A.A. Grillo¹⁴⁶, K. Grimm^{31,l}, S. Grinstein^{14,z}, J.-F. Grivaz¹³², S. Groh⁹⁹, E. Gross¹⁸⁰, J. Grosse-Knetter⁵³, Z.J. Grout⁹⁴, C. Grud¹⁰⁵, A. Grummer¹¹⁷, L. Guan¹⁰⁵, W. Guan¹⁸¹, J. Guenther³⁶, A. Guerguichon¹³², J.G.R. Guerrero Rojas¹⁷⁴, F. Guescini¹¹⁴, D. Guest¹⁷¹, R. Gugel⁵², T. Guillemin⁵, S. Guindon³⁶, U. Gul⁵⁷, J. Guo^{60c}, W. Guo¹⁰⁵, Y. Guo^{60a,t}, Z. Guo¹⁰¹, R. Gupta⁴⁶, S. Gurbuz^{12c}, G. Gustavino¹²⁸, M. Guth⁵², P. Gutierrez¹²⁸, C. Gutschow⁹⁴, C. Guyot¹⁴⁵, C. Gwenlan¹³⁵, C.B. Gwilliam⁹⁰, A. Haas¹²⁴, C. Haber¹⁸, H.K. Hadavand⁸, N. Haddad^{35e}, A. Hadeef^{60a}, S. Hageböck³⁶, M. Haleem¹⁷⁷, J. Haley¹²⁹, G. Halladjian¹⁰⁶, G.D. Hallewell¹⁰¹, K. Hamacher¹⁸², P. Hamal¹³⁰, K. Hamano¹⁷⁶, H. Hamdaoui^{35e}, G.N. Hamity¹⁴⁹, K. Han^{60a,ak}, L. Han^{60a}, S. Han^{15a,15d}, Y.F. Han¹⁶⁷, K. Hanagaki^{81,x}, M. Hance¹⁴⁶, D.M. Handl¹¹³, B. Haney¹³⁷, R. Hankache¹³⁶, E. Hansen⁹⁶, J.B. Hansen⁴⁰, J.D. Hansen⁴⁰, M.C. Hansen²⁴, P.H. Hansen⁴⁰, E.C. Hanson¹⁰⁰, K. Hara¹⁶⁹, T. Harenberg¹⁸², S. Harkusha¹⁰⁷, P.F. Harrison¹⁷⁸, N.M. Hartmann¹¹³, Y. Hasegawa¹⁵⁰, A. Hasib⁵⁰, S. Hassani¹⁴⁵, S. Haug²⁰, R. Hauser¹⁰⁶, L.B. Havener³⁹, M. Havranek¹⁴², C.M. Hawkes²¹, R.J. Hawkings³⁶, D. Hayden¹⁰⁶, C. Hayes¹⁵⁵, R.L. Hayes¹⁷⁵, C.P. Hays¹³⁵, J.M. Hays⁹², H.S. Hayward⁹⁰, S.J. Haywood¹⁴⁴, F. He^{60a}, M.P. Heath⁵⁰, V. Hedberg⁹⁶, L. Heelan⁸, S. Heer²⁴,

K.K. Heidegger⁵², W.D. Heidorn⁷⁸, J. Heilman³⁴, S. Heim⁴⁶, T. Heim¹⁸, B. Heinemann^{46,as},
 J.J. Heinrich¹³¹, L. Heinrich³⁶, C. Heinz⁵⁶, J. Hejbal¹⁴¹, L. Helary^{61b}, A. Held¹⁷⁵, S. Helleund¹³⁴,
 C.M. Helling¹⁴⁶, S. Hellman^{45a,45b}, C. Helsens³⁶, R.C.W. Henderson⁸⁹, Y. Heng¹⁸¹, S. Henkelmann¹⁷⁵,
 A.M. Henriques Correia³⁶, G.H. Herbert¹⁹, H. Herde²⁶, V. Herget¹⁷⁷, Y. Hernández Jiménez^{33c},
 H. Herr⁹⁹, M.G. Herrmann¹¹³, T. Herrmann⁴⁸, G. Herten⁵², R. Hertenberger¹¹³, L. Hervas³⁶,
 T.C. Herwig¹³⁷, G.G. Hesketh⁹⁴, N.P. Hessey^{168a}, A. Higashida¹⁶³, S. Higashino⁸¹, E. Higón-Rodríguez¹⁷⁴,
 K. Hildebrand³⁷, E. Hill¹⁷⁶, J.C. Hill³², K.K. Hill²⁹, K.H. Hiller⁴⁶, S.J. Hillier²¹, M. Hils⁴⁸, I. Hinchliffe¹⁸,
 F. Hinterkeuser²⁴, M. Hirose¹³³, S. Hirose⁵², D. Hirschbuehl¹⁸², B. Hiti⁹¹, O. Hladik¹⁴¹, D.R. Hlaluku^{33c},
 X. Hoad⁵⁰, J. Hobbs¹⁵⁵, N. Hod¹⁸⁰, M.C. Hodgkinson¹⁴⁹, A. Hoecker³⁶, F. Hoenig¹¹³, D. Hohn⁵²,
 D. Hohov¹³², T.R. Holmes³⁷, M. Holzbock¹¹³, L.B.A.H. Hommels³², S. Honda¹⁶⁹, T.M. Hong¹³⁹,
 J.C. Honig⁵², A. Hönle¹¹⁴, B.H. Hooberman¹⁷³, W.H. Hopkins⁶, Y. Horii¹¹⁶, P. Horn⁴⁸, L.A. Horyn³⁷,
 S. Hou¹⁵⁸, A. Hoummada^{35a}, J. Howarth¹⁰⁰, J. Hoya⁸⁸, M. Hrabovsky¹³⁰, J. Hrdinka⁷⁶, I. Hristova¹⁹,
 J. Hrivnac¹³², A. Hrynevich¹⁰⁸, T. Hryn'ova⁵, P.J. Hsu⁶⁴, S.-C. Hsu¹⁴⁸, Q. Hu²⁹, S. Hu^{60c}, Y.F. Hu^{15a},
 D.P. Huang⁹⁴, Y. Huang^{60a}, Y. Huang^{15a}, Z. Hubacek¹⁴², F. Hubaut¹⁰¹, M. Huebner²⁴, F. Huegging²⁴,
 T.B. Huffman¹³⁵, M. Huhtinen³⁶, R.F.H. Hunter³⁴, P. Huo¹⁵⁵, A.M. Hupe³⁴, N. Huseynov^{79,ag},
 J. Huston¹⁰⁶, J. Huth⁵⁹, R. Hyneman¹⁰⁵, S. Hyrych^{28a}, G. Iacobucci⁵⁴, G. Iakovidis²⁹, I. Ibragimov¹⁵¹,
 L. Iconomidou-Fayard¹³², Z. Idrissi^{35e}, P. Iengo³⁶, R. Ignazzi⁴⁰, O. Igonkina^{119,ab,*}, R. Iguchi¹⁶³,
 T. Iizawa⁵⁴, Y. Ikegami⁸¹, M. Ikeno⁸¹, D. Iliadis¹⁶², N. Ilic^{118,167,ae}, F. Iltzsche⁴⁸, G. Introzzi^{70a,70b},
 M. Iodice^{74a}, K. Iordanidou^{168a}, V. Ippolito^{72a,72b}, M.F. Isacson¹⁷², M. Ishino¹⁶³, W. Islam¹²⁹,
 C. Issever¹³⁵, S. Istin¹⁶⁰, F. Ito¹⁶⁹, J.M. Iturbe Ponce^{63a}, R. Iuppa^{75a,75b}, A. Ivina¹⁸⁰, H. Iwasaki⁸¹,
 J.M. Izen⁴³, V. Izzo^{69a}, P. Jacka¹⁴¹, P. Jackson¹, R.M. Jacobs²⁴, B.P. Jaeger¹⁵², V. Jain², G. Jäkel¹⁸²,
 K.B. Jakobi⁹⁹, K. Jakobs⁵², S. Jakobsen⁷⁶, T. Jakoubek¹⁴¹, J. Jamieson⁵⁷, K.W. Janas^{83a}, R. Jansky⁵⁴,
 J. Janssen²⁴, M. Janus⁵³, P.A. Janus^{83a}, G. Jarlskog⁹⁶, N. Javadov^{79,ag}, T. Javůrek³⁶, M. Javurkova⁵²,
 F. Jeanneau¹⁴⁵, L. Jeanty¹³¹, J. Jejelava^{159a,ah}, A. Jelinskas¹⁷⁸, P. Jenni^{52,b}, J. Jeong⁴⁶, N. Jeong⁴⁶,
 S. Jézéquel⁵, H. Ji¹⁸¹, J. Jia¹⁵⁵, H. Jiang⁷⁸, Y. Jiang^{60a}, Z. Jiang^{153,q}, S. Jiggins⁵², F.A. Jimenez Morales³⁸,
 J. Jimenez Pena¹¹⁴, S. Jin^{15c}, A. Jinaru^{27b}, O. Jinnouchi¹⁶⁵, H. Jivan^{33c}, P. Johansson¹⁴⁹, K.A. Johns⁷,
 C.A. Johnson⁶⁵, K. Jon-And^{45a,45b}, R.W.L. Jones⁸⁹, S.D. Jones¹⁵⁶, S. Jones⁷, T.J. Jones⁹⁰, J. Jongmanns^{61a},
 P.M. Jorge^{140a}, J. Jovicevic³⁶, X. Ju¹⁸, J.J. Junggeburth¹¹⁴, A. Juste Rozas^{14,z}, A. Kaczmarska⁸⁴,
 M. Kado^{72a,72b}, H. Kagan¹²⁶, M. Kagan¹⁵³, C. Kahra⁹⁹, T. Kaji¹⁷⁹, E. Kajomovitz¹⁶⁰, C.W. Kalderon⁹⁶,
 A. Kaluza⁹⁹, A. Kamenshchikov¹²², M. Kaneda¹⁶³, L. Kanjir⁹¹, Y. Kano¹⁶³, V.A. Kantserov¹¹¹,
 J. Kanzaki⁸¹, L.S. Kaplan¹⁸¹, D. Kar^{33c}, K. Karava¹³⁵, M.J. Kareem^{168b}, S.N. Karpov⁷⁹, Z.M. Karpova⁷⁹,
 V. Kartvelishvili⁸⁹, A.N. Karyukhin¹²², L. Kashif¹⁸¹, R.D. Kass¹²⁶, A. Kastanas^{45a,45b}, C. Kato^{60d,60c},
 J. Katzy⁴⁶, K. Kawade¹⁵⁰, K. Kawagoe⁸⁷, T. Kawaguchi¹¹⁶, T. Kawamoto¹⁶³, G. Kawamura⁵³, E.F. Kay¹⁷⁶,
 V.F. Kazanin^{121b,121a}, R. Keeler¹⁷⁶, R. Kehoe⁴², J.S. Keller³⁴, E. Kellermann⁹⁶, D. Kelsey¹⁵⁶,
 J.J. Kempster²¹, J. Kendrick²¹, O. Kepka¹⁴¹, S. Kersten¹⁸², B.P. Kerševan⁹¹, S. Ketabchi Haghighat¹⁶⁷,
 M. Khader¹⁷³, F. Khalil-Zada¹³, M. Khandoga¹⁴⁵, A. Khanov¹²⁹, A.G. Kharlamov^{121b,121a},
 T. Kharlamova^{121b,121a}, E.E. Khoda¹⁷⁵, A. Khodinov¹⁶⁶, T.J. Khoo⁵⁴, E. Khramov⁷⁹, J. Khubua^{159b},
 S. Kido⁸², M. Kiehn⁵⁴, C.R. Kilby⁹³, Y.K. Kim³⁷, N. Kimura⁹⁴, O.M. Kind¹⁹, B.T. King^{90,*},
 D. Kirchmeier⁴⁸, J. Kirk¹⁴⁴, A.E. Kiryunin¹¹⁴, T. Kishimoto¹⁶³, D.P. Kisliuk¹⁶⁷, V. Kitali⁴⁶, O. Kivernyk⁵,
 T. Klapdor-Kleingrothaus⁵², M. Klassen^{61a}, M.H. Klein¹⁰⁵, M. Klein⁹⁰, U. Klein⁹⁰, K. Kleinknecht⁹⁹,
 P. Klimek¹²⁰, A. Klimentov²⁹, T. Klingl²⁴, T. Klioutchnikova³⁶, F.F. Klitzner¹¹³, P. Kluit¹¹⁹, S. Kluth¹¹⁴,
 E. Kneringer⁷⁶, E.B.F.G. Knoops¹⁰¹, A. Knue⁵², D. Kobayashi⁸⁷, T. Kobayashi¹⁶³, M. Kobel⁴⁸,
 M. Kocian¹⁵³, P. Kodys¹⁴³, P.T. Koenig²⁴, T. Koffas³⁴, N.M. Köhler³⁶, T. Koi¹⁵³, M. Kolb^{61b}, I. Koletsou⁵,
 T. Komarek¹³⁰, T. Kondo⁸¹, N. Kondrashova^{60c}, K. Köneke⁵², A.C. König¹¹⁸, T. Kono¹²⁵,
 R. Konoplich^{124,an}, V. Konstantinides⁹⁴, N. Konstantinidis⁹⁴, B. Konya⁹⁶, R. Kopeliansky⁶⁵,
 S. Koperny^{83a}, K. Korcyl⁸⁴, K. Kordas¹⁶², G. Koren¹⁶¹, A. Korn⁹⁴, I. Korolkov¹⁴, E.V. Korolkova¹⁴⁹,
 N. Korotkova¹¹², O. Kortner¹¹⁴, S. Kortner¹¹⁴, T. Kosek¹⁴³, V.V. Kostyukhin¹⁶⁶, A. Kotskechagia¹³²,
 A. Kotwal⁴⁹, A. Koulouris¹⁰, A. Kourkouveli-Charalampidi^{70a,70b}, C. Kourkouvelis⁹, E. Kourlitis¹⁴⁹,
 V. Kouskoura²⁹, A.B. Kowalewska⁸⁴, R. Kowalewski¹⁷⁶, C. Kozakai¹⁶³, W. Kozanecki¹⁴⁵, A.S. Kozhin¹²²,
 V.A. Kramarenko¹¹², G. Kramberger⁹¹, D. Krasnopevtsev^{60a}, M.W. Krasny¹³⁶, A. Krasznahorkay³⁶,
 D. Krauss¹¹⁴, J.A. Kremer^{83a}, J. Kretzschmar⁹⁰, P. Krieger¹⁶⁷, F. Krieter¹¹³, A. Krishnan^{61b}, K. Krizka¹⁸,
 K. Kroeninger⁴⁷, H. Kroha¹¹⁴, J. Kroll¹⁴¹, J. Kroll¹³⁷, K.S. Krowpman¹⁰⁶, J. Krstic¹⁶, U. Kruchonak⁷⁹,

H. Krüger²⁴, N. Krumnack⁷⁸, M.C. Kruse⁴⁹, J.A. Krzysiak⁸⁴, T. Kubota¹⁰⁴, O. Kuchinskaia¹⁶⁶, S. Kuday^{4b}, J.T. Kuechler⁴⁶, S. Kuehn³⁶, A. Kugel^{61a}, T. Kuhl⁴⁶, V. Kukhtin⁷⁹, R. Kukla¹⁰¹, Y. Kulchitsky^{107,aj}, S. Kuleshov^{147c}, Y.P. Kulinich¹⁷³, M. Kuna⁵⁸, T. Kunigo⁸⁵, A. Kupco¹⁴¹, T. Kupfer⁴⁷, O. Kuprash⁵², H. Kurashige⁸², L.L. Kurchaninov^{168a}, Y.A. Kurochkin¹⁰⁷, A. Kurova¹¹¹, M.G. Kurth^{15a,15d}, E.S. Kuwertz³⁶, M. Kuze¹⁶⁵, A.K. Kvam¹⁴⁸, J. Kvita¹³⁰, T. Kwan¹⁰³, A. La Rosa¹¹⁴, L. La Rotonda^{41b,41a}, F. La Ruffa^{41b,41a}, C. Lacasta¹⁷⁴, F. Lacava^{72a,72b}, D.P.J. Lack¹⁰⁰, H. Lacker¹⁹, D. Lacour¹³⁶, E. Ladygin⁷⁹, R. Lafaye⁵, B. Laforge¹³⁶, T. Lagouri^{33c}, S. Lai⁵³, S. Lammers⁶⁵, W. Lampl⁷, C. Lampoudis¹⁶², E. Lançon²⁹, U. Landgraf⁵², M.P.J. Landon⁹², M.C. Lanfermann⁵⁴, V.S. Lang⁴⁶, J.C. Lange⁵³, R.J. Langenberg³⁶, A.J. Lankford¹⁷¹, F. Lanni²⁹, K. Lantsch²⁴, A. Lanza^{70a}, A. Lapertosa^{55b,55a}, S. Laplace¹³⁶, J.F. Laporte¹⁴⁵, T. Lari^{68a}, F. Lasagni Manghi^{23b,23a}, M. Lassnig³⁶, T.S. Lau^{63a}, A. Laudrain¹³², A. Laurier³⁴, M. Lavorgna^{69a,69b}, S.D. Lawlor⁹³, M. Lazzaroni^{68a,68b}, B. Le¹⁰⁴, E. Le Guirriec¹⁰¹, M. LeBlanc⁷, T. LeCompte⁶, F. Ledroit-Guillon⁵⁸, A.C.A. Lee⁹⁴, C.A. Lee²⁹, G.R. Lee¹⁷, L. Lee⁵⁹, S.C. Lee¹⁵⁸, S.J. Lee³⁴, S. Lee⁷⁸, B. Lefebvre^{168a}, H.P. Lefebvre⁹³, M. Lefebvre¹⁷⁶, F. Legger¹¹³, C. Leggett¹⁸, K. Lehmann¹⁵², N. Lehmann¹⁸², G. Lehmann Miotto³⁶, W.A. Leight⁴⁶, A. Leisos^{162,y}, M.A.L. Leite^{80d}, C.E. Leitgeb¹¹³, R. Leitner¹⁴³, D. Lellouch^{180,*}, K.J.C. Leney⁴², T. Lenz²⁴, B. Lenzi³⁶, R. Leone⁷, S. Leone^{71a}, C. Leonidopoulos⁵⁰, A. Leopold¹³⁶, G. Lerner¹⁵⁶, C. Leroy¹⁰⁹, R. Les¹⁶⁷, C.G. Lester³², M. Levchenko¹³⁸, J. Levêque⁵, D. Levin¹⁰⁵, L.J. Levinson¹⁸⁰, D.J. Lewis²¹, B. Li^{15b}, B. Li¹⁰⁵, C-Q. Li^{60a}, F. Li^{60c}, H. Li^{60a}, H. Li^{60b}, J. Li^{60c}, K. Li¹⁵³, L. Li^{60c}, M. Li^{15a}, Q. Li^{15a,15d}, Q.Y. Li^{60a}, S. Li^{60d,60c}, X. Li⁴⁶, Y. Li⁴⁶, Z. Li^{60b}, Z. Liang^{15a}, B. Liberti^{73a}, A. Liblong¹⁶⁷, K. Lie^{63c}, C.Y. Lin³², K. Lin¹⁰⁶, T.H. Lin⁹⁹, R.A. Linck⁶⁵, J.H. Lindon²¹, A.L. Lioni⁵⁴, E. Lipeles¹³⁷, A. Lipniacka¹⁷, M. Lisovsky^{61b}, T.M. Liss^{173,au}, A. Lister¹⁷⁵, A.M. Litke¹⁴⁶, J.D. Little⁸, B. Liu⁷⁸, B.L. Liu⁶, H.B. Liu²⁹, H. Liu¹⁰⁵, J.B. Liu^{60a}, J.K.K. Liu¹³⁵, K. Liu¹³⁶, M. Liu^{60a}, P. Liu¹⁸, Y. Liu^{15a,15d}, Y.L. Liu¹⁰⁵, Y.W. Liu^{60a}, M. Livan^{70a,70b}, A. Lleres⁵⁸, J. Llorente Merino¹⁵², S.L. Lloyd⁹², C.Y. Lo^{63b}, F. Lo Sterzo⁴², E.M. Lobodzinska⁴⁶, P. Loch⁷, S. Loffredo^{73a,73b}, T. Lohse¹⁹, K. Lohwasser¹⁴⁹, M. Lokajicek¹⁴¹, J.D. Long¹⁷³, R.E. Long⁸⁹, L. Longo³⁶, K.A. Looper¹²⁶, J.A. Lopez^{147c}, I. Lopez Paz¹⁰⁰, A. Lopez Solis¹⁴⁹, J. Lorenz¹¹³, N. Lorenzo Martinez⁵, M. Losada²², P.J. Lösel¹¹³, A. Lösle⁵², X. Lou⁴⁶, X. Lou^{15a}, A. Lounis¹³², J. Love⁶, P.A. Love⁸⁹, J.J. Lozano Bahilo¹⁷⁴, M. Lu^{60a}, Y.J. Lu⁶⁴, H.J. Lubatti¹⁴⁸, C. Luci^{72a,72b}, A. Lucotte⁵⁸, C. Luedtke⁵², F. Luehring⁶⁵, I. Luise¹³⁶, L. Luminari^{72a}, B. Lund-Jensen¹⁵⁴, M.S. Lutz¹⁰², D. Lynn²⁹, R. Lysak¹⁴¹, E. Lytken⁹⁶, F. Lyu^{15a}, V. Lyubushkin⁷⁹, T. Lyubushkina⁷⁹, H. Ma²⁹, L.L. Ma^{60b}, Y. Ma^{60b}, G. Maccarrone⁵¹, A. Macchiolo¹¹⁴, C.M. Macdonald¹⁴⁹, J. Machado Miguens¹³⁷, D. Madaffari¹⁷⁴, R. Madar³⁸, W.F. Mader⁴⁸, N. Madysa⁴⁸, J. Maeda⁸², S. Maeland¹⁷, T. Maeno²⁹, M. Maerker⁴⁸, A.S. Maevskiy¹¹², V. Magerl⁵², N. Magini⁷⁸, D.J. Mahon³⁹, C. Maidantchik^{80b}, T. Maier¹¹³, A. Maio^{140a,140b,140d}, K. Maj^{83a}, O. Majersky^{28a}, S. Majewski¹³¹, Y. Makida⁸¹, N. Makovec¹³², B. Malaescu¹³⁶, Pa. Malecki⁸⁴, V.P. Maleev¹³⁸, F. Malek⁵⁸, U. Mallik⁷⁷, D. Malon⁶, C. Malone³², S. Maltezos¹⁰, S. Malyukov⁷⁹, J. Mamuzic¹⁷⁴, G. Mancini⁵¹, I. Mandić⁹¹, L. Manhaes de Andrade Filho^{80a}, I.M. Maniatis¹⁶², J. Manjarres Ramos⁴⁸, K.H. Mankinen⁹⁶, A. Mann¹¹³, A. Manousos⁷⁶, B. Mansoulie¹⁴⁵, I. Manthos¹⁶², S. Manzoni¹¹⁹, A. Marantis¹⁶², G. Marceca³⁰, L. Marchese¹³⁵, G. Marchiori¹³⁶, M. Marcisovsky¹⁴¹, L. Marcoccia^{73a,73b}, C. Marcon⁹⁶, C.A. Marin Tobon³⁶, M. Marjanovic¹²⁸, Z. Marshall¹⁸, M.U.F. Martensson¹⁷², S. Marti-Garcia¹⁷⁴, C.B. Martin¹²⁶, T.A. Martin¹⁷⁸, V.J. Martin⁵⁰, B. Martin dit Latour¹⁷, L. Martinelli^{74a,74b}, M. Martinez^{14,z}, V.I. Martinez Outschoorn¹⁰², S. Martin-Haugh¹⁴⁴, V.S. Martoiu^{27b}, A.C. Martyniuk⁹⁴, A. Marzin³⁶, S.R. Maschek¹¹⁴, L. Masetti⁹⁹, T. Mashimo¹⁶³, R. Mashinistov¹¹⁰, J. Masik¹⁰⁰, A.L. Maslennikov^{121b,121a}, L. Massa^{73a,73b}, P. Massarotti^{69a,69b}, P. Mastrandrea^{71a,71b}, A. Mastroberardino^{41b,41a}, T. Masubuchi¹⁶³, D. Matakias¹⁰, A. Matic¹¹³, P. Mättig²⁴, J. Maurer^{27b}, B. Maček⁹¹, D.A. Maximov^{121b,121a}, R. Mazini¹⁵⁸, I. Maznas¹⁶², S.M. Mazza¹⁴⁶, S.P. Mc Kee¹⁰⁵, T.G. McCarthy¹¹⁴, W.P. McCormack¹⁸, E.F. McDonald¹⁰⁴, J.A. McFayden³⁶, G. Mchedlidze^{159b}, M.A. McKay⁴², K.D. McLean¹⁷⁶, S.J. McMahon¹⁴⁴, P.C. McNamara¹⁰⁴, C.J. McNicol¹⁷⁸, R.A. McPherson^{176,ae}, J.E. Mdhuli^{33c}, Z.A. Meadows¹⁰², S. Meehan³⁶, T. Megy⁵², S. Mehlhase¹¹³, A. Mehta⁹⁰, T. Meideck⁵⁸, B. Meirose⁴³, D. Melini¹⁷⁴, B.R. Mellado Garcia^{33c}, J.D. Mellenthin⁵³, M. Melo^{28a}, F. Meloni⁴⁶, A. Melzer²⁴, S.B. Menary¹⁰⁰, E.D. Mendes Gouveia^{140a,140e}, L. Meng³⁶, X.T. Meng¹⁰⁵, S. Menke¹¹⁴, E. Meoni^{41b,41a}, S. Mergelmeyer¹⁹, S.A.M. Merkt¹³⁹, C. Merlassino²⁰, P. Mermod⁵⁴, L. Merola^{69a,69b}, C. Meroni^{68a}, O. Meshkov^{112,110}, J.K.R. Meshreki¹⁵¹, A. Messina^{72a,72b}, J. Metcalfe⁶, A.S. Mete¹⁷¹, C. Meyer⁶⁵, J. Meyer¹⁶⁰, J-P. Meyer¹⁴⁵,

H. Meyer Zu Theenhausen^{61a}, F. Miano¹⁵⁶, M. Michetti¹⁹, R.P. Middleton¹⁴⁴, L. Mijović⁵⁰, G. Mikenberg¹⁸⁰, M. Mikestikova¹⁴¹, M. Mikuž⁹¹, H. Mildner¹⁴⁹, M. Milesi¹⁰⁴, A. Milic¹⁶⁷, D.A. Millar⁹², D.W. Miller³⁷, A. Milov¹⁸⁰, D.A. Milstead^{45a,45b}, R.A. Mina^{153,q}, A.A. Minaenko¹²², M. Miñano Moya¹⁷⁴, I.A. Minashvili^{159b}, A.I. Mincer¹²⁴, B. Mindur^{83a}, M. Mineev⁷⁹, Y. Minegishi¹⁶³, L.M. Mir¹⁴, A. Mirto^{67a,67b}, K.P. Mistry¹³⁷, T. Mitani¹⁷⁹, J. Mitrevski¹¹³, V.A. Mitsou¹⁷⁴, M. Mittal^{60c}, O. Miu¹⁶⁷, A. Miucci²⁰, P.S. Miyagawa¹⁴⁹, A. Mizukami⁸¹, J.U. Mjörnmark⁹⁶, T. Mkrtchyan¹⁸⁴, M. Mlynarikova¹⁴³, T. Moa^{45a,45b}, K. Mochizuki¹⁰⁹, P. Mogg⁵², S. Mohapatra³⁹, R. Moles-Valls²⁴, M.C. Mondragon¹⁰⁶, K. Mönig⁴⁶, J. Monk⁴⁰, E. Monnier¹⁰¹, A. Montalbano¹⁵², J. Montejo Berlingen³⁶, M. Montella⁹⁴, F. Monticelli⁸⁸, S. Monzani^{68a}, N. Morange¹³², D. Moreno²², M. Moreno Llácer³⁶, C. Moreno Martinez¹⁴, P. Morettini^{55b}, M. Morgenstern¹¹⁹, S. Morgenstern⁴⁸, D. Mori¹⁵², M. Morii⁵⁹, M. Morinaga¹⁷⁹, V. Morisbak¹³⁴, A.K. Morley³⁶, G. Mornacchi³⁶, A.P. Morris⁹⁴, L. Morvaj¹⁵⁵, P. Moschovakos³⁶, B. Moser¹¹⁹, M. Mosidze^{159b}, T. Moskalets¹⁴⁵, H.J. Moss¹⁴⁹, J. Moss^{31,n}, E.J.W. Moyses¹⁰², S. Muanza¹⁰¹, J. Mueller¹³⁹, R.S.P. Mueller¹¹³, D. Muenstermann⁸⁹, G.A. Mullier⁹⁶, J.L. Munoz Martinez¹⁴, F.J. Munoz Sanchez¹⁰⁰, P. Murin^{28b}, W.J. Murray^{178,144}, A. Murrone^{68a,68b}, M. Muškinja¹⁸, C. Mwewa^{33a}, A.G. Myagkov^{122,ao}, J. Myers¹³¹, M. Myska¹⁴², B.P. Nachman¹⁸, O. Nackenhorst⁴⁷, A. Nag Nag⁴⁸, K. Nagai¹³⁵, K. Nagano⁸¹, Y. Nagasaka⁶², M. Nagel⁵², J.L. Nagle²⁹, E. Nagy¹⁰¹, A.M. Nairz³⁶, Y. Nakahama¹¹⁶, K. Nakamura⁸¹, T. Nakamura¹⁶³, I. Nakano¹²⁷, H. Nanjo¹³³, F. Napolitano^{61a}, R.F. Naranjo Garcia⁴⁶, R. Narayan⁴², I. Naryshkin¹³⁸, T. Naumann⁴⁶, G. Navarro²², P.Y. Nechaeva¹¹⁰, F. Nechansky⁴⁶, T.J. Neep²¹, A. Negri^{70a,70b}, M. Negrini^{23b}, C. Nellist⁵³, M.E. Nelson¹³⁵, S. Nemecek¹⁴¹, P. Nemethy¹²⁴, M. Nessi^{36,d}, M.S. Neubauer¹⁷³, M. Neumann¹⁸², P.R. Newman²¹, Y.S. Ng¹⁹, Y.W.Y. Ng¹⁷¹, B. Ngair^{35e}, H.D.N. Nguyen¹⁰¹, T. Nguyen Manh¹⁰⁹, E. Nibigira³⁸, R.B. Nickerson¹³⁵, R. Nicolaidou¹⁴⁵, D.S. Nielsen⁴⁰, J. Nielsen¹⁴⁶, N. Nikiforou¹¹, V. Nikolaenko^{122,ao}, I. Nikolic-Audit¹³⁶, K. Nikolopoulos²¹, P. Nilsson²⁹, H.R. Nindhito⁵⁴, Y. Ninomiya⁸¹, A. Nisati^{72a}, N. Nishu^{60c}, R. Nisius¹¹⁴, I. Nitsche⁴⁷, T. Nitta¹⁷⁹, T. Nobe¹⁶³, Y. Noguchi⁸⁵, I. Nomidis¹³⁶, M.A. Nomura²⁹, M. Nordberg³⁶, N. Norjoharuddeen¹³⁵, T. Novak⁹¹, O. Novgorodova⁴⁸, R. Novotny¹⁴², L. Nozka¹³⁰, K. Ntekas¹⁷¹, E. Nurse⁹⁴, F.G. Oakham^{34,ax}, H. Oberlack¹¹⁴, J. Ocariz¹³⁶, A. Ochi⁸², I. Ochoa³⁹, J.P. Ochoa-Ricoux^{147a}, K. O'Connor²⁶, S. Oda⁸⁷, S. Odaka⁸¹, S. Oerdek⁵³, A. Ogrodnik^{83a}, A. Oh¹⁰⁰, S.H. Oh⁴⁹, C.C. Ohm¹⁵⁴, H. Oide¹⁶⁵, M.L. Ojeda¹⁶⁷, H. Okawa¹⁶⁹, Y. Okazaki⁸⁵, Y. Okumura¹⁶³, T. Okuyama⁸¹, A. Olariu^{27b}, L.F. Oleiro Seabra^{140a}, S.A. Olivares Pino^{147a}, D. Oliveira Damazio²⁹, J.L. Oliver¹, M.J.R. Olsson¹⁷¹, A. Olszewski⁸⁴, J. Olszowska⁸⁴, D.C. O'Neil¹⁵², A.P. O'Neill¹³⁵, A. Onofre^{140a,140e}, P.U.E. Onyisi¹¹, H. Oppen¹³⁴, M.J. Oreglia³⁷, G.E. Orellana⁸⁸, D. Orestano^{74a,74b}, N. Orlando¹⁴, R.S. Orr¹⁶⁷, V. O'Shea⁵⁷, R. Ospanov^{60a}, G. Otero y Garzon³⁰, H. Otono⁸⁷, P.S. Ott^{61a}, M. Ouchrif^{35d}, J. Ouellette²⁹, F. Ould-Saada¹³⁴, A. Ouraou¹⁴⁵, Q. Ouyang^{15a}, M. Owen⁵⁷, R.E. Owen²¹, V.E. Ozcan^{12c}, N. Ozturk⁸, J. Pacalt¹³⁰, H.A. Pacey³², K. Pachal⁴⁹, A. Pacheco Pages¹⁴, C. Padilla Aranda¹⁴, S. Pagan Griso¹⁸, M. Paganini¹⁸³, G. Palacino⁶⁵, S. Palazzo⁵⁰, S. Palestini³⁶, M. Palka^{83b}, D. Pallin³⁸, I. Panagoulas¹⁰, C.E. Pandini³⁶, J.G. Panduro Vazquez⁹³, P. Pani⁴⁶, G. Panizzo^{66a,66c}, L. Paolozzi⁵⁴, C. Papadatos¹⁰⁹, K. Papageorgiou^{9,h}, S. Parajuli⁴³, A. Paramonov⁶, D. Paredes Hernandez^{63b}, S.R. Paredes Saenz¹³⁵, B. Parida¹⁶⁶, T.H. Park¹⁶⁷, A.J. Parker³¹, M.A. Parker³², F. Parodi^{55b,55a}, E.W. Parrish¹²⁰, J.A. Parsons³⁹, U. Parzefall⁵², L. Pascual Dominguez¹³⁶, V.R. Pascuzzi¹⁶⁷, J.M.P. Pasner¹⁴⁶, F. Pasquali¹¹⁹, E. Pasqualucci^{72a}, S. Passaggio^{55b}, F. Pastore⁹³, P. Pasuwan^{45a,45b}, S. Patariaia⁹⁹, J.R. Pater¹⁰⁰, A. Pathak^{181,j}, T. Pauly³⁶, B. Pearson¹¹⁴, M. Pedersen¹³⁴, L. Pedraza Diaz¹¹⁸, R. Pedro^{140a}, T. Peiffer⁵³, S.V. Peleganchuk^{121b,121a}, O. Penc¹⁴¹, H. Peng^{60a}, B.S. Peralva^{80a}, M.M. Perego¹³², A.P. Pereira Peixoto^{140a}, D.V. Perepelitsa²⁹, F. Peri¹⁹, L. Perini^{68a,68b}, H. Pernegger³⁶, S. Perrella^{69a,69b}, K. Peters⁴⁶, R.F.Y. Peters¹⁰⁰, B.A. Petersen³⁶, T.C. Petersen⁴⁰, E. Petit¹⁰¹, A. Petridis¹, C. Petridou¹⁶², P. Petroff¹³², M. Petrov¹³⁵, F. Petrucci^{74a,74b}, M. Pettee¹⁸³, N.E. Pettersson¹⁰², K. Petukhova¹⁴³, A. Peyaud¹⁴⁵, R. Pezoa^{147c}, L. Pezzotti^{70a,70b}, T. Pham¹⁰⁴, F.H. Phillips¹⁰⁶, P.W. Phillips¹⁴⁴, M.W. Phipps¹⁷³, G. Piacquadio¹⁵⁵, E. Pianori¹⁸, A. Picazio¹⁰², R.H. Pickles¹⁰⁰, R. Piegaia³⁰, D. Pietreanu^{27b}, J.E. Pilcher³⁷, A.D. Pilkington¹⁰⁰, M. Pinamonti^{73a,73b}, J.L. Pinfold³, M. Pitt¹⁶¹, L. Pizzimento^{73a,73b}, M.-A. Pleier²⁹, V. Pleskot¹⁴³, E. Plotnikova⁷⁹, P. Podberezko^{121b,121a}, R. Poettgen⁹⁶, R. Poggi⁵⁴, L. Poggioli¹³², I. Pogrebnyak¹⁰⁶, D. Pohl²⁴, I. Pokharel⁵³, G. Polesello^{70a}, A. Poley¹⁸, A. Policicchio^{72a,72b}, R. Polifka¹⁴³, A. Polini^{23b}, C.S. Pollard⁴⁶, V. Polychronakos²⁹, D. Ponomarenko¹¹¹, L. Pontecorvo³⁶, S. Popa^{27a}, G.A. Popeneciu^{27d}, L. Portales⁵,

D.M. Portillo Quintero⁵⁸, S. Pospisil¹⁴², K. Potamianos⁴⁶, I.N. Potrap⁷⁹, C.J. Potter³², H. Potti¹¹,
 T. Poulsen⁹⁶, J. Poveda³⁶, T.D. Powell¹⁴⁹, G. Pownall⁴⁶, M.E. Pozo Astigarraga³⁶, P. Pralavorio¹⁰¹,
 S. Prell⁷⁸, D. Price¹⁰⁰, M. Primavera^{67a}, S. Prince¹⁰³, M.L. Proffitt¹⁴⁸, N. Proklova¹¹¹, K. Prokofiev^{63c},
 F. Prokoshin⁷⁹, S. Protopopescu²⁹, J. Proudfoot⁶, M. Przybycien^{83a}, D. Pudzha¹³⁸, A. Puri¹⁷³, P. Puzo¹³²,
 J. Qian¹⁰⁵, Y. Qin¹⁰⁰, A. Quadt⁵³, M. Queitsch-Maitland⁴⁶, A. Qureshi¹, M. Racko^{28a}, P. Rados¹⁰⁴,
 F. Ragusa^{68a,68b}, G. Rahal⁹⁷, J.A. Raine⁵⁴, S. Rajagopalan²⁹, A. Ramirez Morales⁹², K. Ran^{15a,15d},
 T. Rashid¹³², S. Raspopov⁵, D.M. Rauch⁴⁶, F. Rauscher¹¹³, S. Rave⁹⁹, B. Ravina¹⁴⁹, I. Ravinovitch¹⁸⁰,
 J.H. Rawling¹⁰⁰, M. Raymond³⁶, A.L. Read¹³⁴, N.P. Readioff⁵⁸, M. Reale^{67a,67b}, D.M. Rebuffi^{70a,70b},
 A. Redelbach¹⁷⁷, G. Redlinger²⁹, K. Reeves⁴³, L. Rehnisch¹⁹, J. Reichert¹³⁷, D. Reikher¹⁶¹, A. Reiss⁹⁹,
 A. Rej¹⁵¹, C. Rembser³⁶, M. Renda^{27b}, M. Rescigno^{72a}, S. Resconi^{68a}, E.D. Resseguie¹³⁷, S. Rettie¹⁷⁵,
 E. Reynolds²¹, O.L. Rezanova^{121b,121a}, P. Reznicek¹⁴³, E. Ricci^{75a,75b}, R. Richter¹¹⁴, S. Richter⁴⁶,
 E. Richter-Was^{83b}, O. Ricken²⁴, M. Ridel¹³⁶, P. Rieck¹¹⁴, C.J. Riegel¹⁸², O. Rifki⁴⁶, M. Rijssenbeek¹⁵⁵,
 A. Rimoldi^{70a,70b}, M. Rimoldi⁴⁶, L. Rinaldi^{23b}, G. Ripellino¹⁵⁴, I. Riu¹⁴, J.C. Rivera Vergara¹⁷⁶,
 F. Rizatdinova¹²⁹, E. Rizvi⁹², C. Rizzi³⁶, R.T. Roberts¹⁰⁰, S.H. Robertson^{103,ae}, M. Robin⁴⁶, D. Robinson³²,
 J.E.M. Robinson⁴⁶, C.M. Robles Gajardo^{147c}, A. Robson⁵⁷, A. Rocchi^{73a,73b}, E. Rocco⁹⁹, C. Roda^{71a,71b},
 S. Rodriguez Bosca¹⁷⁴, A. Rodriguez Perez¹⁴, D. Rodriguez Rodriguez¹⁷⁴, A.M. Rodríguez Vera^{168b},
 S. Roe³⁶, O. Røhne¹³⁴, R. Röhrig¹¹⁴, R.A. Rojas^{147c}, C.P.A. Roland⁶⁵, J. Roloff⁵⁹, A. Romaniouk¹¹¹,
 M. Romano^{23b,23a}, N. Rompotis⁹⁰, M. Ronzani¹²⁴, L. Roos¹³⁶, S. Rosati^{72a}, K. Rosbach⁵², G. Rosin¹⁰²,
 B.J. Rosser¹³⁷, E. Rossi⁴⁶, E. Rossi^{74a,74b}, E. Rossi^{69a,69b}, L.P. Rossi^{55b}, L. Rossini^{68a,68b}, R. Rosten¹⁴,
 M. Rotaru^{27b}, J. Rothberg¹⁴⁸, D. Rousseau¹³², G. Rovelli^{70a,70b}, A. Roy¹¹, D. Roy^{33c}, A. Rozanov¹⁰¹,
 Y. Rozen¹⁶⁰, X. Ruan^{33c}, F. Rubbo¹⁵³, F. Rühr⁵², A. Ruiz-Martinez¹⁷⁴, A. Rummeler³⁶, Z. Rurikova⁵²,
 N.A. Rusakovich⁷⁹, H.L. Russell¹⁰³, L. Rustige^{38,47}, J.P. Rutherford⁷, E.M. Rüttinger¹⁴⁹, M. Rybar³⁹,
 G. Rybkin¹³², E.B. Rye¹³⁴, A. Ryzhov¹²², P. Sabatini⁵³, G. Sabato¹¹⁹, S. Sacerdoti¹³²,
 H.F-W. Sadrozinski¹⁴⁶, R. Sadykov⁷⁹, F. Safai Tehrani^{72a}, B. Safarzadeh Samani¹⁵⁶, P. Saha¹²⁰, S. Saha¹⁰³,
 M. Sahinsoy^{61a}, A. Sahu¹⁸², M. Saimpert⁴⁶, M. Saito¹⁶³, T. Saito¹⁶³, H. Sakamoto¹⁶³, A. Sakharov^{124,an},
 D. Salamani⁵⁴, G. Salamanna^{74a,74b}, J.E. Salazar Loyola^{147c}, P.H. Sales De Bruin¹⁷², A. Salnikov¹⁵³,
 J. Salt¹⁷⁴, D. Salvatore^{41b,41a}, F. Salvatore¹⁵⁶, A. Salvucci^{63a,63b,63c}, A. Salzburger³⁶, J. Samarati³⁶,
 D. Sammel⁵², D. Sampsonidis¹⁶², D. Sampsonidou¹⁶², J. Sánchez¹⁷⁴, A. Sanchez Pineda^{66a,66c},
 H. Sandaker¹³⁴, C.O. Sander⁴⁶, I.G. Sanderswood⁸⁹, M. Sandhoff¹⁸², C. Sandoval²², D.P.C. Sankey¹⁴⁴,
 M. Sannino^{55b,55a}, Y. Sano¹¹⁶, A. Sansoni⁵¹, C. Santoni³⁸, H. Santos^{140a,140b}, S.N. Santpur¹⁸,
 A. Santra¹⁷⁴, A. Saponov⁷⁹, J.G. Saraiva^{140a,140d}, O. Sasaki⁸¹, K. Sato¹⁶⁹, F. Sauerburger⁵², E. Sauvan⁵,
 P. Savard^{167,ax}, N. Savic¹¹⁴, R. Sawada¹⁶³, C. Sawyer¹⁴⁴, L. Sawyer^{95,al}, C. Sbarra^{23b}, A. Sbrizzi^{23a},
 T. Scanlon⁹⁴, J. Schaarschmidt¹⁴⁸, P. Schacht¹¹⁴, B.M. Schachtner¹¹³, D. Schaefer³⁷, L. Schaefer¹³⁷,
 J. Schaeffer⁹⁹, S. Schaepe³⁶, U. Schäfer⁹⁹, A.C. Schaffer¹³², D. Schaile¹¹³, R.D. Schamberger¹⁵⁵,
 N. Scharmberg¹⁰⁰, V.A. Schegelsky¹³⁸, D. Scheirich¹⁴³, F. Schenck¹⁹, M. Schernau¹⁷¹, C. Schiavi^{55b,55a},
 S. Schier¹⁴⁶, L.K. Schildgen²⁴, Z.M. Schillaci²⁶, E.J. Schioppa³⁶, M. Schioppa^{41b,41a}, K.E. Schleicher⁵²,
 S. Schlenker³⁶, K.R. Schmidt-Sommerfeld¹¹⁴, K. Schmieden³⁶, C. Schmitt⁹⁹, S. Schmitt⁴⁶, S. Schmitz⁹⁹,
 J.C. Schmoeckel⁴⁶, U. Schnoor⁵², L. Schoeffel¹⁴⁵, A. Schoening^{61b}, P.G. Scholer⁵², E. Schopf¹³⁵,
 M. Schott⁹⁹, J.F.P. Schouwenberg¹¹⁸, J. Schovancova³⁶, S. Schramm⁵⁴, F. Schroeder¹⁸², A. Schulte⁹⁹,
 H-C. Schultz-Coulon^{61a}, M. Schumacher⁵², B.A. Schumm¹⁴⁶, Ph. Schune¹⁴⁵, A. Schwartzman¹⁵³,
 T.A. Schwarz¹⁰⁵, Ph. Schwemling¹⁴⁵, R. Schwienhorst¹⁰⁶, A. Sciandra¹⁴⁶, G. Sciolla²⁶, M. Scodreggio⁴⁶,
 M. Scornajenghi^{41b,41a}, F. Scuri^{71a}, F. Scutti¹⁰⁴, L.M. Scyboz¹¹⁴, C.D. Sebastiani^{72a,72b}, P. Seema¹⁹,
 S.C. Seidel¹¹⁷, A. Seiden¹⁴⁶, B.D. Seidlitz²⁹, T. Seiss³⁷, J.M. Seixas^{80b}, G. Sekhniaidze^{69a}, K. Sekhon¹⁰⁵,
 S.J. Sekula⁴², N. Semprini-Cesari^{23b,23a}, S. Sen⁴⁹, S. Senkin³⁸, C. Serfon⁷⁶, L. Serin¹³², L. Serkin^{66a,66b},
 M. Sessa^{60a}, H. Severini¹²⁸, T. Šfiligoj⁹¹, F. Sforza^{55b,55a}, A. Sfyrla⁵⁴, E. Shabalina⁵³, J.D. Shahinian¹⁴⁶,
 N.W. Shaikh^{45a,45b}, D. Shaked Renous¹⁸⁰, L.Y. Shan^{15a}, R. Shang¹⁷³, J.T. Shank²⁵, M. Shapiro¹⁸,
 A. Sharma¹³⁵, A.S. Sharma¹, P.B. Shatalov¹²³, K. Shaw¹⁵⁶, S.M. Shaw¹⁰⁰, A. Shcherbakova¹³⁸,
 M. Shehade¹⁸⁰, Y. Shen¹²⁸, N. Sherafati³⁴, A.D. Sherman²⁵, P. Sherwood⁹⁴, L. Shi^{158,at}, S. Shimizu⁸¹,
 C.O. Shimmin¹⁸³, Y. Shimogama¹⁷⁹, M. Shimojima¹¹⁵, I.P.J. Shipsey¹³⁵, S. Shirabe⁸⁷, M. Shiyakova^{79,ac},
 J. Shlomi¹⁸⁰, A. Shmeleva¹¹⁰, M.J. Shochet³⁷, J. Shojaii¹⁰⁴, D.R. Shope¹²⁸, S. Shrestha¹²⁶, E.M. Shrif^{33c},
 E. Shulga¹⁸⁰, P. Sicho¹⁴¹, A.M. Sickles¹⁷³, P.E. Sidebo¹⁵⁴, E. Sideras Haddad^{33c}, O. Sidiropoulou³⁶,
 A. Sidoti^{23b,23a}, F. Siegert⁴⁸, Dj. Sijacki¹⁶, M.Jr. Silva¹⁸¹, M.V. Silva Oliveira^{80a}, S.B. Silverstein^{45a},

S. Simion¹³², E. Simioni⁹⁹, R. Simoniello⁹⁹, S. Simsek^{12b}, P. Sinervo¹⁶⁷, V. Sinetckii^{112,110}, N.B. Sinev¹³¹, M. Sioli^{23b,23a}, I. Siral¹⁰⁵, S.Yu. Sivoklokov¹¹², J. Sjölin^{45a,45b}, E. Skorda⁹⁶, P. Skubic¹²⁸, M. Slawinska⁸⁴, K. Sliwa¹⁷⁰, R. Slovak¹⁴³, V. Smakhtin¹⁸⁰, B.H. Smart¹⁴⁴, J. Smiesko^{28a}, N. Smirnov¹¹¹, S.Yu. Smirnov¹¹¹, Y. Smirnov¹¹¹, L.N. Smirnova^{112,v}, O. Smirnova⁹⁶, J.W. Smith⁵³, M. Smizanska⁸⁹, K. Smolek¹⁴², A. Smykiewicz⁸⁴, A.A. Snesev¹¹⁰, H.L. Snoek¹¹⁹, I.M. Snyder¹³¹, S. Snyder²⁹, R. Sobie^{176,ae}, A. Soffer¹⁶¹, A. Søgaard⁵⁰, F. Sohns⁵³, C.A. Solans Sanchez³⁶, E.Yu. Soldatov¹¹¹, U. Soldevila¹⁷⁴, A.A. Solodkov¹²², A. Soloshenko⁷⁹, O.V. Solovyanov¹²², V. Solovyev¹³⁸, P. Sommer¹⁴⁹, H. Son¹⁷⁰, W. Song¹⁴⁴, W.Y. Song^{168b}, A. Sopczak¹⁴², F. Sopkova^{28b}, C.L. Sotiropoulou^{71a,71b}, S. Sottocornola^{70a,70b}, R. Soualah^{66a,66c,g}, A.M. Soukharev^{121b,121a}, D. South⁴⁶, S. Spagnolo^{67a,67b}, M. Spalla¹¹⁴, M. Spangenberg¹⁷⁸, F. Spanò⁹³, D. Sperlich⁵², T.M. Spieker^{61a}, R. Spighi^{23b}, G. Spigo³⁶, M. Spina¹⁵⁶, D.P. Spiteri⁵⁷, M. Spousta¹⁴³, A. Stabile^{68a,68b}, B.L. Stamas¹²⁰, R. Stamen^{61a}, M. Stamenkovic¹¹⁹, E. Stanecka⁸⁴, B. Stanislaus¹³⁵, M.M. Stanitzki⁴⁶, M. Stankaityte¹³⁵, B. Stapf¹¹⁹, E.A. Starchenko¹²², G.H. Stark¹⁴⁶, J. Stark⁵⁸, S.H. Stark⁴⁰, P. Staroba¹⁴¹, P. Starovoitov^{61a}, S. Stärz¹⁰³, R. Staszewski⁸⁴, G. Stavropoulos⁴⁴, M. Stegler⁴⁶, P. Steinberg²⁹, A.L. Steinhebel¹³¹, B. Stelzer¹⁵², H.J. Stelzer¹³⁹, O. Stelzer-Chilton^{168a}, H. Stenzel⁵⁶, T.J. Stevenson¹⁵⁶, G.A. Stewart³⁶, M.C. Stockton³⁶, G. Stoicea^{27b}, M. Stolarski^{140a}, S. Stonjek¹¹⁴, A. Straessner⁴⁸, J. Strandberg¹⁵⁴, S. Strandberg^{45a,45b}, M. Strauss¹²⁸, P. Strizenec^{28b}, R. Ströhmer¹⁷⁷, D.M. Strom¹³¹, R. Stroynowski⁴², A. Strubig⁵⁰, S.A. Stucci²⁹, B. Stugu¹⁷, J. Stupak¹²⁸, N.A. Styles⁴⁶, D. Su¹⁵³, S. Suchek^{61a}, V.V. Sulin¹¹⁰, M.J. Sullivan⁹⁰, D.M.S. Sultan⁵⁴, S. Sultansoy^{4c}, T. Sumida⁸⁵, S. Sun¹⁰⁵, X. Sun³, K. Suruliz¹⁵⁶, C.J.E. Suster¹⁵⁷, M.R. Sutton¹⁵⁶, S. Suzuki⁸¹, M. Svatos¹⁴¹, M. Swiatlowski³⁷, S.P. Swift², T. Swirski¹⁷⁷, A. Sydorenko⁹⁹, I. Sykora^{28a}, M. Sykora¹⁴³, T. Sykora¹⁴³, D. Ta⁹⁹, K. Tackmann^{46,aa}, J. Taenzer¹⁶¹, A. Taffard¹⁷¹, R. Tafirout^{168a}, H. Takai²⁹, R. Takashima⁸⁶, K. Takeda⁸², T. Takeshita¹⁵⁰, E.P. Takeva⁵⁰, Y. Takubo⁸¹, M. Talby¹⁰¹, A.A. Talyshev^{121b,121a}, N.M. Tamir¹⁶¹, J. Tanaka¹⁶³, M. Tanaka¹⁶⁵, R. Tanaka¹³², S. Tapia Araya¹⁷³, S. Tapprogge⁹⁹, A. Tarek Abouelfadl Mohamed¹³⁶, S. Tarem¹⁶⁰, K. Tariq^{60b}, G. Tarna^{27b,c}, G.F. Tartarelli^{68a}, P. Tas¹⁴³, M. Tasevsky¹⁴¹, T. Tashiro⁸⁵, E. Tassi^{41b,41a}, A. Tavares Delgado^{140a,140b}, Y. Tayalati^{35e}, A.J. Taylor⁵⁰, G.N. Taylor¹⁰⁴, W. Taylor^{168b}, A.S. Tee⁸⁹, R. Teixeira De Lima¹⁵³, P. Teixeira-Dias⁹³, H. Ten Kate³⁶, J.J. Teoh¹¹⁹, S. Terada⁸¹, K. Terashi¹⁶³, J. Terron⁹⁸, S. Terzo¹⁴, M. Testa⁵¹, R.J. Teuscher^{167,ae}, S.J. Thais¹⁸³, T. Theveneaux-Pelzer⁴⁶, F. Thiele⁴⁰, D.W. Thomas⁹³, J.O. Thomas⁴², J.P. Thomas²¹, A.S. Thompson⁵⁷, P.D. Thompson²¹, L.A. Thomsen¹⁸³, E. Thomson¹³⁷, E.J. Thorpe⁹², R.E. Ticse Torres⁵³, V.O. Tikhomirov^{110,ap}, Yu.A. Tikhonov^{121b,121a}, S. Timoshenko¹¹¹, P. Tipton¹⁸³, S. Tisserant¹⁰¹, K. Todome^{23b,23a}, S. Todorova-Nova⁵, S. Todt⁴⁸, J. Tojo⁸⁷, S. Tokár^{28a}, K. Tokushuku⁸¹, E. Tolley¹²⁶, K.G. Tomiwa^{33c}, M. Tomoto¹¹⁶, L. Tompkins^{153,q}, B. Tong⁵⁹, P. Tornambe¹⁰², E. Torrence¹³¹, H. Torres⁴⁸, E. Torró Pastor¹⁴⁸, C. Tosciri¹³⁵, J. Toth^{101,ad}, D.R. Tovey¹⁴⁹, A. Traeet¹⁷, C.J. Treado¹²⁴, T. Trefzger¹⁷⁷, F. Tresoldi¹⁵⁶, A. Tricoli²⁹, I.M. Trigger^{168a}, S. Trincaz-Duvoid¹³⁶, W. Trischuk¹⁶⁷, B. Trocmé⁵⁸, A. Trofymov¹⁴⁵, C. Troncon^{68a}, M. Trovatelli¹⁷⁶, F. Trovato¹⁵⁶, L. Truong^{33b}, M. Trzebinski⁸⁴, A. Trzupek⁸⁴, F. Tsai⁴⁶, J.C-L. Tseng¹³⁵, P.V. Tsiarehka^{107,qj}, A. Tsigotis¹⁶², V. Tsiskaridze¹⁵⁵, E.G. Tskhadadze^{159a}, M. Tsopoulou¹⁶², I.I. Tsukerman¹²³, V. Tsulaia¹⁸, S. Tsuno⁸¹, D. Tsybychev¹⁵⁵, Y. Tu^{63b}, A. Tudorache^{27b}, V. Tudorache^{27b}, T.T. Tulbure^{27a}, A.N. Tuna⁵⁹, S. Turchikhin⁷⁹, D. Turgeman¹⁸⁰, I. Turk Cakir^{4b,w}, R.J. Turner²¹, R.T. Turra^{68a}, P.M. Tuts³⁹, S. Tzamarias¹⁶², E. Tzovara⁹⁹, G. Uccielli⁴⁷, K. Uchida¹⁶³, I. Ueda⁸¹, M. Ughetto^{45a,45b}, F. Ukegawa¹⁶⁹, G. Unal³⁶, A. Undrus²⁹, G. Unel¹⁷¹, F.C. Ungaro¹⁰⁴, Y. Unno⁸¹, K. Uno¹⁶³, J. Urban^{28b}, P. Urquijo¹⁰⁴, G. Usai⁸, Z. Uysal^{12d}, L. Vacavant¹⁰¹, V. Vacek¹⁴², B. Vachon¹⁰³, K.O.H. Vadla¹³⁴, A. Vaidya⁹⁴, C. Valderanis¹¹³, E. Valdes Santurio^{45a,45b}, M. Valente⁵⁴, S. Valentinetti^{23b,23a}, A. Valero¹⁷⁴, L. Valéry⁴⁶, R.A. Vallance²¹, A. Vallier³⁶, J.A. Valls Ferrer¹⁷⁴, T.R. Van Daalen¹⁴, P. Van Gemmeren⁶, I. Van Vulpen¹¹⁹, M. Vanadia^{73a,73b}, W. Vandelli³⁶, E.R. Vandewall¹²⁹, A. Vaniachine¹⁶⁶, D. Vannicola^{72a,72b}, R. Vari^{72a}, E.W. Varnes⁷, C. Varni^{55b,55a}, T. Varol¹⁵⁸, D. Varouchas¹³², K.E. Varvell¹⁵⁷, M.E. Vasile^{27b}, G.A. Vasquez¹⁷⁶, J.G. Vasquez¹⁸³, F. Vazeille³⁸, D. Vazquez Furelos¹⁴, T. Vazquez Schroeder³⁶, J. Veatch⁵³, V. Vecchio^{74a,74b}, M.J. Veen¹¹⁹, L.M. Veloce¹⁶⁷, F. Veloso^{140a,140c}, S. Veneziano^{72a}, A. Ventura^{67a,67b}, N. Venturi³⁶, A. Verbitskyi¹¹⁴, V. Vercesi^{70a}, M. Verducci^{71a,71b}, C.M. Vergel Infante⁷⁸, C. Vergis²⁴, W. Verkerke¹¹⁹, A.T. Vermeulen¹¹⁹, J.C. Vermeulen¹¹⁹, M.C. Vetterli^{152,ax}, N. Viaux Maira^{147c}, M. Vicente Barreto Pinto⁵⁴, T. Vickey¹⁴⁹, O.E. Vickey Boeriu¹⁴⁹, G.H.A. Viehhauser¹³⁵, L. Viganì^{61b}, M. Villa^{23b,23a}, M. Villaplana Perez^{68a,68b}, E. Vilucchi⁵¹,

M.G. Vincter³⁴, G.S. Virdee²¹, A. Vishwakarma⁴⁶, C. Vittori^{23b,23a}, I. Vivarelli¹⁵⁶, M. Vogel¹⁸², P. Vokac¹⁴², S.E. von Buddenbrock^{33c}, E. Von Toerne²⁴, V. Vorobel¹⁴³, K. Vorobev¹¹¹, M. Vos¹⁷⁴, J.H. Vosseveld⁹⁰, M. Vozak¹⁰⁰, N. Vranjes¹⁶, M. Vranjes Milosavljevic¹⁶, V. Vrba¹⁴², M. Vreeswijk¹¹⁹, R. Vuillermet³⁶, I. Vukotic³⁷, P. Wagner²⁴, W. Wagner¹⁸², J. Wagner-Kuhr¹¹³, S. Wahdan¹⁸², H. Wahlberg⁸⁸, V.M. Walbrecht¹¹⁴, J. Walder⁸⁹, R. Walker¹¹³, S.D. Walker⁹³, W. Walkowiak¹⁵¹, V. Wallangen^{45a,45b}, A.M. Wang⁵⁹, C. Wang^{60c}, C. Wang^{60b}, F. Wang¹⁸¹, H. Wang¹⁸, H. Wang³, J. Wang^{63a}, J. Wang¹⁵⁷, J. Wang^{61b}, P. Wang⁴², Q. Wang¹²⁸, R.-J. Wang⁹⁹, R. Wang^{60a}, R. Wang⁶, S.M. Wang¹⁵⁸, W.T. Wang^{60a}, W. Wang^{15c,af}, W.X. Wang^{60a,af}, Y. Wang^{60a,am}, Z. Wang^{60c}, C. Wanotayaroj⁴⁶, A. Warburton¹⁰³, C.P. Ward³², D.R. Wardrope⁹⁴, N. Warrack⁵⁷, A. Washbrook⁵⁰, A.T. Watson²¹, M.F. Watson²¹, G. Watts¹⁴⁸, B.M. Waugh⁹⁴, A.F. Webb¹¹, S. Webb⁹⁹, C. Weber¹⁸³, M.S. Weber²⁰, S.A. Weber³⁴, S.M. Weber^{61a}, A.R. Weidberg¹³⁵, J. Weingarten⁴⁷, M. Weirich⁹⁹, C. Weiser⁵², P.S. Wells³⁶, T. Wenaus²⁹, T. Wengler³⁶, S. Wenig³⁶, N. Vermes²⁴, M.D. Werner⁷⁸, M. Wessels^{61a}, T.D. Weston²⁰, K. Whalen¹³¹, N.L. Whallon¹⁴⁸, A.M. Wharton⁸⁹, A.S. White¹⁰⁵, A. White⁸, M.J. White¹, D. Whiteson¹⁷¹, B.W. Whitmore⁸⁹, W. Wiedenmann¹⁸¹, M. Wieler¹⁴⁴, N. Wieseotte⁹⁹, C. Wiglesworth⁴⁰, L.A.M. Wiik-Fuchs⁵², F. Wilk¹⁰⁰, H.G. Wilkens³⁶, L.J. Wilkins⁹³, H.H. Williams¹³⁷, S. Williams³², C. Willis¹⁰⁶, S. Willocq¹⁰², J.A. Wilson²¹, I. Wingerter-Seez⁵, E. Winkels¹⁵⁶, F. Winklmeier¹³¹, O.J. Winston¹⁵⁶, B.T. Winter⁵², M. Wittgen¹⁵³, M. Wobisch⁹⁵, A. Wolf⁹⁹, T.M.H. Wolf¹¹⁹, R. Wolff¹⁰¹, R.W. Wölker¹³⁵, J. Wollrath⁵², M.W. Wolter⁸⁴, H. Wolters^{140a,140c}, V.W.S. Wong¹⁷⁵, N.L. Woods¹⁴⁶, S.D. Worm²¹, B.K. Wosiek⁸⁴, K.W. Woźniak⁸⁴, K. Wraight⁵⁷, S.L. Wu¹⁸¹, X. Wu⁵⁴, Y. Wu^{60a}, T.R. Wyatt¹⁰⁰, B.M. Wynne⁵⁰, S. Xella⁴⁰, Z. Xi¹⁰⁵, L. Xia¹⁷⁸, X. Xiao¹⁰⁵, I. Xiotidis¹⁵⁶, D. Xu^{15a}, H. Xu^{60a,c}, L. Xu²⁹, T. Xu¹⁴⁵, W. Xu¹⁰⁵, Z. Xu^{60b}, Z. Xu¹⁵³, B. Yabsley¹⁵⁷, S. Yacoob^{33a}, K. Yajima¹³³, D.P. Yallup⁹⁴, D. Yamaguchi¹⁶⁵, Y. Yamaguchi¹⁶⁵, A. Yamamoto⁸¹, M. Yamatani¹⁶³, T. Yamazaki¹⁶³, Y. Yamazaki⁸², Z. Yan²⁵, H.J. Yang^{60c,60d}, H.T. Yang¹⁸, S. Yang⁷⁷, X. Yang^{60b,58}, Y. Yang¹⁶³, W.-M. Yao¹⁸, Y.C. Yap⁴⁶, Y. Yasu⁸¹, E. Yatsenko^{60c,60d}, J. Ye⁴², S. Ye²⁹, I. Yeletsikh⁷⁹, M.R. Yexley⁸⁹, E. Yigitbasi²⁵, K. Yorita¹⁷⁹, K. Yoshihara¹³⁷, C.J.S. Young³⁶, C. Young¹⁵³, J. Yu⁷⁸, R. Yuan^{60b,i}, X. Yue^{61a}, S.P.Y. Yuen²⁴, M. Zaazoua^{35e}, B. Zabinski⁸⁴, G. Zacharis¹⁰, E. Zaffaroni⁵⁴, J. Zahreddine¹³⁶, A.M. Zaitsev^{122,ao}, T. Zakareishvili^{159b}, N. Zakharchuk³⁴, S. Zambito⁵⁹, D. Zanzi³⁶, D.R. Zaripovas⁵⁷, S.V. Zeiβner⁴⁷, C. Zeitnitz¹⁸², G. Zemaityte¹³⁵, J.C. Zeng¹⁷³, O. Zenin¹²², T. Ženiš^{28a}, D. Zerwas¹³², M. Zgubič¹³⁵, B. Zhang^{15c}, D.F. Zhang^{15b}, G. Zhang^{15b}, H. Zhang^{15c}, J. Zhang⁶, L. Zhang^{15c}, L. Zhang^{60a}, M. Zhang¹⁷³, R. Zhang²⁴, X. Zhang^{60b}, Y. Zhang^{15a,15d}, Z. Zhang^{63a}, Z. Zhang¹³², P. Zhao⁴⁹, Y. Zhao^{60b}, Z. Zhao^{60a}, A. Zhemchugov⁷⁹, Z. Zheng¹⁰⁵, D. Zhong¹⁷³, B. Zhou¹⁰⁵, C. Zhou¹⁸¹, M.S. Zhou^{15a,15d}, M. Zhou¹⁵⁵, N. Zhou^{60c}, Y. Zhou⁷, C.G. Zhu^{60b}, C. Zhu^{15a,15d}, H.L. Zhu^{60a}, H. Zhu^{15a}, J. Zhu¹⁰⁵, Y. Zhu^{60a}, X. Zhuang^{15a}, K. Zhukov¹¹⁰, V. Zhulanov^{121b,121a}, D. Zieminska⁶⁵, N.I. Zimine⁷⁹, S. Zimmermann⁵², Z. Zinonos¹¹⁴, M. Ziolkowski¹⁵¹, L. Živković¹⁶, G. Zobernig¹⁸¹, A. Zoccoli^{23b,23a}, K. Zoch⁵³, T.G. Zorbas¹⁴⁹, R. Zou³⁷, L. Zwalinski³⁶

¹ Department of Physics, University of Adelaide, Adelaide, Australia

² Physics Department, SUNY Albany, Albany, NY, United States of America

³ Department of Physics, University of Alberta, Edmonton, AB, Canada

⁴ (a) Department of Physics, Ankara University, Ankara; (b) Istanbul Aydin University, Istanbul; (c) Division of Physics, TOBB University of Economics and Technology, Ankara, Turkey

⁵ LAPP, Université Grenoble Alpes, Université Savoie Mont Blanc, CNRS/IN2P3, Annecy, France

⁶ High Energy Physics Division, Argonne National Laboratory, Argonne, IL, United States of America

⁷ Department of Physics, University of Arizona, Tucson, AZ, United States of America

⁸ Department of Physics, University of Texas at Arlington, Arlington, TX, United States of America

⁹ Physics Department, National and Kapodistrian University of Athens, Athens, Greece

¹⁰ Physics Department, National Technical University of Athens, Zografou, Greece

¹¹ Department of Physics, University of Texas at Austin, Austin, TX, United States of America

¹² (a) Bahcesehir University, Faculty of Engineering and Natural Sciences, Istanbul; (b) Istanbul Bilgi University, Faculty of Engineering and Natural Sciences, Istanbul; (c) Department of Physics, Bogazici University, Istanbul; (d) Department of Physics Engineering, Gaziantep University, Gaziantep, Turkey

¹³ Institute of Physics, Azerbaijan Academy of Sciences, Baku, Azerbaijan

¹⁴ Institut de Física d'Altes Energies (IFAE), Barcelona Institute of Science and Technology, Barcelona, Spain

¹⁵ (a) Institute of High Energy Physics, Chinese Academy of Sciences, Beijing; (b) Physics Department, Tsinghua University, Beijing; (c) Department of Physics, Nanjing University, Nanjing;

(d) University of Chinese Academy of Science (UCAS), Beijing, China

¹⁶ Institute of Physics, University of Belgrade, Belgrade, Serbia

¹⁷ Department for Physics and Technology, University of Bergen, Bergen, Norway

¹⁸ Physics Division, Lawrence Berkeley National Laboratory and University of California, Berkeley, CA, United States of America

¹⁹ Institut für Physik, Humboldt Universität zu Berlin, Berlin, Germany

²⁰ Albert Einstein Center for Fundamental Physics and Laboratory for High Energy Physics, University of Bern, Bern, Switzerland

²¹ School of Physics and Astronomy, University of Birmingham, Birmingham, United Kingdom

²² Facultad de Ciencias y Centro de Investigaciones, Universidad Antonio Nariño, Bogota, Colombia

²³ (a) INFN Bologna and Università di Bologna, Dipartimento di Fisica; (b) INFN Sezione di Bologna, Italy

- ²⁴ Physikalisches Institut, Universität Bonn, Bonn, Germany
- ²⁵ Department of Physics, Boston University, Boston, MA, United States of America
- ²⁶ Department of Physics, Brandeis University, Waltham, MA, United States of America
- ²⁷ ^(a) Transilvania University of Brasov, Brasov; ^(b) Horia Hulubei National Institute of Physics and Nuclear Engineering, Bucharest; ^(c) Department of Physics, Alexandru Ioan Cuza University of Iasi, Iasi; ^(d) National Institute for Research and Development of Isotopic and Molecular Technologies, Physics Department, Cluj-Napoca; ^(e) University Politehnica Bucharest, Bucharest; ^(f) West University in Timisoara, Timisoara, Romania
- ²⁸ ^(a) Faculty of Mathematics, Physics and Informatics, Comenius University, Bratislava; ^(b) Department of Subnuclear Physics, Institute of Experimental Physics of the Slovak Academy of Sciences, Kosice, Slovak Republic
- ²⁹ Physics Department, Brookhaven National Laboratory, Upton, NY, United States of America
- ³⁰ Departamento de Física, Universidad de Buenos Aires, Buenos Aires, Argentina
- ³¹ California State University, CA, United States of America
- ³² Cavendish Laboratory, University of Cambridge, Cambridge, United Kingdom
- ³³ ^(a) Department of Physics, University of Cape Town, Cape Town; ^(b) Department of Mechanical Engineering Science, University of Johannesburg, Johannesburg; ^(c) School of Physics, University of the Witwatersrand, Johannesburg, South Africa
- ³⁴ Department of Physics, Carleton University, Ottawa, ON, Canada
- ³⁵ ^(a) Faculté des Sciences Ain Chock, Réseau Universitaire de Physique des Hautes Energies - Université Hassan II, Casablanca; ^(b) Faculté des Sciences, Université Ibn-Tofail, Kénitra; ^(c) Faculté des Sciences Semlalia, Université Cadi Ayyad, LPHEA-Marrakech; ^(d) Faculté des Sciences, Université Mohamed Premier and LPTPM, Oujda; ^(e) Faculté des sciences, Université Mohammed V, Rabat, Morocco
- ³⁶ CERN, Geneva, Switzerland
- ³⁷ Enrico Fermi Institute, University of Chicago, Chicago, IL, United States of America
- ³⁸ LPC, Université Clermont Auvergne, CNRS/IN2P3, Clermont-Ferrand, France
- ³⁹ Nevis Laboratory, Columbia University, Irvington, NY, United States of America
- ⁴⁰ Niels Bohr Institute, University of Copenhagen, Copenhagen, Denmark
- ⁴¹ ^(a) Dipartimento di Fisica, Università della Calabria, Rende; ^(b) INFN Gruppo Collegato di Cosenza, Laboratori Nazionali di Frascati, Italy
- ⁴² Physics Department, Southern Methodist University, Dallas, TX, United States of America
- ⁴³ Physics Department, University of Texas at Dallas, Richardson, TX, United States of America
- ⁴⁴ National Centre for Scientific Research "Demokritos", Agia Paraskevi, Greece
- ⁴⁵ ^(a) Department of Physics, Stockholm University; ^(b) Oskar Klein Centre, Stockholm, Sweden
- ⁴⁶ Deutsches Elektronen-Synchrotron DESY, Hamburg and Zeuthen, Germany
- ⁴⁷ Lehrstuhl für Experimentelle Physik IV, Technische Universität Dortmund, Dortmund, Germany
- ⁴⁸ Institut für Kern- und Teilchenphysik, Technische Universität Dresden, Dresden, Germany
- ⁴⁹ Department of Physics, Duke University, Durham, NC, United States of America
- ⁵⁰ SUPA - School of Physics and Astronomy, University of Edinburgh, Edinburgh, United Kingdom
- ⁵¹ INFN e Laboratori Nazionali di Frascati, Frascati, Italy
- ⁵² Physikalisches Institut, Albert-Ludwigs-Universität Freiburg, Freiburg, Germany
- ⁵³ II. Physikalisches Institut, Georg-August-Universität Göttingen, Göttingen, Germany
- ⁵⁴ Département de Physique Nucléaire et Corpusculaire, Université de Genève, Genève, Switzerland
- ⁵⁵ ^(a) Dipartimento di Fisica, Università di Genova, Genova; ^(b) INFN Sezione di Genova, Italy
- ⁵⁶ II. Physikalisches Institut, Justus-Liebig-Universität Giessen, Giessen, Germany
- ⁵⁷ SUPA - School of Physics and Astronomy, University of Glasgow, Glasgow, United Kingdom
- ⁵⁸ LPSC, Université Grenoble Alpes, CNRS/IN2P3, Grenoble INP, Grenoble, France
- ⁵⁹ Laboratory for Particle Physics and Cosmology, Harvard University, Cambridge, MA, United States of America
- ⁶⁰ ^(a) Department of Modern Physics and State Key Laboratory of Particle Detection and Electronics, University of Science and Technology of China, Hefei; ^(b) Institute of Frontier and Interdisciplinary Science and Key Laboratory of Particle Physics and Particle Irradiation (MOE), Shandong University, Qingdao; ^(c) School of Physics and Astronomy, Shanghai Jiao Tong University, KLPPAC-MoE, SKLPPC, Shanghai; ^(d) Tsung-Dao Lee Institute, Shanghai, China
- ⁶¹ ^(a) Kirchhoff-Institut für Physik, Ruprecht-Karls-Universität Heidelberg, Heidelberg; ^(b) Physikalisches Institut, Ruprecht-Karls-Universität Heidelberg, Heidelberg, Germany
- ⁶² Faculty of Applied Information Science, Hiroshima Institute of Technology, Hiroshima, Japan
- ⁶³ ^(a) Department of Physics, Chinese University of Hong Kong, Shatin, N.T., Hong Kong; ^(b) Department of Physics, University of Hong Kong, Hong Kong; ^(c) Department of Physics and Institute for Advanced Study, Hong Kong University of Science and Technology, Clear Water Bay, Kowloon, Hong Kong, China
- ⁶⁴ Department of Physics, National Tsing Hua University, Hsinchu, Taiwan
- ⁶⁵ Department of Physics, Indiana University, Bloomington, IN, United States of America
- ⁶⁶ ^(a) INFN Gruppo Collegato di Udine, Sezione di Trieste, Udine; ^(b) ICTP, Trieste; ^(c) Dipartimento Politecnico di Ingegneria e Architettura, Università di Udine, Udine, Italy
- ⁶⁷ ^(a) INFN Sezione di Lecce; ^(b) Dipartimento di Matematica e Fisica, Università del Salento, Lecce, Italy
- ⁶⁸ ^(a) INFN Sezione di Milano; ^(b) Dipartimento di Fisica, Università di Milano, Milano, Italy
- ⁶⁹ ^(a) INFN Sezione di Napoli; ^(b) Dipartimento di Fisica, Università di Napoli, Napoli, Italy
- ⁷⁰ ^(a) INFN Sezione di Pavia; ^(b) Dipartimento di Fisica, Università di Pavia, Pavia, Italy
- ⁷¹ ^(a) INFN Sezione di Pisa; ^(b) Dipartimento di Fisica E. Fermi, Università di Pisa, Pisa, Italy
- ⁷² ^(a) INFN Sezione di Roma; ^(b) Dipartimento di Fisica, Sapienza Università di Roma, Roma, Italy
- ⁷³ ^(a) INFN Sezione di Roma Tor Vergata; ^(b) Dipartimento di Fisica, Università di Roma Tor Vergata, Roma, Italy
- ⁷⁴ ^(a) INFN Sezione di Roma Tre; ^(b) Dipartimento di Matematica e Fisica, Università Roma Tre, Roma, Italy
- ⁷⁵ ^(a) INFN-TIFPA; ^(b) Università degli Studi di Trento, Trento, Italy
- ⁷⁶ Institut für Astro- und Teilchenphysik, Leopold-Franzens-Universität, Innsbruck, Austria
- ⁷⁷ University of Iowa, Iowa City, IA, United States of America
- ⁷⁸ Department of Physics and Astronomy, Iowa State University, Ames, IA, United States of America
- ⁷⁹ Joint Institute for Nuclear Research, Dubna, Russia
- ⁸⁰ ^(a) Departamento de Engenharia Elétrica, Universidade Federal de Juiz de Fora (UFJF), Juiz de Fora; ^(b) Universidade Federal do Rio De Janeiro COPPE/EE/IF, Rio de Janeiro; ^(c) Universidade Federal de São João del Rei (UFSJ), São João del Rei; ^(d) Instituto de Física, Universidade de São Paulo, São Paulo, Brazil
- ⁸¹ KEK, High Energy Accelerator Research Organization, Tsukuba, Japan
- ⁸² Graduate School of Science, Kobe University, Kobe, Japan
- ⁸³ ^(a) AGH University of Science and Technology, Faculty of Physics and Applied Computer Science, Krakow; ^(b) Marian Smoluchowski Institute of Physics, Jagiellonian University, Krakow, Poland
- ⁸⁴ Institute of Nuclear Physics Polish Academy of Sciences, Krakow, Poland
- ⁸⁵ Faculty of Science, Kyoto University, Kyoto, Japan
- ⁸⁶ Kyoto University of Education, Kyoto, Japan
- ⁸⁷ Research Center for Advanced Particle Physics and Department of Physics, Kyushu University, Fukuoka, Japan
- ⁸⁸ Instituto de Física La Plata, Universidad Nacional de La Plata and CONICET, La Plata, Argentina
- ⁸⁹ Physics Department, Lancaster University, Lancaster, United Kingdom
- ⁹⁰ Oliver Lodge Laboratory, University of Liverpool, Liverpool, United Kingdom
- ⁹¹ Department of Experimental Particle Physics, Jožef Stefan Institute and Department of Physics, University of Ljubljana, Ljubljana, Slovenia

- ⁹² School of Physics and Astronomy, Queen Mary University of London, London, United Kingdom
- ⁹³ Department of Physics, Royal Holloway University of London, Egham, United Kingdom
- ⁹⁴ Department of Physics and Astronomy, University College London, London, United Kingdom
- ⁹⁵ Louisiana Tech University, Ruston, LA, United States of America
- ⁹⁶ Fysiska institutionen, Lunds universitet, Lund, Sweden
- ⁹⁷ Centre de Calcul de l'Institut National de Physique Nucléaire et de Physique des Particules (IN2P3), Villeurbanne, France
- ⁹⁸ Departamento de Física Teórica C-15 and CIAFF, Universidad Autónoma de Madrid, Madrid, Spain
- ⁹⁹ Institut für Physik, Universität Mainz, Mainz, Germany
- ¹⁰⁰ School of Physics and Astronomy, University of Manchester, Manchester, United Kingdom
- ¹⁰¹ CPPM, Aix-Marseille Université, CNRS/IN2P3, Marseille, France
- ¹⁰² Department of Physics, University of Massachusetts, Amherst, MA, United States of America
- ¹⁰³ Department of Physics, McGill University, Montreal, QC, Canada
- ¹⁰⁴ School of Physics, University of Melbourne, Victoria, Australia
- ¹⁰⁵ Department of Physics, University of Michigan, Ann Arbor, MI, United States of America
- ¹⁰⁶ Department of Physics and Astronomy, Michigan State University, East Lansing, MI, United States of America
- ¹⁰⁷ B.I. Stepanov Institute of Physics, National Academy of Sciences of Belarus, Minsk, Belarus
- ¹⁰⁸ Research Institute for Nuclear Problems of Byelorussian State University, Minsk, Belarus
- ¹⁰⁹ Group of Particle Physics, University of Montreal, Montreal, QC, Canada
- ¹¹⁰ P.N. Lebedev Physical Institute of the Russian Academy of Sciences, Moscow, Russia
- ¹¹¹ National Research Nuclear University MEPhI, Moscow, Russia
- ¹¹² D.V. Skobel'syn Institute of Nuclear Physics, M.V. Lomonosov Moscow State University, Moscow, Russia
- ¹¹³ Fakultät für Physik, Ludwig-Maximilians-Universität München, München, Germany
- ¹¹⁴ Max-Planck-Institut für Physik (Werner-Heisenberg-Institut), München, Germany
- ¹¹⁵ Nagasaki Institute of Applied Science, Nagasaki, Japan
- ¹¹⁶ Graduate School of Science and Kobayashi-Maskawa Institute, Nagoya University, Nagoya, Japan
- ¹¹⁷ Department of Physics and Astronomy, University of New Mexico, Albuquerque, NM, United States of America
- ¹¹⁸ Institute for Mathematics, Astrophysics and Particle Physics, Radboud University Nijmegen/Nikhef, Nijmegen, Netherlands
- ¹¹⁹ Nikhef National Institute for Subatomic Physics and University of Amsterdam, Amsterdam, Netherlands
- ¹²⁰ Department of Physics, Northern Illinois University, DeKalb, IL, United States of America
- ¹²¹ ^(a) Budker Institute of Nuclear Physics and NSU, SB RAS, Novosibirsk; ^(b) Novosibirsk State University Novosibirsk, Russia
- ¹²² Institute for High Energy Physics of the National Research Centre Kurchatov Institute, Protvino, Russia
- ¹²³ Institute for Theoretical and Experimental Physics named by A.I. Alikhanov of National Research Centre "Kurchatov Institute", Moscow, Russia
- ¹²⁴ Department of Physics, New York University, New York, NY, United States of America
- ¹²⁵ Ochanomizu University, Otsuka, Bunkyo-ku, Tokyo, Japan
- ¹²⁶ Ohio State University, Columbus, OH, United States of America
- ¹²⁷ Faculty of Science, Okayama University, Okayama, Japan
- ¹²⁸ Homer L. Dodge Department of Physics and Astronomy, University of Oklahoma, Norman, OK, United States of America
- ¹²⁹ Department of Physics, Oklahoma State University, Stillwater, OK, United States of America
- ¹³⁰ Palacký University, RCPTM, Joint Laboratory of Optics, Olomouc, Czech Republic
- ¹³¹ Center for High Energy Physics, University of Oregon, Eugene, OR, United States of America
- ¹³² LAL, Université Paris-Sud, CNRS/IN2P3, Université Paris-Saclay, Orsay, France
- ¹³³ Graduate School of Science, Osaka University, Osaka, Japan
- ¹³⁴ Department of Physics, University of Oslo, Oslo, Norway
- ¹³⁵ Department of Physics, Oxford University, Oxford, United Kingdom
- ¹³⁶ LPNHE, Sorbonne Université, Université de Paris, CNRS/IN2P3, Paris, France
- ¹³⁷ Department of Physics, University of Pennsylvania, Philadelphia, PA, United States of America
- ¹³⁸ Konstantinov Nuclear Physics Institute of National Research Centre "Kurchatov Institute", PNPI, St. Petersburg, Russia
- ¹³⁹ Department of Physics and Astronomy, University of Pittsburgh, Pittsburgh, PA, United States of America
- ¹⁴⁰ ^(a) Laboratório de Instrumentação e Física Experimental de Partículas - LIP, Lisboa; ^(b) Departamento de Física, Faculdade de Ciências, Universidade de Lisboa, Lisboa; ^(c) Departamento de Física, Universidade de Coimbra, Coimbra; ^(d) Centro de Física Nuclear da Universidade de Lisboa, Lisboa; ^(e) Departamento de Física, Universidade do Minho, Braga; ^(f) Departamento de Física Teórica y del Cosmos, Universidad de Granada, Granada (Spain); ^(g) Dep Física and CEFITEC of Faculdade de Ciências e Tecnologia, Universidade Nova de Lisboa, Caparica;
- ^(h) Instituto Superior Técnico, Universidade de Lisboa, Lisboa, Portugal
- ¹⁴¹ Institute of Physics of the Czech Academy of Sciences, Prague, Czech Republic
- ¹⁴² Czech Technical University in Prague, Prague, Czech Republic
- ¹⁴³ Charles University, Faculty of Mathematics and Physics, Prague, Czech Republic
- ¹⁴⁴ Particle Physics Department, Rutherford Appleton Laboratory, Didcot, United Kingdom
- ¹⁴⁵ IRFU, CEA, Université Paris-Saclay, Gif-sur-Yvette, France
- ¹⁴⁶ Santa Cruz Institute for Particle Physics, University of California Santa Cruz, Santa Cruz, CA, United States of America
- ¹⁴⁷ ^(a) Departamento de Física, Pontificia Universidad Católica de Chile, Santiago; ^(b) Universidad Andres Bello, Department of Physics, Santiago; ^(c) Departamento de Física, Universidad Técnica Federico Santa María, Valparaíso, Chile
- ¹⁴⁸ Department of Physics, University of Washington, Seattle, WA, United States of America
- ¹⁴⁹ Department of Physics and Astronomy, University of Sheffield, Sheffield, United Kingdom
- ¹⁵⁰ Department of Physics, Shinshu University, Nagano, Japan
- ¹⁵¹ Department Physik, Universität Siegen, Siegen, Germany
- ¹⁵² Department of Physics, Simon Fraser University, Burnaby, BC, Canada
- ¹⁵³ SLAC National Accelerator Laboratory, Stanford, CA, United States of America
- ¹⁵⁴ Physics Department, Royal Institute of Technology, Stockholm, Sweden
- ¹⁵⁵ Departments of Physics and Astronomy, Stony Brook University, Stony Brook, NY, United States of America
- ¹⁵⁶ Department of Physics and Astronomy, University of Sussex, Brighton, United Kingdom
- ¹⁵⁷ School of Physics, University of Sydney, Sydney, Australia
- ¹⁵⁸ Institute of Physics, Academia Sinica, Taipei, Taiwan
- ¹⁵⁹ ^(a) E. Andronikashvili Institute of Physics, Iv. Javakishvili Tbilisi State University, Tbilisi; ^(b) High Energy Physics Institute, Tbilisi State University, Tbilisi, Georgia
- ¹⁶⁰ Department of Physics, Technion, Israel Institute of Technology, Haifa, Israel
- ¹⁶¹ Raymond and Beverly Sackler School of Physics and Astronomy, Tel Aviv University, Tel Aviv, Israel
- ¹⁶² Department of Physics, Aristotle University of Thessaloniki, Thessaloniki, Greece
- ¹⁶³ International Center for Elementary Particle Physics and Department of Physics, University of Tokyo, Tokyo, Japan
- ¹⁶⁴ Graduate School of Science and Technology, Tokyo Metropolitan University, Tokyo, Japan
- ¹⁶⁵ Department of Physics, Tokyo Institute of Technology, Tokyo, Japan
- ¹⁶⁶ Tomsk State University, Tomsk, Russia

- ¹⁶⁷ Department of Physics, University of Toronto, Toronto, ON, Canada
¹⁶⁸ ^(a) TRIUMF, Vancouver, BC; ^(b) Department of Physics and Astronomy, York University, Toronto, ON, Canada
¹⁶⁹ Division of Physics and Tomonaga Center for the History of the Universe, Faculty of Pure and Applied Sciences, University of Tsukuba, Tsukuba, Japan
¹⁷⁰ Department of Physics and Astronomy, Tufts University, Medford, MA, United States of America
¹⁷¹ Department of Physics and Astronomy, University of California Irvine, Irvine, CA, United States of America
¹⁷² Department of Physics and Astronomy, University of Uppsala, Uppsala, Sweden
¹⁷³ Department of Physics, University of Illinois, Urbana, IL, United States of America
¹⁷⁴ Instituto de Física Corpuscular (IFIC), Centro Mixto Universidad de Valencia - CSIC, Valencia, Spain
¹⁷⁵ Department of Physics, University of British Columbia, Vancouver, BC, Canada
¹⁷⁶ Department of Physics and Astronomy, University of Victoria, Victoria, BC, Canada
¹⁷⁷ Fakultät für Physik und Astronomie, Julius-Maximilians-Universität Würzburg, Würzburg, Germany
¹⁷⁸ Department of Physics, University of Warwick, Coventry, United Kingdom
¹⁷⁹ Waseda University, Tokyo, Japan
¹⁸⁰ Department of Particle Physics, Weizmann Institute of Science, Rehovot, Israel
¹⁸¹ Department of Physics, University of Wisconsin, Madison, WI, United States of America
¹⁸² Fakultät für Mathematik und Naturwissenschaften, Fachgruppe Physik, Bergische Universität Wuppertal, Wuppertal, Germany
¹⁸³ Department of Physics, Yale University, New Haven, CT, United States of America
¹⁸⁴ Yerevan Physics Institute, Yerevan, Armenia

- ^a Also at Borough of Manhattan Community College, City University of New York, New York, NY; United States of America.
^b Also at CERN, Geneva; Switzerland.
^c Also at CPPM, Aix-Marseille Université, CNRS/IN2P3, Marseille; France.
^d Also at Département de Physique Nucléaire et Corpusculaire, Université de Genève, Genève; Switzerland.
^e Also at Departament de Física de la Universitat Autònoma de Barcelona, Barcelona; Spain.
^f Also at Departamento de Física, Instituto Superior Técnico, Universidade de Lisboa, Lisboa; Portugal.
^g Also at Department of Applied Physics and Astronomy, University of Sharjah, Sharjah; United Arab Emirates.
^h Also at Department of Financial and Management Engineering, University of the Aegean, Chios; Greece.
ⁱ Also at Department of Physics and Astronomy, Michigan State University, East Lansing, MI; United States of America.
^j Also at Department of Physics and Astronomy, University of Louisville, Louisville, KY; United States of America.
^k Also at Department of Physics, Ben Gurion University of the Negev, Beer Sheva; Israel.
^l Also at Department of Physics, California State University, East Bay; United States of America.
^m Also at Department of Physics, California State University, Fresno; United States of America.
ⁿ Also at Department of Physics, California State University, Sacramento; United States of America.
^o Also at Department of Physics, King's College London, London; United Kingdom.
^p Also at Department of Physics, St. Petersburg State Polytechnical University, St. Petersburg; Russia.
^q Also at Department of Physics, Stanford University, Stanford, CA; United States of America.
^r Also at Department of Physics, University of Adelaide, Adelaide; Australia.
^s Also at Department of Physics, University of Fribourg, Fribourg; Switzerland.
^t Also at Department of Physics, University of Michigan, Ann Arbor, MI; United States of America.
^u Also at Dipartimento di Matematica, Informatica e Fisica, Università di Udine, Udine; Italy.
^v Also at Faculty of Physics, M.V. Lomonosov Moscow State University, Moscow; Russia.
^w Also at Giresun University, Faculty of Engineering, Giresun; Turkey.
^x Also at Graduate School of Science, Osaka University, Osaka; Japan.
^y Also at Hellenic Open University, Patras; Greece.
^z Also at Institutio Catalana de Recerca i Estudis Avancats, ICREA, Barcelona; Spain.
^{aa} Also at Institut für Experimentalphysik, Universität Hamburg, Hamburg; Germany.
^{ab} Also at Institute for Mathematics, Astrophysics and Particle Physics, Radboud University Nijmegen/Nikhef, Nijmegen; Netherlands.
^{ac} Also at Institute for Nuclear Research and Nuclear Energy (INRNE) of the Bulgarian Academy of Sciences, Sofia; Bulgaria.
^{ad} Also at Institute for Particle and Nuclear Physics, Wigner Research Centre for Physics, Budapest; Hungary.
^{ae} Also at Institute of Particle Physics (IPP), Vancouver; Canada.
^{af} Also at Institute of Physics, Academia Sinica, Taipei; Taiwan.
^{ag} Also at Institute of Physics, Azerbaijan Academy of Sciences, Baku; Azerbaijan.
^{ah} Also at Institute of Theoretical Physics, Ilia State University, Tbilisi; Georgia.
^{ai} Also at Instituto de Física Teórica, IFT-UAM/CSIC, Madrid; Spain.
^{aj} Also at Joint Institute for Nuclear Research, Dubna; Russia.
^{ak} Also at LAL, Université Paris-Sud, CNRS/IN2P3, Université Paris-Saclay, Orsay; France.
^{al} Also at Louisiana Tech University, Ruston, LA; United States of America.
^{am} Also at LPNHE, Sorbonne Université, Université de Paris, CNRS/IN2P3, Paris; France.
^{an} Also at Manhattan College, New York, NY; United States of America.
^{ao} Also at Moscow Institute of Physics and Technology State University, Dolgoprudny; Russia.
^{ap} Also at National Research Nuclear University MEPhI, Moscow; Russia.
^{aq} Also at Physics Department, An-Najah National University, Nablus; Palestine.
^{ar} Also at Physics Dept, University of South Africa, Pretoria; South Africa.
^{as} Also at Physikalisches Institut, Albert-Ludwigs-Universität Freiburg, Freiburg; Germany.
^{at} Also at School of Physics, Sun Yat-sen University, Guangzhou; China.
^{au} Also at The City College of New York, New York, NY; United States of America.
^{av} Also at The Collaborative Innovation Center of Quantum Matter (CICQM), Beijing; China.
^{aw} Also at Tomsk State University, Tomsk, and Moscow Institute of Physics and Technology State University, Dolgoprudny; Russia.
^{ax} Also at TRIUMF, Vancouver, BC; Canada.
^{ay} Also at Università di Napoli Parthenope, Napoli; Italy.
^{*} Deceased.